Quantum Coherence in Biological Systems

Elisabeth Rieper

Diplom Physikerin, Universität Braunschweig, Germany

Centre for Quantum Technologies

National University of Singapore

A thesis submitted for the degree of

PhilosophiæDoctor (PhD)

2011

Habe nun, ach! Mathematik,
Quantenphysik und Biologie,
Und leider auch Spinchemie!
Durchaus studiert, mit heißem Bemühn.
Da steh ich nun, ich armer Tor!
Und bin so klug als wie zuvor.

Abstract

In this PhD thesis I investigate the occurrence of quantum coherences and their consequences in biological systems. I consider both finite (spin) and infinite (vibrations) degrees of freedom.

Chapter 1 gives a general introduction to quantum biology. I summarize key features of quantum effects and point out how they could matter in biological systems.

Chapter 2 deals with the avian compass, where spin coherences play a fundamental role. The experimental evidence on how weak oscillating fields disrupt a bird's ability to navigate is summarized. Detailed calculations show that the experimental evidence can only be explained by long lived coherence of the electron spin.

In chapter 3 I investigate entanglement and thus coherence in infinite degrees of freedoms, i.e. vibrations in coupled harmonic oscillators. Two entanglement measures show critical behavior at the quantum phase transition from a linear chain to a zig-zag configuration of a harmonic lattice.

The methods developed for the chain of coupled harmonic oscillators will be applied in chapter 4 to the electronic degree of freedom in DNA. I model the electron clouds of nucleic acids in DNA as a chain of coupled quantum harmonic oscillators with dipole-dipole interaction between nearest neighbours resulting in a van der Waals type bonding. Crucial parameters in my model are the distances between the acids and the coupling between them, which I estimate from numerical simulations. I show that for realistic parameters nearest neighbour entanglement is present even at room temperature. I

find that the strength of the single base von Neumann entropy depends on the neighbouring sites, thus questioning the notion of treating the quantum state of single bases as independent units. I derive an analytical expression for the binding energy of the coupled chain in terms of entanglement and show the connection between entanglement and correlation energy, a quantity commonly used in quantum chemistry.

Chapter 5 deals with general aspects of classical information processing using quantum channels. Biological information processing takes place at the challenging regime where quantum meets classical physics. The majority of information in a cell is classical information which has the advantage of being reliable and easy to store. The quantum aspects enter when information is processed. Any interaction in a cell relies on chemical reactions, which are dominated by quantum aspects of electron shells, i.e. quantum mechanics controls the flow of information. I will give examples of biological information processing and introduce the concepts of classical-quantum (cq) states in biology. This formalism is able to keep track of the combined classical-quantum aspects of information processing. In more detail I will study information processing in DNA. The impact of quantum noise on the classical information processing is investigated in detail for copying genetic information. For certain parameter values the model of copying genetic information allows for non-random mutations. This is compared to biological evidence on adaptive mutations.

Chapter 6 gives the conclusion and the outlook.

Acknowledgements

I would like to acknowledge all the people who helped me in the past years. Thanks to everybody at CQT, because working here is just cool! And thanks to the small army of people proof-reading my thesis!

Giovanni: My office mate, for entertainment and teaching me the relaxed Italian style, and keeping swearing in office to a minimum.

Mile: My colleague and flat mate, for good discussions about Go and the world, and teaching me so many things.

Oli & Jing: My good friends, who got me out the science world and distracted me from my work, thanks for emotional support, patient Chinese teaching, and most importantly, constant supply of fantastic food!

Pauline & Paul: Thanks for a fantastic stay in Arizona, great discussions ranging from the beginning of the universe, to quantum effects in biological systems, to make-up tips and many more things.

Susanne: Thanks for sharing our PhD problems, I enjoyed our travelling.

Alexandra: Thanks for the great time we had, and sharing the post-PhD problems!

Janet: You have been a great mentor, friend, and colleague!

Karoline: I enjoyed working with you, thanks for the cool project!

Carmen & Daniel: Good friends ask you, upon arrival at 3am in the morning: Tea or coffee? Thanks for being that kind of friends, thanks for visiting me, and all the emotional support in the past years.

Andrea & Björn: Thanks for the good discussions and advices, from quantum mechanics to dating.

Markus B.: I enjoyed organising the conference with you, and some good German chatting.

Evon: Thanks for doing all the admin stuff! Without you none of my official documents would ever have been written.

Steph: I enjoyed the good discussions. Thanks for making me understand what I am doing.

Rami: Thanks for the disgusting Syrian tea and helping me to find a job!

Ivona: You have a great personality! I will miss chatting to you.

Artur: Thanks for good advice beyond physics. I appreciate drinking coffee with you.

Vlatko: You are a great supervisor! Thanks for giving me the liberty to research whatever I wanted to. And thanks for never attempting to make me smoke.

Alexander & Annabel & Amelie & Fabian & Katharina: Without all of you I would not have been able to do my PhD.

Gabriele & Walter Rieper: Ich danke Euch!

Contents

List of Figures ix

List of Tables xi

1 Introduction 1

1.1 Motivation . . . 1

1.2 The breakdown of the k_BT argument . . . 2

1.2.1 Non-equilibrium . . . 3

1.2.2 Entanglement . . . 4

1.3 Quantum enhanced processing of classical information . . . 4

1.3.1 Single particle - Coherence . . . 5

1.3.1.1 Ion channel . . . 6

1.3.1.2 Photosynthesis . . . 7

1.3.2 Two particles - Entanglement . . . 7

1.3.2.1 Avian compass . . . 8

1.3.3 Many particles - vibrations . . . 9

2 Avian Compass 11

2.1 Experimental evidence on European Robins . . . 12

2.2 The Radical Pair model . . . 12

2.2.1 Quantum correlations . . . 17

2.2.2 Pure phase noise . . . 19

2.3 Alternative Explanations - Critical Review . . . 22

3 Entanglement at the quantum phase transition in a harmonic lattice 25
3.1 Introduction . . . 25
3.2 The model . . . 27
3.3 Calculation of entanglement measures . . . 29
3.3.1 Thermodynamical limit ($N \to \infty$) . . . 33
3.4 Behaviour of entanglement at zero temperature . . . 34
3.4.1 Block Entropy . . . 36
3.5 Witnessing entanglement at finite temperature . . . 38
3.6 Conclusions . . . 40

4 Quantum information in DNA 41
4.1 Introduction . . . 41
4.2 Dispersion energies between nucleic acids . . . 43
4.3 Entanglement and Energy . . . 47
4.4 Aperiodic potentials and information processing in DNA . . . 50
4.5 Conclusions and discussion . . . 53

5 Information flow in biological systems 55
5.1 Information theory . . . 57
5.1.1 Channels - sending and storing . . . 58
5.1.2 Identity Channel . . . 59
5.1.3 More channel capacities . . . 60
5.1.4 Examples of information processing in biology . . . 62
5.1.5 Biology's measurement problem . . . 64
5.1.6 Does QM play a non-trivial role in genetic information processing? 66
5.1.7 Classical quantum states in genetic information . . . 67
5.1.8 Weak external fields . . . 70
5.2 Copying genetic information . . . 73
5.2.1 Mutations and its causes . . . 75
5.2.2 Tautomeric base pairing . . . 75
5.2.3 Non-coding tautomeric base pairing . . . 76
5.2.3.1 Double proton tunnelling . . . 77
5.2.3.2 Single proton tunneling . . . 78
5.2.4 The thermal error channel . . . 78

5.2.5 Channel picture of genetic information 80
5.2.5.1 Results for quantum capacity 87
5.2.5.2 Results for one-shot classical capacity 88
5.2.5.3 Results for entanglement assisted classical capacity C_E 89
5.3 Sequence dependent mutations 90
5.3.1 Codon bias 91
5.3.2 Adaptive mutations 93
5.4 A quantum resonance model 94
5.4.1 Directed generation or directed capture 96
5.4.2 Vibrational states of base pairs 98
5.4.3 Electron scattering 99
5.4.3.1 Excitation mechanism 104
5.4.4 The importance of selective pressure 104
5.5 Change or die! 105
5.6 Summary 108

6 Conclusions and Outlook **111**
6.1 Predictive power and QM 112
6.2 Life, levers and quantum biology 114

References **117**

List of Figures

1.1 Fourier Transform of a Cat 2
1.2 Double Slit 6
1.3 Ion channel 7
1.4 Avian compass 9

2.1 Spin Chemistry 13
2.2 Bird's retina 14
2.3 Effect of noise field 16
2.4 Noise and decoherence 17
2.5 Entanglement in avian compass 19
2.6 Pure Phase Noise 21

3.1 Sketch of harmonic lattice 28
3.2 Entanglement measures 35
3.3 Geometry of trapping potential 36
3.4 Block entropy 37
3.5 Negativity at finite temperature 39

4.1 Sketch of DNA's electron cloud 44
4.2 Single strand of DNA 45
4.3 Entanglement in DNA 48
4.4 Classical and quantum entropy for different sequences 52

5.1 Born-Oppenheimer approximation and information processing 56
5.2 General description of a channel 59
5.3 Classical one shot capacity 61

LIST OF FIGURES

5.4 Entanglement assisted capacity 62
5.5 DNA 63
5.6 Proton tunneling in cytosine 68
5.7 Genetic two level system 69
5.8 Noise induced errors 72
5.9 Base pairs in keto form 74
5.10 Base pairs in tautomeric form 76
5.11 Processing of a point mutation 77
5.12 Thermal excitation 1 80
5.13 Thermal excitation 2 80
5.14 Genetic Information Channel 82
5.15 Effective Temperature 87
5.16 One-shot classical capacity 89
5.17 Entanglement assisted classical capacity 90
5.18 Mutational hotspot in E. Coli 95
5.19 Mutation flow chart 96
5.20 Excitation model 97
5.21 Quantum Resonance Model 98
5.22 Vibrations for AT-AT pair 99
5.23 Proton distance AT-AT pair 100
5.24 Vibrations for CG-GC pair 100
5.25 Proton distance for CG-GC pair 101
5.26 Excitation probability 102
5.27 Comparison of thermal and resonant excitation mechanism 105
5.28 One-shot classical capacity for p and σ 107
5.29 Consequences of SDM 110

List of Tables

4.1 Polarizability of nucleic acids 46
4.2 Von Neumann entropy 53

5.1 Comparision 85
5.2 Codon Code 92

Previously published work

Large portions of Chapters 2 have appeared in the following paper:

> "Sustained quantum coherence and entanglement in the avian compass", E. M. Gauger, Elisabeth Rieper, J. J. L. Morton, S. C. Benjamin and V. Vedral, Phys. Rev. Lett. **106**, 040503 (2011).

Chapter 3 appears in its entirety as

> "Entanglement at the quantum phase transition in a harmonic lattice", Elisabeth Rieper, J. Anders and V. Vedral, New J. Phys. **12**, 025016 (2010).

Most of Chapter 4 is available as eprint

> "Quantum entanglement between the electron clouds of nucleic acids in DNA", Elisabeth Rieper, J. Anders and V. Vedral, arxiv 1006.4053 , (2010).

The eprint

> "Sharpening Occams Razor with Quantum Mechanics", M. Gu, K. Wiesner, Elisabeth Rieper and V. Vedral, arxiv 1102.1994 , (2011).

is submitted to journal.

The publications and eprints

> "Inadequacy of von Neumann entropy for characterizing extractable work", O. C. O. Dahlsten, R. Renner, Elisabeth Rieper and V. Vedral, New J. Phys. **13**, 053015 (2011).

and

"Information-theoretic bound on the energy cost of stochastic simulation", K. Wiesner, M. Gu, Elisabeth Rieper and V. Vedral, arXiv:1110.4217, (2011).

are not mentioned is this thesis.

LIST OF TABLES

1

Introduction

1.1 Motivation

Quantum effects are subtle. The fundamental unit of quantum mechanics has the very small value of $\hbar \approx 10^{-34} J/s$. In addition, quantum effects, like superposition and entanglement, are easily destroyed by interaction with the environment. This explains why we usually do not observe quantum effects in the macroscopic world [1]. A rule of thumb is the (in)famous $k_B T$ argument, stating that whenever the interaction energies are smaller than room temperature, quantum effects cannot persist. However, as quantum mechanical laws are fundamental, in special situations the consequences of quantum mechanics can be macroscopic. The explanation of the photoelectric effect (1) revealed the quantised nature of energy carriers (photons) and the importance of energy levels. But what about quantum effects in biology? For a long time the prevailing view was that in 'warm and wet' biological systems quantum effects cannot survive beyond the trivial, i.e. explaining the stability of molecules. In the first part of this introduction I will explain why the $k_B T$ argument fails. There might be similarities to the question how weak electrical and magnetic fields can have an influence on biological systems, see (2) for more details. In the second part I will briefly outline how quantum effects can be harnessed in biological systems. Examples include ion channels, photosynthesis and the olfactory sense, which are not covered in this thesis. I discuss in more detail

[1] It is a matter of taste what to classify as a quantum effect. Magnetism cannot be explained without spins, and is consequently also a quantum effect. However, Maxwell's equations provide an efficient classical description of magnetic fields. In this context 'quantum effects' describe phenomena which are unexpected given every day's life intuition.

the avian magneto reception and special mutagenic events in DNA. Also, Schrödinger's cat will not be rescued here, see fig. 1.1

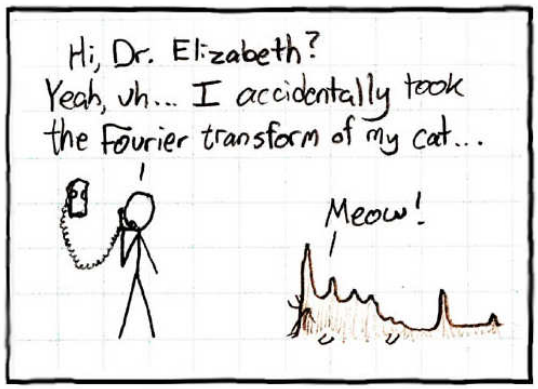

Figure 1.1: Xkcd web comic (http://imgs.xkcd.com/comics/fourier.jpg): The Schrödinger cat is usually assumed to be in a superposition state of the form of $|Alive\rangle + |Dead\rangle$. Thus a fourier transformation can potentially save its life. However, due to unforeseen complications, cat owners are advised not to use this method until further knowledge is available on the side effects of Fourier transforms on cats.

1.2 The breakdown of the k_BT argument

The k_BT argument is a mean-field argument that is very useful for many systems to estimate the possible impact of quantum mechanics on a given physical system. The most simplistic argument against quantum effects in biological systems is that life usually operates at $300-310K$, which is by far too hot to allow for quantum effects. Let me explain the argument in more detail to show where it breaks down when dealing with living systems. A physical system with given Hamiltonian $\hat{H}$ in thermal equilibrium is described by the density operator

$$\rho_{Thermal} = \frac{e^{-\beta\hat{H}}}{Z} = p_0|0\rangle\langle 0| + p_1|1\rangle\langle 1| + \dots \ , \tag{1.1}$$

where $\beta = \frac{1}{k_BT}$ denotes the inverse temperature, $|i\rangle$ the orthonormal basis of the Hamiltonian, $Z = Tr(e^{-\beta\hat{H}})$ and $p_i = \frac{e^{-\beta E_i}}{Z}$ the probability to be in state $|i\rangle$ with

corresponding energy E_i. If the energies $\{E_i\}$ are small compared to the temperature, then all probabilities are roughly equal, $p_i \approx \frac{1}{Z}$. Due to thermal fluctuations, it is impossible to predict which state $|i\rangle$ the system occupies, and thus the thermal state is the totally mixed state $\rho_T = \frac{\mathbb{1}}{d}$ with d the dimension of the Hilbert space. It is impossible to process any information with the maximally mixed state, as any unitary operation will leave the maximally mixed state unchanged. On the other hand, if the energies are very small compared to the temperature, then the k_BT argument presumes the system to be in its ground state. However, there are many situations where this line of argument fails, among them non-equilibrium dynamics, entanglement and effective temperatures in complex systems.

1.2.1 Non-equilibrium

Some quantum effects are sensitive to temperature. For quantum computing using ion traps or quantum dots, the systems have to be cooled to few Kelvin (3). But the thermal argument is only true for equilibrium states. Let us consider spin systems in more details. Electron spins have two possible states. For typical organic molecules, the energy difference between these two states is much smaller than thermal energy. At room temperature the spin is in a fully mixed state. Thus the quick conclusion is that spins cannot be entangled at room temperature. However, dynamical systems avoid the equilibrium state. It was shown theoretically that two spins, given a suitable cycling driving, can maintain their entanglement even at finite temperature and coupled to the environment (4). This is a good example to show how our intuition fails in non-equilibrium situations. Even though every thermal state in the parameter regime is separable, the non-thermal state passing along the parameter curve is not!

Another possibility is to use quantum effects before the system had time to equilibrate with the environment. In spin chemistry, a weak magnetic field, on the order of $1-10mT$ is shown to influence the rate of chemical reactions (5). This fields are incredibly weak compared to thermal noise, the ratio is around $\mu_B B/k_BT \approx 10^{-5}$. The only explanation how such weak fields can alter the outcome of chemical reactions is by manipulating the spins of the involved molecules. This is of fundamental importance for animal magneto reception. A species of birds, the European Robin, is believed to use this sort of electron entanglement to measure earth magnetic field (6) for navigation. This will be discussed in more detail in chapter 2.

1.2.2 Entanglement

Now there are two ways to fall off the horse, and the next system, van der Waals forces in DNA, shows how the k_BT argument fails in the other direction. Van der Waals bonding is one of the weakest chemical bonds and a special case of Casimir forces. As will be explained in more detail in chapter 4 and 5, DNA consists of a sequence of the four nucleic acids. The electron clouds of neighbouring sites have dipole-dipole interaction, resulting in an attractive van der Waals bonding. The coupling between nucleic acids leads to phonons with frequencies ω in the optical range. The interaction energies are thus large compared to thermal energy, $k_BT/\hbar\omega << 1$. The simple k_BT argument says that as the first excited state has so much more energy than thermally available, the DNA has to be in its electronic ground state. For each single uncoupled nucleic acids this is true, but the situation changes in a strand of DNA due to the coupling. The attractive part of the dipole dipole interaction reduces energy, and also creates entanglement between the π electron clouds of the bases. The electronic system is *globally* in the ground state. As a consequence of the global entanglement, the system has to be *locally* in a mixed state. It is impossible to distinguish with local measurements whether a local state is mixed due to temperature or due to entanglement. In chapter 4 it will be shown that entanglement creates local mixtures that correspond to more than $2000K$ of thermal energy.

1.3 Quantum enhanced processing of classical information

In the above paragraph I argued why quantum effects can exist in biological systems. Here I will show how they can be advantageous. The first two examples of biological systems, photosynthesis and ion channels, use coherence for transport problems. The other examples, avian compass, olfactory sense and DNA, deal with the determination of classical information using quantum channels. Spin correlations enable European robins to measure earth magnetic field. The interacting spins constitute quantum channels, which lead to the classical knowledge needed for navigation. In the olfactory sense a quantum channel, phonon assisted electron tunnelling, is employed to identify

different molecules. Finally, a quantum resonance phenomenon would in principle allow to address specific base pairs in specific genes, leading to the phenomena of non-random mutations.

1.3.1 Single particle - Coherence

Coherence effects play a fundamental role in transport problems, which is of importance for systems like ion channels or photosynthetic complexes (transferring electronic excitations).

Describing coherence keeps track of more information than just the probabilities to be in a certain state. Consider the most simple quantum state, a qubit,

$$\rho = \begin{pmatrix} p_0 & c_{01} \\ c_{10} & p_1 \end{pmatrix} \tag{1.2}$$

where p_i are the probabilities to be in state $|i\rangle$ and $c_{01} = c_{10}^*$ quantify the coherence $|0\rangle\langle 1|$ between the two states. While the p_i's can be directly measured, the coherences are more subtle. The state ρ will have a different time evolution for different values of c_{01}. This is known as interference effects. If $c_{01} = 0$, then the particle is in a mixture of states (either $|0\rangle\langle 0|$ or $|1\rangle\langle 1|$), which is unknown to the observer. If $c_{01} \neq 0$, then the particle can be in superposition of both states. While it is always possible to find a basis in which the state ρ is diagonal, some bases are intuitively preferred. In the case of the double slit experiment, see Fig. 1.2, this basis is the left ($|L\rangle$) and right ($|R\rangle$) path. In this experiment the key question is whether a single particle passes through either the left or right slit (no coherence), or both slits simultaneously (requires $|L\rangle\langle R|$ coherence terms). If there is no path coherence, the particle will go through either of the slits, and give rise to a classical pattern on the screen. With path coherence, the particle goes through both slits simultaneously and will interfere with itself giving rise to an interference pattern on the detector screen.

Coherence describes a particle's ability to exist in several distinct states simultaneously. These states can represent, for example, position, energy or spin. In case of position superposition, a particle can gather non-local information.

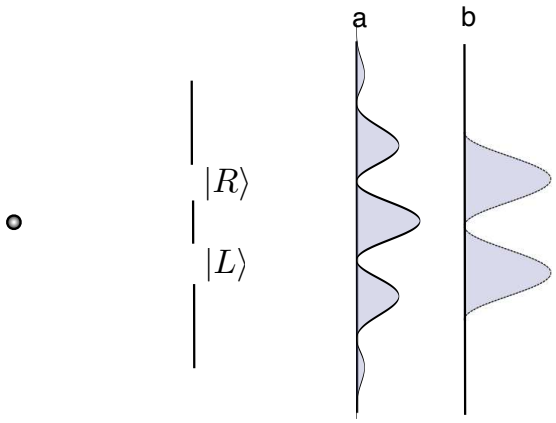

Figure 1.2: This graphic shows a typical double slit experiment. Photons are sent through the double slit, leading to either pattern a or b on the detection screen. If it can be known through which slit a photon passed, there exists no path coherence and the detection screen shows a classical pattern (b), with highest arrival probability directly behind the open slits. However, if no path information leaves the system, the photons fly through both slits simultaneously. This path coherence leads to the typical interference pattern (a). With coherence the photons can arrive at positions on the detector screen which are classically forbidden, i.e. in the centre of the screen. Because of this ability to change arrival destinations, interference effects are important for transport problems.

1.3.1.1 Ion channel

Coherence can be utilised in transport problems, because interference patterns are very sensitive to a couple of parameters, e.g. the mass of the particle. It is a standing conjecture (7) that interference effects might explain the efficiency of ion channels in cells.

For a cell or bacterium to function properly it needs to maintain a delicate balance of different ions inside and outside the cell. This non-equilibrium steady state is achieved with the use of ion pumps and channels. The problem for an ion channel is to be highly permeable for one species of ions, but tight for other ions. The potassium channel for example transmits around 10^8 potassium ions per second through the membrane, while only 1 in 10^4 transmitted ions is sodium. As both sodium and potassium ions carry the same charge, the key difference between the ions is their mass. It is thus postulated that the ion channels use interference effects leading to **ion selected transport**.

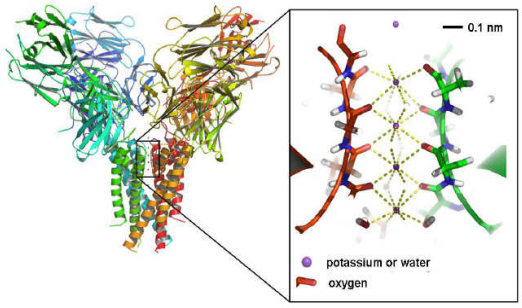

Figure 1.3: Schematic illustration of the KcsA postassium channel after PDB 1K4C taken from (7) . KcsA protein complex with four transmembrane subunits (left) and the selectivity with four axial trapping sites formed by the carbonyl oxygen atoms in which a potassium ion or a water molecule can be trapped. Path coherence along the trapping sites can lead to ion species selected transport.

1.3.1.2 Photosynthesis

The transport problem that received the most scientific attention is photosynthesis. After photon absorption the electron excitation needs to be transported to the reaction centre, where a chemical reaction converts the energy into sugar. It was shown experimentally at low temperatures that the photosynthetic complex FMO supports coherent transport over a short period (8). There are a number of papers investigating the details of the transport and the importance of coherence in the system. There is good numerical evidence that the existence of **coherence speeds up the transport** in the first part of the time evolution (see (9) and references therein). In the second part interaction with the environment decoheres the system. It turns out that this decoherence further speeds up the excitation transfer, as it keeps the system from being trapped in dark states.

1.3.2 Two particles - Entanglement

When discussing the behaviour of two particles, the most interesting point is the correlations between them. Quantum information typically distinguishes two kinds of correlations: classical correlations and entanglement. Entanglement is a strange quantum mechanical property that allows two or more particles to be stronger than classically correlated. This also means that while the global state is perfectly known, the local

state is fully mixed. Let us consider a spin singlet state in more detail. I ignore the thermal influence for now and focus on the properties of the ground state of the two particle system at zero temperature. The wavefunction is given by $|\psi\rangle = \frac{1}{\sqrt{2}}(|\uparrow\downarrow\rangle - |\downarrow\uparrow\rangle)$, or as a density operator

$$\rho = |\psi\rangle\langle\psi| = \frac{1}{2}\begin{pmatrix} 1 & 0 & 0 & -1 \\ 0 & 0 & 0 & 0 \\ 0 & 0 & 0 & 0 \\ -1 & 0 & 0 & 1 \end{pmatrix} \quad . \tag{1.3}$$

While this state looks somewhat similar to the above coherence example, there are distinct differences. The coherence terms in the corner show that the spins of **two** spatially separated electrons simultaneously are anti-correlated. That means that each individual electron has not a defined spin. Mathematically this is more clear when taking the partial trace of the state, i.e. write down the individual state (density operator) of a single electron

$$\rho_A = Tr_B|\psi\rangle\langle\psi| = \frac{1}{2}\begin{pmatrix} 1 & 0 \\ 0 & 1 \end{pmatrix} \quad , \tag{1.4}$$

which is the fully mixed state. As previously mentioned, the simple k_BT fails in the presence of entanglement. How can a single particle be in a fully mixed state at zero temperature? Also note, that when a single particle is entangled with another one, it cannot have the above described self-coherence. **Entanglement creates non-local correlations and non-thermal excitations.**

1.3.2.1 Avian compass

The field of spin chemistry investigates the influence of spin correlations between two spatially separated electrons on chemical reactions. There is experimental evidence (10, 11, 12) that a migrating species of birds, the European Robin, exploits this feature to navigate in Earth magnetic field. The ratio of Earth magnetic field energy to thermal energy is about $\mu_B 60\mu T/k_B 310K \approx 10^{-8}$. It is still puzzling for the scientific community how birds are able to detect this miniscule signal. For the avian compass to work, the spins of the two electrons need to be correlated. The easiest way to create the correlations is by using Pauli exclusion principle to initialise the two electrons in a singlet state. Coherent single electron photoexcitation and subsequent electron translocation leads to an entangled state, which provides the necessary spin

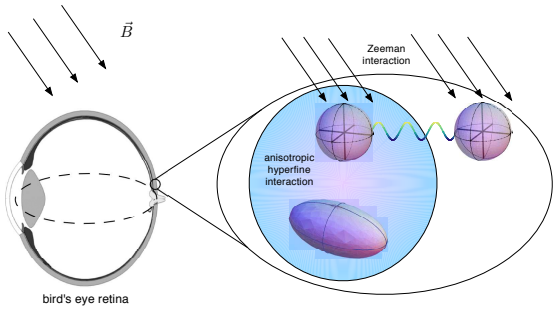

Figure 1.4: According to the RP model, the back of the bird's eye contains numerous molecules for magnetoreception (13). These molecules give rise to a pattern, discernible to the bird, which indicates the orientation of the field. In the simplest variant, each such molecule involves three crucial components (see inset): there are two electrons, initially photo-excited to a singlet state, and a nuclear spin that couples to *one* of the electrons. This coupling is anisotropic, so that the molecule has a directionality to it.

correlations. While both electron spins interact with earth magnetic field, one of them additionally interacts with a nuclear spin. This causes the state of the electrons to oscillate between singlets and triplets. After some time the excited states relax either in a singlet or triplet state, leading to different chemical end products. The required information about earth magnetic field is encoded in the oscillation frequency and can be recovered by detecting the relative amount of singlet or triplet chemicals. This will be covered in chapter 2.

1.3.3 Many particles - vibrations

For many particle systems vibrations are a common phenomenon. Vibrations, or phonons, describe the collective movement of many particles. Dependent on whether the movement of particles needs to be described by quantum or classical laws, the dynamics of vibrations is either quantum or classical. One characteristic parameter of vibrations is their frequency. Molecules have a unique spatial arrangement of atoms, linked by chemical bonds acting as springs. Each molecule thus has an individual set of characteristic vibrations. In the olfactory sense, experimental evidence supports the hypothesis that these vibrations are measured using phonon assisted electron transport (14, 15). Even though molecular vibrations can be described efficiently using classical methods, this mechanism still has a remarkable sensitivity to the quantum details of

a molecule. It has been demonstrated that fruit flies can distinguish between normal fragrant molecules and deuterium enriched molecules, although the molecules have a very similar shape.

In chapter 4 of this thesis I will investigate phonons in DNA. As a preparation for that, I will look at phonons in coupled harmonic oscillators in chapter 3. One conclusions of chapter 4 is that the electronic degree of freedom in DNA is delocalised even at body temperature. This insight will be of importance in chapter 5, where information flow in biological systems is investigated at a more abstract level.

In this thesis I propose to use classical-quantum (cq) states for describing information stored in DNA. The idea of cq states originates in quantum cryptography, where classical information is encoded in quantum degrees, for example in the polarization of photons. While cryptography aims at hiding information, biology faces the opposite problem of making genetic information easily accessible inside a cell. DNA consists of four nucleic acids; each nucleic acid encodes two bits of classical information. But how exactly is this information accessed? Contrary to computers, where classical transistors process the information, in a biological system everything depends on chemical reactions. But chemistry is nothing but the quantum physics of a molecule's electron shell and single protons. This motivates the use of quantum channels for storing and processing classical genetic information. There is a well developed mathematical framework for determining exactly how much quantum and classical information can be processed for a given physical system. In chapter 5 I will discuss how this concept can explain the experimental occurrence of non-random mutations.

Finally, in the last chapter, I will discuss two ideas about the consequences of quantum mechanics in biological system on a very general level.

2

Avian Compass

Many animals have a magnetic sense, which allows them to navigate in earth magnetic field. Examples include bacteria, sharks and birds (16). It is not yet fully understood which physical process allows these animals to measure earth magnetic field, which is very weak, around $B \approx 40\mu T$. Often the magnetic energy μB is equal or smaller than the thermal energy kT. This makes it a challenge to measure earth magnetic field against thermal noise. There are several mechanisms by which this sense may operate (16). In certain species (including certain birds (17, 18), fruit flies (19, 20) and even plants (21)), the evidence supports a so-called Radical Pair (RP) mechanism. This process involves the quantum evolution of a spatially-separated pair of electron spins (12, 17), and such a model is supported by several results from the field of spin chemistry (5, 6, 22, 23, 24). An artificial chemical compass operating according to this principle has been demonstrated experimentally (25), and a very recent theoretical study examines the presence of entanglement within such a system (26). In this chapter I consider the timescales for the persistence of full quantum coherence, and entanglement, within a specific living system: the European Robin. The analysis uses recent data from experiments on live birds. I conclude that the RP model implies a decoherence time in the birds' compass which is extraordinarily long – beyond that of any artificial molecular system.

2.1 Experimental evidence on European Robins

By manipulating a captive bird's magnetic environment and recording its response, one can make inferences about the mechanism of the magnetic sensor (10, 11, 12, 27). Specifically, European Robins are only sensitive to the inclination and not the polarization of the magnetic field (10), and this sensor is evidently activated by photons entering the bird's eye (11, 28). Importantly for the present analysis, a very small oscillating magnetic field can disrupt the bird's ability to orientate (12, 27). It is also significant that birds are able to 'train' to different field strengths, suggesting that the navigation sense is robust, and unlikely to depend on very special values for the parameter in the model (27).

2.2 The Radical Pair model

The basic idea of the RP model is as follows: there are molecular structures in the bird's eye which can each absorb an optical photon and give rise to a spatially separated electron pair in a singlet spin state, see Fig. 2.1. Because of the differing local environments of the two electron spins, a singlet-triplet evolution occurs. This evolution depends on the inclination of the molecule with respect to the Earth's magnetic field. Recombination occurs either from the singlet or triplet state, leading to different chemical end products. The concentration of these products constitutes a chemical signal correlated to the Earth's field orientation. The specific molecule involved is unknown, but the molecule cryptochrome is thought to be involved (32).

Making as few assumptions as possible about the detailed structure of the molecule, a family of models with the necessary complexity to support this RP mechanism is examined. The aim is to understand whether full quantum coherence and entanglement exist for long durations in the European Robin's compass system. Figure 2.2 depicts the most basic form of the model: two electronic spins (17) and one nuclear spin. The nucleus interacts with only one of the electron spins, thus providing the asymmetry required for singlet-triplet oscillations. In this model, as with the other models considered, I employ the Hamiltonian corresponding to the system once the two electrons have become separated. That is, $t = 0$ corresponds to the moment of RP formation.

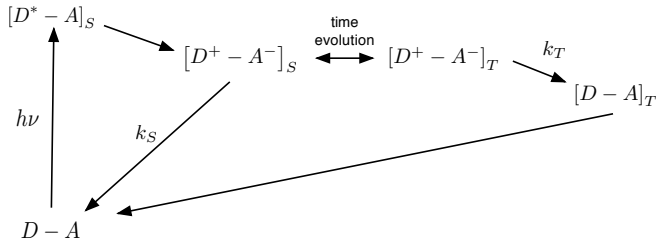

Figure 2.1: In a spin chemistry scenario a molecule consisting of a donor (D) and acceptor (A) part is initially in the electronic ground state, which constitutes a spin singlet state. A photon of energy $h\nu$ coherently excites one of the electrons. This excited electron moves from the donor to the acceptor part. Now the two spatially separated electrons interact with different local magnetic fields. While both electrons interact with earth magnetic field, one electron in addition interacts with a nuclear spin. This leads to an oscillation between singlet and triplet states. The time evolution of this oscillation depends on the angle with earth magnetic field. Both states decay with a rate constant of k_S or k_T into a singlet or triplet state. These two molecules can be chemically distinguished. The relative concentration of singlet to triplet molecules varies over the bird's retina, giving rise to a pattern that encodes the angle with earth magnetic field.

The anisotropic hyperfine tensor coupling the nucleus and electron 1, is conveniently written in its diagonal basis $A = \mathrm{diag}(A_x, A_y, A_z)$, and an axially symmetric (or cigar-shaped) molecule with $A_z = 10^{-5}$ meV and $A_x = A_y = A_z/2$ is assumed. This is the simplest assumption that can provide directionality, and the general shape and magnitude of the tensor is chosen to be consistent with (29). The Hamiltonian is

$$H = \hat{I} \cdot \mathbf{A} \cdot \hat{S}_1 + \gamma \mathbf{B} \cdot (\hat{S}_1 + \hat{S}_2),$$

where $\hat{I}$ is the nuclear spin operator, $\hat{S}_i = (\sigma_x, \sigma_y, \sigma_z)_i$ are the electron spin operators $(i = 1, 2)$, $\mathbf{B}$ is the magnetic field vector and $\gamma = \frac{1}{2}\mu_0 g$ the gyromagnetic ratio with μ_0 being Bohr's magneton and $g = 2$ the g-factor. The factor $1/2$ in the gyromagnetic ratio accounts for the fact that there is a spin one-half system, but here Pauli matrices such as $\sigma_z = \mathrm{diag}\{1, -1\}$ etc are used. Here only one electron is coupled to one nucleus, whereas the remote electron is so weakly interacting that it is described as free.

A family of variants involving different hyperfine tensors, adding a second nuclear spin (following previous studies where more than one nucleus couples to the system (6, 26, 27, 30)), and replacing the nuclear asymmetry with an anisotropic electron g-factor is also considered. These models, and the results of the corresponding simulations, are

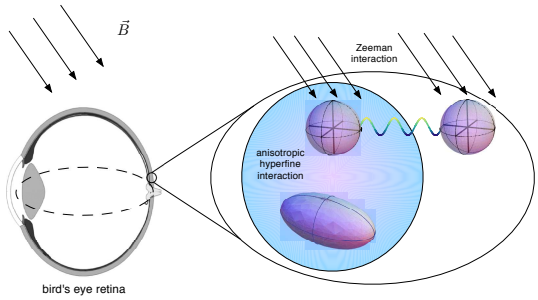

Figure 2.2: According to the RP model, the back of the bird's eye contains numerous molecules for magnetoreception (13). These molecules give rise to a pattern, discernible to the bird, which indicates the orientation of the field. Note that this implies that the molecules involved are at least fixed in orientation, and possibly ordered with respect to one another (17). In the simplest variant, each such molecule involves three crucial components (see inset): there are two electrons, initially photo-excited to a singlet state, and a nuclear spin that couples to *one* of the electrons. This coupling is anisotropic, so that the molecule has a directionality to it.

presented in (31). In essence all models give rise to the same qualitative behavior as the basic model described here. This is not surprising since there is a basic underlying principle: The electron spins of the RP must be protected from an irreversible loss of quantum coherence in order to be susceptible to the experimentally applied RF field. The extremely low strength of this applied field dictates the timescale over which quantum coherence must be preserved. Thus the inference of extraordinarily long coherence times does not vary significantly over the various models.

Generally, the magnetic field is

$$\begin{aligned} \mathbf{B} &= B_0(\cos\varphi\sin\vartheta, \sin\varphi\sin\vartheta, \cos\vartheta) \\ &+ B_{\mathrm{rf}}\cos\omega t(\cos\phi\sin\theta, \sin\phi\sin\theta, \cos\theta), \end{aligned} \tag{2.1}$$

where $B_0 = 47\ \mu$T is the Earth's magnetic field in Frankfurt (27), and the angles describe the orientation of magnetic field to the basis of the HF tensor. $B_{\mathrm{rf}} = 150$ nT is an additional oscillatory field only applied in the simulations where explicitly mentioned. For resonant excitation with the uncoupled electron spin, $\hbar\omega = 2\gamma B_0$, so that $\nu = \omega/(2\pi) = 1.316$ MHz.

The axial symmetry of the HF tensor allows to set $\varphi = 0$ and focus on ϑ in the range $[0, \pi/2]$ without loss of generality. For the oscillatory field I set $\phi = 0$.

To model the dynamics of the system with a quantum master equation (ME) approach, two 'shelving states' to the 8 dimensional Hilbert space of the three spins are added. I employ Operators to represent the spin-selective relaxation into the singlet shelf $|S\rangle$ from the electron singlet state, or the triplet shelf $|T\rangle$ from the triplet configurations. One of the two events will occur, and the final populations of $|S\rangle$ and $|T\rangle$ give the singlet and triplet yield.

With the usual definition of singlet $|s\rangle$ and triplet states $|t_i\rangle$ in the electronic subspace, while $|\uparrow\rangle$ and $|\downarrow\rangle$ describe the states of the nuclear spin, the following decay operators are defined: $P_{S,\uparrow} = |S\rangle\langle s,\uparrow|$, $P_{T_0,\uparrow} = |T\rangle\langle t_0,\uparrow|$, $P_{T_+,\uparrow} = |T\rangle\langle t_+,\uparrow|$, $P_{T_-,\uparrow} = |T\rangle\langle t_-,\uparrow|$, and similarly for the 'down' nuclear states. This gives a total of two singlet and six triplet projectors to discriminate the respective decays with a standard Lindblad ME,

$$\dot{\rho} = -\frac{i}{\hbar}[H,\rho] + k\sum_{i=1}^{8} P_i\rho P_i^\dagger - \frac{1}{2}P_i^\dagger P_i\rho + \rho P_i^\dagger P_i \ . \tag{2.2}$$

For simplicity and because this choice corresponds exactly to the expression for the singlet yield used in the previous literature, all eight projectors have been assigned the same decay rate k. Note that Eqn. (2.2) does not yet contain environmental noise, though this will not alter the estimate of k.

In the previous literature it has been common to employ a Liouville equation to model the RP dynamics. In fact, a term-by-term comparison of the evolution of the density matrix readily confirms that this former approach and this ME are exactly equivalent in the absence of environmental noise. For equal singlet and triplet reaction rates, both give rise to the same singlet yield that is often defined as the integral $\Phi = \int_0^\infty \langle\psi^-|Tr_n(\rho(t))|\psi^-\rangle k e^{-kt} dt$ in the prior literature. Specifically, the ultimate population of this singlet shelf $|S\rangle$ corresponds to Φ. However, when one presently wishes to introduce various kinds of noise operators, the ME approach provides the more intuitive framework.

The initial state of the model ρ_0 assigns a pure singlet state to the electrons, and a completely mixed state to the nucleus, $\rho(0) = (|s,\downarrow\rangle\langle s,\downarrow| + |s,\uparrow\rangle\langle s,\uparrow|)/2$.

In the next step an appropriate choice for the parameter k in Eqn. 2.2 is determined. In Ref. (27), the authors report that a perturbing magnetic field of frequency of 1.316 MHz (i.e. the resonance frequency of the 'remote' electron) can disrupt the avian

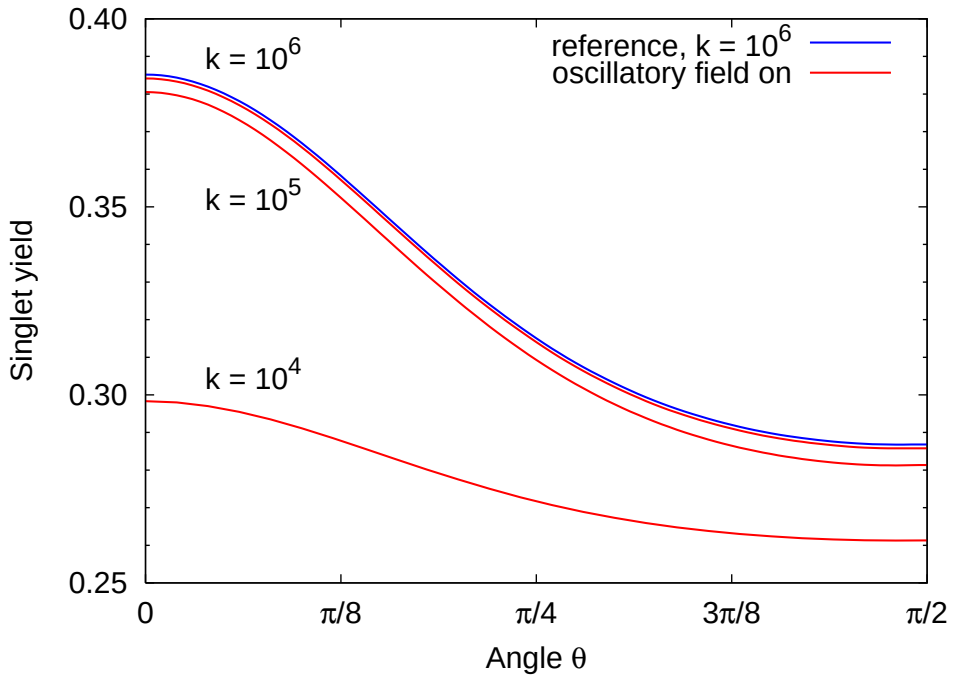

Figure 2.3: Angular dependence of the singlet yield in the presence of an oscillatory field. The blue curve provides a reference of the singlet yield in the Earth's magnetic field ($B_0 = 47\mu$T). The reference is independent of the decay rate for $k \leq 10^7$ s^{-1}, but has been shifted upwards by 0.001 for better visibility. The red curves show the singlet yield when a 150 nT field oscillating at 1.316 MHz (i.e. resonant with the Zeeman frequency of the uncoupled electron) is superimposed perpendicular to the direction of the static field. This only has an appreciable effect on the singlet yield once k is of order 10^4 s^{-1}.

compass. They note that this immediately implies a bound on the decay rate k (since the field would appear static for sufficiently rapid decay). Here the aim is to refine this bound on k by considering the oscillating magnetic field *strength* which suffices to completely disorient the bird's compass, i.e. 150 nT. (Indeed, even a 15 nT field was reported as being disruptive, but to be conservative in the conclusions the larger value is taken here.) To model this effect, the oscillatory field component defined in Eqn. 2.1 is activated and the singlet yield as a function of the angle between the Earth's field and the molecular axis is examined. Consistent with the experimental work, it is found that there is no effect at such weak fields when the oscillatory field is parallel to the Earth's field. Therefore the oscillatory field is set to be perpendicular. The results are

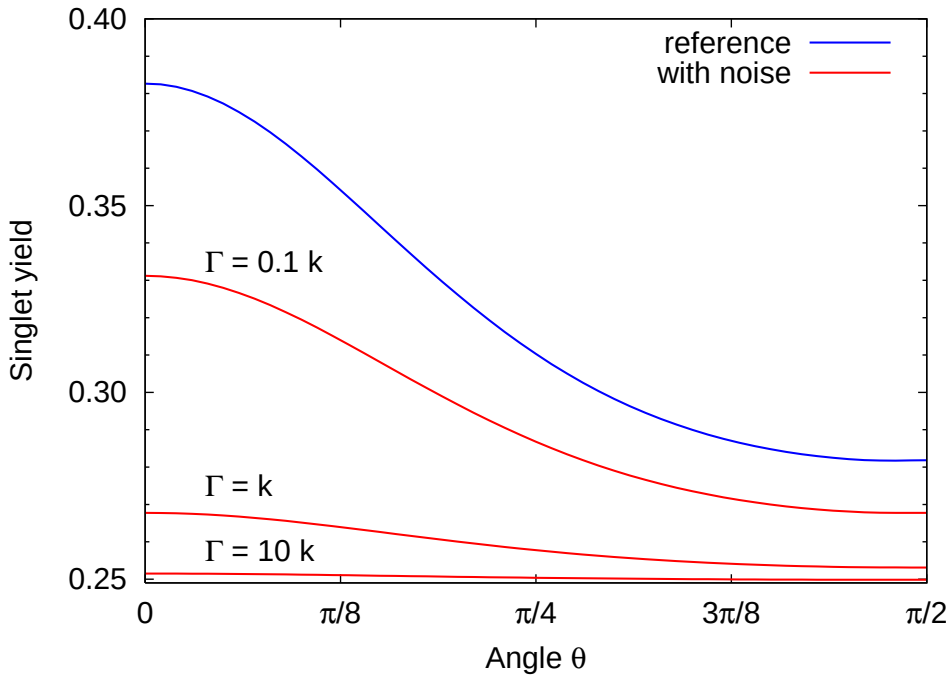

Figure 2.4: Angular dependence of the singlet yield in the presence of noise (for $k = 10^4/s$). The blue curve provides a reference in the absence of noise and the red curves show the singlet yield for different noise rates. As is apparent from the plot a noise rate $\Gamma > 0.1k$ has a dramatic effect on the magnitude and contrast of the singlet yield.

shown in Figure 2.3. I conclude that if the oscillating field is to disorient the bird, as experiments showed, then the decay rate k should be approximately 10^4 s^{-1} or less. For higher values of k (shorter timescales for the overall process) there is no time for the weak oscillatory field to significantly perturb the system; it relaxes before it has suffered any effect. Such a value for the decay rate is consistent with the long RP lifetimes in certain candidate cryptochrome molecules found in migratory birds (32).

2.2.1 Quantum correlations

Taking the value $k = 10^4$ s^{-1}, the primary question of interest is targeted: how robust this mechanism is against environmental noise. There are several reasons for decoherence, e.g. dipole interactions, electron-electron distance fluctuations and other particles' spin interactions with the electrons. Such environmental noise is described

by extending Eqn. 2.2 with a standard Lindblad dissipator

$$\dot{\rho} = -\frac{i}{\hbar}[H,\rho] + k\sum_{i=1}^{8} P_i\rho P_i^\dagger - \frac{1}{2}P_i^\dagger P_i\rho + \rho P_i^\dagger P_i + \sum_i \Gamma_i\left(L_i\rho L_i^\dagger - \frac{1}{2}\left(L_i^\dagger L_i\rho + \rho L_i^\dagger L_i\right)\right) \quad (2.3)$$

This is a general formalism for Markovian noise. Several noise models are considered: first, a physically reasonable generic model in which both phase and amplitude are perturbed with equal probability. In this model, the noise operators L_i are σ_x, σ_y, σ_z for each electron spin individually (i.e. tensored with identity matrices for the nuclear spin and the other electron spin). This gives a total of six different noise operators L_i and the same decoherence rate Γ is used for all of them. The level of noise which the compass may suffer can be approximated, by finding the magnitude of Γ for which the angular sensitivity fails.

This is shown in Fig. 2.4. Conservatively, when $\Gamma \geq k$, the angular sensitivity is highly degraded. This is remarkable, since it implies the decoherence time of the two-electron compass system is of order 100 μs or more [1]! To provide context for this number, the best laboratory experiment involving preservation of a molecular electron spin state has accomplished a decoherence time of 80 μs (33).

It is interesting to characterise the duration of quantum entanglement in this living system. Having inferred approximate values for the key parameters, entanglement from the initial singlet generation to the eventual decay can be monitored. The metric I use is negativity: $N(\rho) = ||\rho^{T_A/2}||$, where $||\rho^{T_A}||$ is the trace norm of the partial transpose of the system's density matrix. The transpose is applied to the uncoupled electron, thus performing the natural partitioning between the electron, on one side, and the coupled electron plus its nucleus, on the other. Fig. 2.5 shows how this negativity evolves under the generic noise model. Clearly, the initial singlet state is maximally entangled. Under noise, entanglement falls off at a faster rate than the decay of population from the excited state.

[1] One could assume the bird to be more easily perturbed by the oscillatory field (Fig. 2.3), and obtain a larger k. However, that same assumption of high sensitivity should then be applied to the noise analysis (Fig. 2.4) and in fact the two assumptions would cancel to give the same basic estimate for the decoherence rate. This cancellation is robust, being valid over an order of magnitude in k.

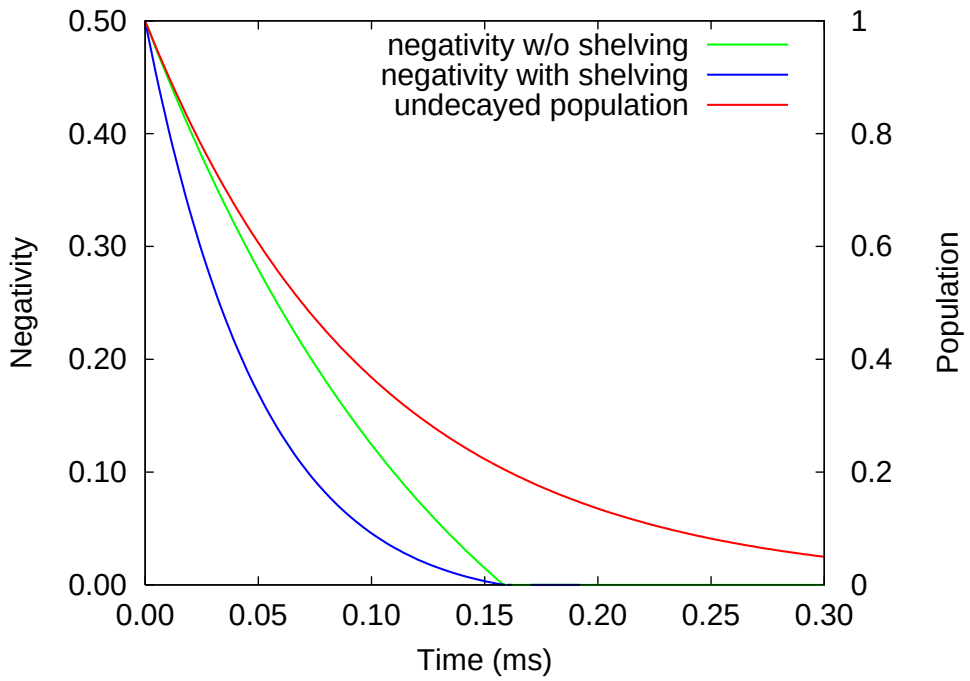

Figure 2.5: The decline and disappearance of entanglement in the compass system, given the parameter k and the noise severity Γ defined above. Here the angle between the Earth's field and the molecular axis is $\pi/4$, although the behavior at other angles is similar.

2.2.2 Pure phase noise

Interestingly, if the simulation starts with a completely dephased state: $(|s\rangle\langle s| + |t_0\rangle\langle t_0|)/2$, the classical correlations are still sufficient for achieving adequate angular visibility and neither quantum phase coherence nor entanglement seems to be a prerequisite for the efficiency of the avian compass.

To explore this idea further, the effect of 'pure dephasing' occurring *during* the singlet-triplet interconversion is studied. In essence energy conserving noise operators, Eqn. (2.4) are used, which are known to be the dominant source of decoherence in so many other artificially made quantum systems. By applying this specific noise, it is confirmed that the compass mechanism's performance is essentially immune, while of course the coherence of the quantum state of the electrons would be degraded.

One might be inclined to conclude that, if pure dephasing noise is indeed dominant, then the avian compass need not protect quantum coherence for the long time scales

suggested above. But crucially, it is also shown that if such noise were naturally present at a high level in the compass (exceeding the generic noise level Γ by more than an order of magnitude) then it would render the bird immune to the weak oscillatory magnetic fields studied by Ritz *et al.* (34). Thus the sensitivity to oscillatory fields implies that both amplitude and phase, and thus entanglement, are indeed protected within the avian compass on timescales exceeding tens of microseconds.

Since the electron spin singlet state is not an eigenstate of the Hamiltonian, the dephasing operators will be different from the ones mixing the phase of the singlet and triplet state within the electronic subspace. Instead, the previously defined noise operators of L_i of Eq. (3) are replaced by appropriate dephasing operators as follows: the remote electron and the electron nuclear spin subsystem are treated separately. Within both subsystems, dephasing operators are defined as

$$\begin{aligned} Z_i &= \frac{1}{\sqrt{2}}\left(\sum_{j\neq i} |\lambda_j\rangle\langle\lambda_j| - |\lambda_i\rangle\langle\lambda_i|\right) \\ &= \frac{1}{\sqrt{2}}\left(I_4 - 2|\lambda_i\rangle\langle\lambda_i|\right), \end{aligned} \tag{2.4}$$

where $\{|\lambda_i\rangle\}$ are the set of normalised eigenvectors of this subsystem. This results in two dephasing operators for the remote electron (these can be combined to a single σ_z operator rotated with the field) and four operators for the electron nuclear spin subsystem. Each of these dephasing operators corresponds to fluctuations of one of the (subsystem's) energy levels.

Strikingly, the singlet yield is entirely unaffected by this particular kind of noise, i.e. it is entirely independent of the dephasing rate Γ_z. Thus, a curve obtained with this model coincides perfectly with the reference curve of Fig. 2.3. However, I show in the following that the dephasing rate of this model can be at most ten times faster than the generic noise rate to retain sensitivity to the oscillatory field. Fig. 2.6 shows the singlet yield as a function of θ for different pure dephasing rates Γ_z. Pure phase noise would actually *protect* the compass from the harmful effect of an applied oscillatory field (by suppressing the Rabi oscillations caused by such a field). We see that an aggressive pure dephasing rate of $1/\Gamma_z = 10$ μs almost completely recovers the reference curve (corresponding to a noise-free system without oscillatory field).

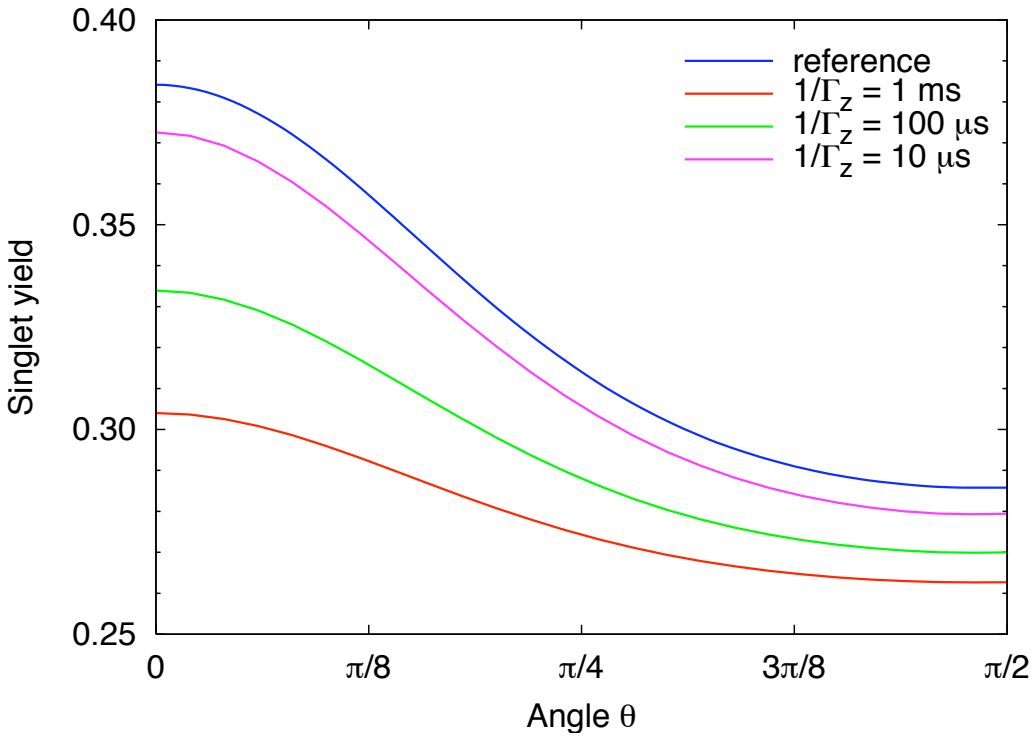

Figure 2.6: Angular dependence of the singlet yield at $k = 10^4$ s^{-1} in the presence of the oscillatory field for different pure dephasing rates Γ_z. This is to be compared with the $k = 10^4$ s^{-1} line in Fig. 2.3. See text for an explanation.

2.3 Alternative Explanations - Critical Review

The conclusions of this chapter seem indeed remarkable. Throughout the calculation a value of $150nT$ for the amplitude of the noise magnetic field was used. Indeed, disruption of magneto reception was reported even for $15nT$. This value would lead to even longer coherence times. The estimated duration of the coherence is surprising, especially as the model does not explain why such a long coherence time would be advantageous. One might assume that the radical pair sensor is extremely sensitive to minute changes in the magnetic field. This general statement, however, would be in contradiction with the experimental evidence that the European Robin's sense of magneto reception is not disturbed when the oscillating field is orthogonal to earth magnetic field. More precisely, it could be that the radical pair magneto receptor is exquisitely sensitive to tiny changes non-orthogonal to earth magnetic field. This requires that the interaction of the sensor with the weak oscillating noise effect is of the same order of magnitude as the interaction with the static field. As the amplitude of the noise field is at least 2 orders of magnitude smaller than the static field, this would either imply disproportionately insensitive interaction with the static field, which seems unlikely given that this detector evolved for detecting static fields of the order of earth magnetic field. Or, the detector interacts disproportionally strongly with oscillating fields at $1.3MHz$. At first sight this seems irrelevant for a bird's evolution. However, such a quantum resonance effect, which interacts disproportionally strongly with a small range of frequencies, might have evolved accidentally. As oscillating fields of this frequency are rare in natural conditions, a hypothetical detector having this sensitivity would not suffer bad side effects. Additionally, the frequency of $1.3MHz$ corresponds to the resonance frequency of a free electron spin, which supports the hypothesis of accidental evolution. While it is not impossible for such a detector to evolve, this model still does not explain the need for such sensitivity. Even worse, the paragraph on pure phase noise indicates that the radical pair detector has to be shielded well from environmental phase noise for keeping the sensitivity to weak oscillating fields. Given that the required long coherence time for such a quantum resonance effect is very difficult to achieve with lab methods, this answer, although possible, is still not very satisfying, and the search for alternative explanations should continue. On the one hand, it is desirable to find a theoretical model explaining why a long coherence time

would be beneficial for a static magnetic field detector. On the other hand, one should explore whether the reported loss of orientation of European Robins in the presence of weak oscillating fields might be caused not by the noise field - detector interaction, but some other physical effect inside the birds. It is still not fully understood how the birds process the presumed singlet - triplet pattern on their retina. It cannot be ruled out that the signal of earth magnetic field is corrupted in a subsequent part of the information processing.

3

Entanglement at the quantum phase transition in a harmonic lattice

The entanglement properties of the phase transition in a two dimensional harmonic lattice, similar to the one observed in recent ion trap experiments, are discussed both, for finite number of particles and thermodynamical limit. We show that for the ground state at the critical value of the trapping potential two entanglement measures, the negativity between two neighbouring sites and the block entropy for blocks of size 1, 2 and 3, change abruptly. Entanglement thus indicates quantum phase transitions in general; not only in the finite dimensional case considered in (35). Finally, I consider the thermal state and compare its exact entanglement with a temperature entanglement witness introduced in (36)

3.1 Introduction

Coupled harmonic chains with short and long range interactions are ubiquitous in science and engineering. Their application to calculate the phononic heat capacity by Einstein (37) marks the birth of solid state physics. Beyond physics, harmonic chains feature in chemistry and biology, where they are used to model behaviour of macromolecules, such as DNA (38) and cell membranes (39). In the last decade harmonic systems have been revised using techniques developed in quantum information science

to study correlation properties in the quantum regime and particularly at small temperatures (40, 41, 42, 43). Thermodynamics has been very successful in characterising "standard" phase transitions that occur at finite temperature when a macroscopic parameter, such as pressure, is changed (44). Quantum phase transitions (QPTs) appear at zero temperature (45) and are due to the change of an external parameter, such as the trapping potential of an ion trap. These transitions are driven by quantum fluctuations and have been linked to entanglement for the case of finite dimensional systems (35, 46).

Here I study a QPT in a continuous variable system: a system of trapped ions which I model as a harmonic lattice (36, 47). The ions interact via a long-range Coulomb repulsion and are trapped by two external potentials, see Fig. 3.1. They align in a linear configuration for big enough transversal trapping potential, ν_t however when ν_t is decreased the system undergoes a phase transition and the new equilibrium state forms a zig-zag configuration. This model is motivated by ion trap experiments (48, 49, 50), where such a QPT occurs (51, 52). Recent analytical studies of the transition using Landau theory (53) allowed to determine the system's classical behaviour at the transition point. Moreover, the numerical treatment of the quantised system of a few ions promised the possibility of simulating linear and nonlinear Klein-Gordon fields on a lattice (54). However, a comprehensive analytical study of the quantised system has so far been lacking due to the complexity of the system.

Here I model the ion trap scenario as a lattice of harmonically coupled oscillators and present a quantitative characterization of the entanglement inherent in both ground state configurations of the ions. For finite dimensional systems QPTs of first (second) order are characterised by a discontinuity (a discontinuity in or divergence of the first derivative) of the negativity (35). I show that also in the here considered continuous variable system the structure of entanglement, measured by the negativity and the von Neumann entropy, changes abruptly at the critical point and indicates the occurrence of a QPT, in a similar way as classical correlations indicate standard phase transitions. The first derivative of the negativity between two neighbouring ions has a finite discontinuity and the von Neumann entropy of contiguous blocks of a single ion, two and three ions all show a divergence in the first derivative. The long-ranged nature of the Coulomb interaction leads to an increase of the block entropy with increasing block size. This is in contrast to models with only nearest neighbour interaction where

'area laws' apply (55) and entanglement does not increase with block size, i.e. volume, as long as the surface of the block is constant. However, the results show that the increase in block entropy with the block size is quite small due to the fast decline of the Coulomb potential.

The quantum fluctuations that cause the QPT are most dominant at zero temperature. However, as experiments are performed at small, but finite temperatures it is important to know how temperature affects these fluctuations (56). In the final part I discuss thermal states and find that the sharpness of the QPT, indicated by the entanglement, fades out with increasing temperature. Another macroscopic consequence of quantum fluctuations is the lowering of the energy of the system (36). I compute up to which temperature the thermal state has a lower energy than any separable state. This temperature witness could be implemented in an ion trap experiment by measuring the average energy (i.e. mean excitation). Although the model is motivated by ion traps realisations include the vibrational motion of molecules (38) (nuclei in the electronic potential) and optical lattices (57).

3.2 The model

I consider the Hamiltonian, see Fig. 3.1,

$$H(\nu_t) = \sum_{j=1}^{N} \left(\frac{p_{x_j}^2 + p_{y_j}^2}{2m} + \frac{m\nu^2}{2}(\tilde{x}_j - \tilde{x}_{j,0})^2 + \frac{m\nu_t^2}{2}\tilde{y}_j^2 + V_j \right), \tag{3.1}$$

where $V_j = \frac{1}{2}\sum_{k\neq j} \frac{Q^2}{|\vec{r}_k - \vec{r}_j|}$ are the Coulomb potentials of the sites with $\vec{r}_j = (\tilde{x}_j, \tilde{y}_j)$ absolute coordinates of the sites and $\tilde{x}_{j,0}$ are the equilibrium positions in x direction. N is the number of particles, Q is the charge of the ions and ν (ν_t) are the trapping potentials in x (y) direction. I assume periodic boundary conditions, $\vec{r}_j = \vec{r}_{j+N}$.

To calculate the entanglement measures I approximate the Coulomb potential to second order and expand about the equilibrium positions. The key step is then to diagonalise the Hamiltonian into a set of uncoupled modes, the lattice vibrations, with which analytic expressions for the measures can be obtained. Similar to the classical calculation (53), I use a simplified model with equidistant equilibrium position in x direction, spaced by the lattice constant a. Such condition can be realised for the central ions of a long ion chain inside a linear Paul trap (58) or for ions confined in a ring of large radius (51, 59).

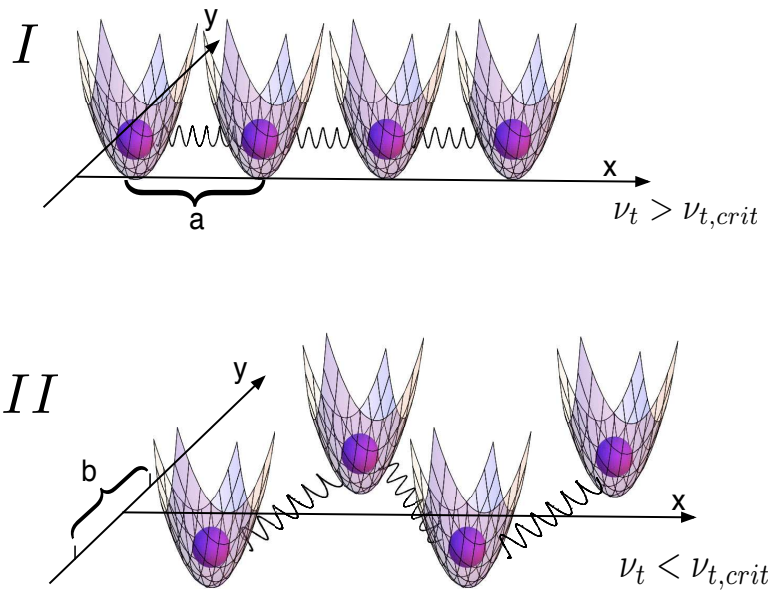

Figure 3.1: Sketch of the harmonic lattice under consideration: Each site is trapped by two external potentials, ν in x direction and ν_t in y direction. For clearness only the nearest neighbour coupling is indicated, however all ions interact via a long-range potential which we approximate harmonically. This could be for instance a Coulomb potential such as is common in ion experiments. The equilibrium distances between the sites are assumed to be equidistant, with lattice constant a in x-direction and b along the y-direction. In I, the transverse trapping potential ν_t is larger than the critical value and the ions arrange linearly. As displayed in II, decreasing the transverse trapping potential below the critical value $\nu_{t,crit}$ leads to a QPT causing the ions to move outwards and form a two-dimensional zig-zag structure.

For big trapping potential the sites are arranged on a single line, i.e. $\tilde{x}_{j,0} = a\,j$ and $\tilde{y}_{j,0} = 0$, while for small enough ν_t, the equilibrium positions become $\tilde{x}_{j,0} = a\,j$ and $\tilde{y}_{j,0} = (-1)^j \frac{b}{2}$ and a two-dimensional zig-zag configuration is formed. The equation determining the deviation b in y direction is obtained by summing the linear terms over all sites and requiring it to vanish,

$$\frac{1}{2} m \nu_t^2 = Q^2 \sum_{\tau=2l+1} \frac{1}{\sqrt{\tau^2 a^2 + b^2}^3}, \tag{3.2}$$

where $\tau = k - j$ numbers the neighbours of each sites. The harmonically approximated

Hamiltonian becomes

$$H = \sum_{j=1}^{N} \left(\frac{p_{xj}^2 + p_{yj}^2}{2m} + \frac{m\nu^2}{2} x_j^2 + \frac{m\nu_t^2}{2} y_j^2 \right) \tag{3.3}$$
$$+ \frac{Q^2}{2} \sum_{j=1}^{N} \sum_{\tau>0} \left(d_\tau^x \, (x_j - x_{j+\tau})^2 + d_\tau^y \, (y_j - y_{j+\tau})^2 + d_\tau^{xy} \, (x_j - x_{j+\tau})(y_j - y_{j+\tau}) \right),$$

with $x_j = \tilde{x}_j - \tilde{x}_{j,0}$ and $y_j = \tilde{y}_j - \tilde{y}_{j,0}$ the deviations from equilibrium. Furthermore, the $d_{x,y,xy}$ denote the second order Taylor coefficients of the Coulomb potential which are, for the linear and zig-zag configuration,

$$d_\tau^x = \frac{1}{(a\,\tau)^3} \quad \text{and} \quad d_\tau^x = \frac{2\tau^2 a^2 - \delta_{\tau,odd}\, b^2}{2\sqrt{(\tau a)^2 + \delta_{\tau,odd}\, b^2}^5}, \tag{3.4}$$

$$d_\tau^y = -\frac{1}{2(a\tau)^3} \quad \text{and} \quad d_\tau^y = \frac{2\delta_{\tau,odd}\, b^2 - \tau^2 a^2}{2\sqrt{(\tau a)^2 + \delta_{\tau,odd}\, b^2}^5}, \tag{3.5}$$

$$d_\tau^{xy} = 0 \quad \text{and} \quad d_\tau^{xy} = \delta_{\tau,odd}\, (-1)^j \frac{3\tau a b}{2\sqrt{(\tau a)^2 + b^2}^5}. \tag{3.6}$$

3.3 Calculation of entanglement measures

I am interested in the behaviour of the entanglement between the sites in the chain for varying transverse trapping potential, ν_t, and particularly at the point of criticality, $\nu_{t,crit}$. I calculate the *negativity*, E_N, for two modes regardless of all others, for instance, the x degrees of freedom of two (neighbouring) sites. To measure the correlation of one mode with all other modes, for instance the entanglement between the y degree of freedom of a single site or block of sites with all the other degrees of freedom in the chain, the *von Neumann entropy*, S_V, is used. Other entanglement measures are available, such as the entanglement of formation (60). Yet they are very hard to calculate in this continuous variable scenario and I will be content with the two measures as stated. To see the effect of the long-range interaction I compare the full long-range (LR) Coulomb Hamiltonian with a cut-off version in which only nearest neighbours interact (NN) and the interaction with more distant neighbours is set to zero.

For the *linear configuration* the Hamiltonian decouples into x and y parts. A discrete Fourier transformation for the x (similar in y direction) of the form

$$x_j = \frac{1}{\sqrt{N}} \sum_{l=1}^{N} e^{i\frac{2\pi}{N} jl} X_l \;\text{ and }\; p_{xj} = \frac{1}{\sqrt{N}} \sum_{l=1}^{N} e^{-i\frac{2\pi}{N} jl} P_{xl} \;, \tag{3.7}$$

maps the space coordinates of the sites into diagonal modes, the lattice vibrations or phonons. The diagonal Hamiltonian is then $H = \sum_{l=1}^{N} \hbar\omega_{xl} \left(\hat{n}_{xl} + \frac{1}{2}\right) + \sum_{l=1}^{N} \hbar\omega_{yl} \left(\hat{n}_{yl} + \frac{1}{2}\right)$ where $\hat{n}_{xl} = \frac{P_{xl}^{\dagger} P_{xl}}{2\hbar m\omega_{xl}} + \frac{m\omega_{xl} X_l^{\dagger} X_l}{2\hbar} - \frac{1}{2}$, and similarly $\hat{n}_{yl}$, are the number operators in x and y direction for mode l, and the frequencies are

$$\omega_{xl} = \sqrt{\nu^2 + C \sum_{\tau>0} \frac{\sin^2\left(\frac{\pi l\tau}{N}\right)}{\tau^3}} \text{ and } \omega_{yl} = \sqrt{\nu_t^2 - \frac{C}{2} \sum_{\tau>0} \frac{\sin^2\left(\frac{\pi l\tau}{N}\right)}{\tau^3}} \tag{3.8}$$

where $C = \frac{4Q^2}{ma^3}$. The asymmetry of the system is reflected in the dispersion relations. ω_{xl} is always real, whereas ω_{yl} would become complex for small values of transverse trapping potential ν_t. This is where the quantum phase transition occurs. The critical value $\nu_{t,crit}$ for LR interaction is $\nu_{t,crit} \approx \sqrt{0.6C}$ while for NN interaction it is $\nu_{t,crit} = \sqrt{0.5C}$.

To diagonalise the Hamiltonian in the emerging *zig-zag configuration*, where the previously independent phonons now couple in $x-y$-direction, see Eq. (3.3), I need to amend the transformation in the y direction Eq. (3.7) and transform with

$$y_j = \frac{i}{\sqrt{N}} \sum_l e^{i\frac{2\pi}{N} j(l+N/2)} Y_l \text{ and } p_{yj} = \frac{i}{\sqrt{N}} \sum_l e^{-i\frac{2\pi}{N} j(l+N/2)} P_{yl}. \tag{3.9}$$

The additional factor $e^{i\pi j} = (-1)^j$ compensates the alternating sign of the $x-y$ coupling in the Hamiltonian. Expressed with a coupling matrix

$$M_l = \begin{pmatrix} \frac{m}{2}\tilde{\omega}_{xl}^2 & 0 & \frac{m}{2}\tilde{\omega}_{xyl} & 0 \\ 0 & \frac{1}{2m} & 0 & 0 \\ \frac{m}{2}\tilde{\omega}_{xyl} & 0 & \frac{m}{2}\tilde{\omega}_{yl}^2 & 0 \\ 0 & 0 & 0 & \frac{1}{2m} \end{pmatrix}. \tag{3.10}$$

the Hamiltonian can now be written as

$$H = \sum_{l=1}^{N} (X_l^{\dagger}, P_{x_l}^{\dagger}, Y_l^{\dagger}, P_{y_l}^{\dagger})\, M_l \begin{pmatrix} X_l \\ P_{x_l} \\ Y_l \\ P_{y_l} \end{pmatrix}, \tag{3.11}$$

with coefficients

$$\tilde{\omega}_{u,l} = \sqrt{\nu_u^2 + \frac{4Q^2}{m} \sum_{\tau>0} d_{u,\tau} \sin^2(\pi l\tau/N)} \text{ , u=x,y} \tag{3.12}$$

and

$$\tilde{\omega}_{xyl} = \frac{Q^2}{m} \sum_{\tau>0,odd} \frac{3\tau ab}{2\sqrt{(\tau a)^2 + b^2}^5} \sin(2\pi l\tau/N) \text{ .} \tag{3.13}$$

For each l I need the symplectic transformation (61), denoted by S_l, that diagonalises the matrix M_l,

$$S_l\, M_l\, S_l^T = \mathrm{diag}\left(\frac{\omega_{v,l}}{2}, \frac{\omega_{v,l}}{2}, \frac{\omega_{w,l}}{2}, \frac{\omega_{w,l}}{2}\right) \tag{3.14}$$

where

$$\omega_{v,l} = \frac{1}{2\sqrt{2}}\sqrt{\tilde{\omega}_{xl}^2 + \tilde{\omega}_{yl}^2 + \sqrt{(\tilde{\omega}_{xl}^2 - \tilde{\omega}_{yl}^2)^2 + 4\tilde{\omega}_{xyl}^2}} \tag{3.15}$$

$$\omega_{w,l} = \frac{1}{2\sqrt{2}}\sqrt{\tilde{\omega}_{xl}^2 + \tilde{\omega}_{yl}^2 - \sqrt{(\tilde{\omega}_{xl}^2 - \tilde{\omega}_{yl}^2)^2 + 4\tilde{\omega}_{xyl}^2}} \tag{3.16}$$

are the symplectic eigenvalues of M_l. These transformations are given by

$$S_l = \begin{pmatrix} 0 & -\phi_l\sqrt{\frac{\omega_{v,l}m}{\psi_l}} & 0 & -2\tilde{\omega}_{xyl}\sqrt{\frac{\omega_{v,l}m}{\psi_l}} \\ \frac{\phi_l}{\sqrt{2m\omega_{v,l}\,\psi_l}} & 0 & \frac{\tilde{\omega}_{xyl}}{\sqrt{\omega_{v,l}m\,\psi_l}} & 0 \\ 0 & -2\tilde{\omega}_{xyl}\sqrt{\frac{\omega_{v,l}m}{\psi_l}} & 0 & \phi_l\sqrt{\frac{\omega_{v,l}m}{\psi_l}} \\ \frac{\tilde{\omega}_{xyl}}{\sqrt{\omega_{v,l}m\,\psi_l}} & 0 & -\frac{\phi_l}{2\sqrt{\omega_{v,l}m\,\psi_l}} & 0 \end{pmatrix} \tag{3.17}$$

where $\phi_l = \tilde{\omega}_{xl}^2 - \tilde{\omega}_{yl}^2 + \sqrt{(\tilde{\omega}_{xl}^2 - \tilde{\omega}_{yl}^2)^2 + 4\tilde{\omega}_{xyl}^2}$ and $\psi_l = (\tilde{\omega}_{xl}^2 - \tilde{\omega}_{yl}^2)^2 + 4\tilde{\omega}_{xyl}^2 + (\tilde{\omega}_{xl}^2 - \tilde{\omega}_{yl}^2)\sqrt{(\tilde{\omega}_{xl}^2 - \tilde{\omega}_{yl}^2)^2 + 4\tilde{\omega}_{xyl}^2}$. The new normal modes are

$$\begin{pmatrix} v_l \\ P_{v_l} \\ w_l \\ P_{w_l} \end{pmatrix} = S_l^{-T} \begin{pmatrix} X_l \\ P_{x_l} \\ Y_l \\ P_{y_l} \end{pmatrix}, \tag{3.18}$$

and using the number operators $\hat{n}_{v,l} = \frac{P_{v_l}^\dagger P_{v_l}}{2\hbar} + \frac{v_l^\dagger v_l}{2\hbar} - \frac{1}{2}$, and similarly for w, I find the fully diagonalised Hamiltonian for the zig-zag configuration

$$H = \sum_l \left[\hbar\omega_{v,l}\left(\hat{n}_{v,l} + \frac{1}{2}\right) + \hbar\omega_{w,l}\left(\hat{n}_{w,l} + \frac{1}{2}\right)\right] . \tag{3.19}$$

The calculation of the two-site negativity requires the evaluation of the covariance matrix of the partially transposed state of the two sites (36, 47). In two dimensions this is a 8×8 matrix of which the symplectic eigenvalues have to be found. However, in the linear configuration of the ions, x and y degrees of freedom completely decouple and it is sufficient to consider two 4×4 covariance matrices independently. In contrast the zig-zag configuration contains xy-coupling terms and it is *a priori* necessary to

consider the full 8×8 matrix. As a result no entanglement occurs between the x and y direction in the linear configuration while the zig-zag configuration could sustain xy entanglement. However, I found that all expectation values coupling the x and y direction, i.e. $\langle x_i\, y_j\rangle$, $\langle p_{x_i}\, p_{y_j}\rangle$ etc., vanish also in the zig-zag configuration.

To characterise the entanglement between two sites two sets of each two conditions, as used in (36), emerge. For each site j these separability conditions are

$$0 \leq S_{1,2}(\nu_t, \tau) = \frac{1}{\hbar^2} \left\langle (x_j \pm x_{j+\tau})^2 \right\rangle \left\langle (p_{x_j} \mp p_{x_{j+\tau}})^2 \right\rangle - 1 \tag{3.20}$$

and similarly for the y direction. The expectation values needed here can be calculated using the transformation rules into the diagonal modes, Eq. (3.7) in the linear chain, and Eq. (3.9) and Eq. (3.18) in the zig-zag configuration. If one of the inequalities is violated then entanglement exists between the j-th site and its τ's neighbour and the negativity,

$$E_N = \sum_{k=1}^{2} \max\left[0, -\ln\sqrt{S_k + 1}\right], \tag{3.21}$$

measures their degree of entanglement. The two criteria S_1 and S_2 witness two types of entanglement. For example, the EPR pair originally considered in (62) shows violation for S_2 but not S_1.

The von Neumann entropy of a single site j in either x or y dimension is obtained following (63) with the formula

$$S_V(r_j) = \frac{r_j + 1}{2} \ln\left(\frac{r_j + 1}{2}\right) - \frac{r_j - 1}{2} \ln\left(\frac{r_j - 1}{2}\right) \tag{3.22}$$

where $r_j = \sqrt{\langle x_j^2\rangle \langle p_{x_j}^2\rangle}$, and similiarly for the y direction, is the symplectic eigenvalue of its reduced state. To evaluate the entropy of a block of n neighbouring sites the block entropy is then simply

$$S_V(n) = \sum_{j=1}^{n} S_V(r_j) \tag{3.23}$$

where the sum is taken over all n symplectic eigenvalues r_j in either x or y dimension within the block.

3.3.1 Thermodynamical limit ($N \to \infty$)

To obtain the negativity in x direction at zero temperature in the thermodynamical limit in the linear configuration, I evaluate Eq. (4.8) in the ground state leading to

$$S_{1,2}(\nu_t,\tau) = \frac{1}{N^2}\sum_{l,k}\frac{\omega_{x,k}}{\omega_{x,l}}\left(1 \pm \cos\left(\frac{2\pi l}{N}\tau\right)\right)\left(1 \mp \cos\left(\frac{2\pi k}{N}\tau\right)\right) - 1,$$

and similarly for the entanglement in y direction. For the zig-zag configuration transformation 3.18 gives a more complicated expression for the $S_{1,2}$ criteria. The formula is long and not enlightening, therefore I omit it. In the thermodynamical limit I substitute $\frac{\pi k}{N} = \alpha$, $\frac{\pi l}{N} = \beta$, and replace the sums with integrals,

$$S_{1,2}(\nu_t,\tau) = \frac{1}{\pi^2}\int_{-\pi/2}^{\pi/2}\omega_{x,\alpha}\left(1 \pm \cos\left(2\alpha\tau\right)\right)d\alpha \int_{-\pi/2}^{\pi/2}\frac{\left(1 \mp \cos\left(2\beta\tau\right)\right)}{\omega_{x,\beta}}d\beta - 1$$

These integrals can be evaluated numerically and the plots are shown in Fig. 3.2 (red-solid line). For one special set of parameters the above expression can be easily calculated analytically, namely for y direction in the linear configuration at the critical point $\nu^2_{t,crit} = \frac{C}{2}$ for NN interaction. The S_1 criterion between nearest neighbours becomes

$$\begin{aligned} S_1(\nu_{t,crit},1) &= \frac{4}{\pi^2}\int_0^{\pi/2}\sqrt{\frac{C}{2}}\cdot\cos(\alpha)\left(1-\cos\left(2\alpha\right)\right)d\alpha \\ &\times \int_0^{\pi/2}\frac{\left(1+\cos\left(2\beta\right)\right)}{\sqrt{\frac{C}{2}}\cdot\cos(\beta)}d\beta - 1 = \frac{4}{\pi^2}\cdot\frac{2}{3}\cdot 2 - 1 \approx -0.46 \end{aligned} \tag{3.24}$$

which leads to a value of the negativity of $E_N \approx 0.308$.

In a similar fashion, the single-site von Neumann entropy for both, x and y direction, can be evaluated in the thermodynamical limit. Here I show the calculation for the y direction. The symplectic eigenvalue for a single site in y direction is $r_j = \sqrt{\langle y_j^2\rangle\langle p_{y_j}^2\rangle} = \sqrt{\sum_{k,l=1}^{N}\frac{1}{N^2}\langle Y_l^2\rangle\langle P_{y_l}^2\rangle}$. Again I substitute sums with integrals and $\frac{\pi k}{N} = \alpha$, which gives an integral expression for the symplectic eigenvalue

$$r_j = \sqrt{\frac{1}{\pi^2}\int_0^{\pi/2}\frac{1}{\sqrt{\nu_t^2 - C/2\sin^2(\alpha)}}d\alpha \int_0^{\pi/2}\sqrt{\nu_t^2 - C/2\sin^2(\beta)}d\beta}. \tag{3.25}$$

At the critical point $\nu^2_{t,crit} = \frac{C}{2}$ and for NN interaction this can be simplified to

$$r_j = \sqrt{\frac{1}{\pi^2}\int_0^{\pi/2}\frac{1}{\cos(\alpha)}d\alpha \int_0^{\pi/2}\cos(\beta)d\beta} \to \infty\ . \tag{3.26}$$

The first integral diverges and hence the symplectic eigenvalue and the von Neumann entropy diverge at the QPT.

3.4 Behaviour of entanglement at zero temperature

Here I study the entanglement behaviour at zero temperature. Fig. 3.2 displays both entanglement measures for decreasing transverse trapping potential ν_t. In the upper plots (a and b) both measures for the x-entanglement are constant in the linear regime. This is because the phonons in x direction are independent of the trapping in y direction. At the critical point both negativity and entropy are not differentiable. Decreasing the trapping potential beyond the critical value, where the zig-zag configuration is formed, the x-entanglement is reduced due to the emerging $x-y$ coupling. Because each site in (b) couples to several different neighbours, the entanglement between two distinct sites disappears.

In the lower plots (c and d) both entanglement measures for the y-entanglement grow with decreasing trapping potential ν_t in the linear configuration. The even numbered ions oscillate exactly out of phase with the odd numbered ions due to the repulsive Coulomb potential. The smaller ν_t, the larger these quantum fluctuations around equilibrium position become. At the critical point the fluctuations become strong enough for causing the ions to move outward. The entropy diverges and the negativity reaches its maximal value of $E_N \approx 0.308$ where it is not differentiable.

For the nearest neighbour coupling (a and c) the negativity and entropy show qualitatively the same behaviour. This can be understood easily as any entanglement of a site with the rest of the chain, measured by the von Neumann entropy, is created by the coupling with only the nearest neighbours. For the long-range interaction (b and d), where a single site couples to all other sites, there are significant differences between the two entanglement measures. While the negativity of two nearest neighbour sites vanishes after a threshold value of ν_t, each single site remains entangled with the rest of the chain, as seen by the positive value of the von Neumann entropy.

Both entanglement measures are functions of the eigenvalues of the Hamiltonian. Therefore abrupt changes in entanglement can signal non-analyticity of ground state energy, which is associated with QPT's. In (35) it was shown for finite dimensional systems that (under certain conditions) a discontinuity in or divergence of the first

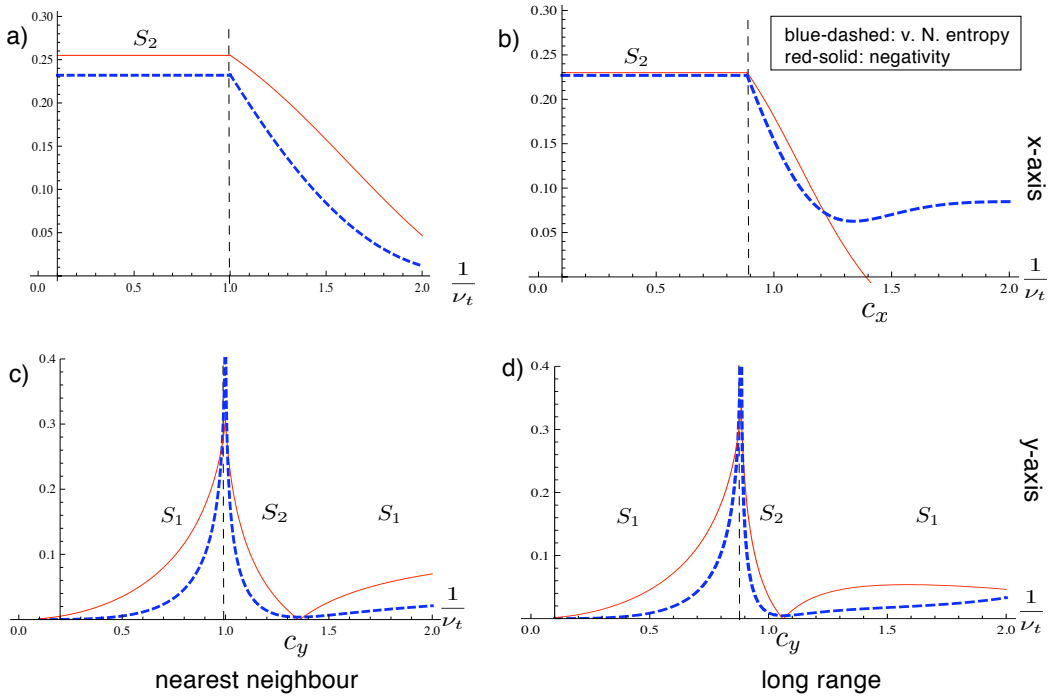

Figure 3.2: This graphic shows the von Neumann entropy of a single site and the negativity between two neighbouring sites both, for x-entanglement (upper plots) and y-entanglement (lower plots) of the ground state ($T = 0$). I compare the case where only nearest neighbours interact (left plots) with the long-range Coulomb Hamiltonian (right plots). Both models are approximated up to second order. The numerical values for the plots are for the ground state ($T = 0K$) in the thermodynamical limit ($N \to \infty$) and $Q = 1$, $m = 2$. For NN the lattice constant is set to $a = 1$, and for LR it is $a = 14/15$ and the plots include interactions up to the fourth neighbour. The change of entanglement at the critical point, indicated by the vertical line, is clearly visible in all four plots.

derivative of the negativity is both necessary and sufficient to signal a QPT. It seems intuitive that a similar characterisation holds also for continuous variable systems. Here the divergence of entropy and finite discontinuity of the first derivative of negativity shows a QPT of second order. After the phase transition the violated negativity criterion switches from S_1 to S_2. Lowering the trapping potential further leads to another "critical" point c_y at which the negativity becomes zero while the entropy reaches its minimal (non-zero) value.

The additional critical point c_y (and c_x in (b)) only appears when the interaction is harmonic as is the case in our second order approximation of the Coulomb model.

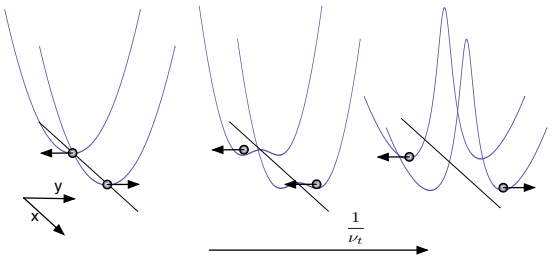

Figure 3.3: This graphic shows the change of trapping potential in y direction. Different geometries favour different momenta, as indicated with the arrows.

The point is due to a sign change of the second order coefficient d_τ^y (d_τ^x) at c_y (c_x). As a consequence the interaction switches from repulsive to attractive. When anharmonic terms are taken into account, as in the numerical treatment in (54), these points vanish. An intuitive way of understanding the switching between S_1 and S_2 is as follows, see Fig. 3.3. Decreasing the trapping potential changes the relative strengths of the inner and outer potential for the motion in the y direction. This leads to the change in phase in the relative momenta of neighbouring sites. In one configuration the relative potential favours momenta in the opposite directions, while the other configuration favours motion in the same direction. This is reflected in the change from S_1 to S_2. However, although the negativity vanishes at these points, a single site is still entangled with the rest of the chain.

3.4.1 Block Entropy

The block entropy measures how much entanglement exists between a block of sites of the lattice and the rest. For nearest neighbour interaction models there exist scaling laws showing that the amount of entanglement scales with the boundary area and not the volume of the reduced state (55). For a translational invariant chain with NN interaction there exists even a computable analytical result for the negativity of a bisected harmonic chain (40). Here I investigate the block entropy for blocks up to three sites in the long-ranged Coulomb lattice. Due to the complexity of LR interactions few results are known so far. The inset (c) illustrates the increase of correlation across the block boundary with increasing block size. Correlations stretch to nearest neighbours (NN) and next-nearest neighbour (NNN), as shown in Fig. 3.4 while third neighbour

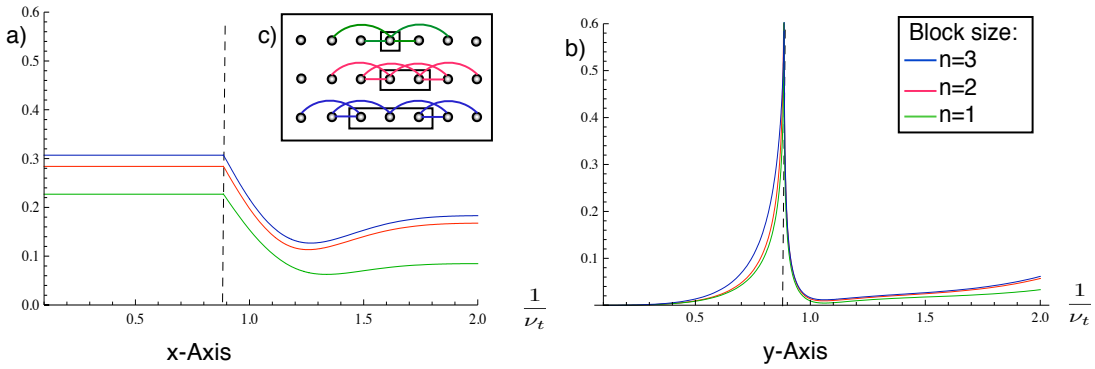

Figure 3.4: This graphic shows the block entropy for different number of sites in x (a) and y (b) dimension for long range interaction in the thermodynamical limit. The entropy increases with number of sites. The inset (c) shows the entanglement connections between nearest neighbour and next nearest neigbour (NNN) sites.

entanglement is negligible. Increasing the block size from one to two there are twice as many NNN connections across the boundary and hence the block entropy for two sites is expected to increase. This intuition is confirmed in a) and b) showing the block entropy in x and y direction, repectively. However, it can be seen that while the entropy increases slightly with number of sites, no qualitative difference can be observed. This is due to the fact that the additional, long range entanglement is much weaker because the Coulomb potential falls off quickly, with $1/\tau^3$ where τ is the distance of sites. In y dimension (b) already the single site entropy is a good approximation for larger blocks. This is because transversal next nearest neighbour entanglement turns out to be very small. In x direction (a) there are significant differences for growing block sites. Here next nearest neighbour entanglement cannot be neglected. Although the number of connections between two and three sites is the same, the block three entropy is still higher. This might be due to multipartite entanglement. Larger block sites are difficult to evaluate, as the symplectic eigenvalues of the covariance matrix become very complicated.

3.5 Witnessing entanglement at finite temperature

One consequence of the entanglement of the sites is a lowering of the energy of the system (36). This can be seen by assuming that the thermal state of the system is separable, i.e. decoupled between modes. Then an effective, single site Hamiltonian can be obtained by removing all second order couplings between the different sites, i.e. $\langle (x_j - x_{j+\tau})^2 \rangle_{\rho_S} = \langle x_j^2 + x_{j+\tau}^2 - 2x_j x_{j+\tau} \rangle_{\rho_S} = 2\langle x_j^2 \rangle_{\rho_S}$ etc.. The total Hamiltonian becomes the sum of the single site Hamiltonian $H_{\text{eff}} = \sum_j H_j$ with

$$H_j = \frac{p_{xj}^2 + p_{yj}^2}{2m} + \frac{m}{2}\left(\Omega_x^2 x_j^2 + \Omega_y^2 y_j^2 + \Omega_{xy} x_j y_j\right) \tag{3.27}$$

where

$$\Omega_x = \sqrt{\nu^2 + \frac{2Q^2}{m}\sum_{\tau\neq 0} d_\tau^x} \text{ and } \Omega_y = \sqrt{\nu_t^2 + \frac{2Q^2}{m}\sum_{\tau\neq 0} d_\tau^y}$$
$$\text{and } \Omega_{xy} = \frac{2Q^2}{m}\sum_{\tau\neq 0} d_{\tau,j}^{xy} \tag{3.28}$$

Then the thermal state takes the form

$$\rho_S = \bigotimes_{j=1}^{N} \frac{e^{-\beta H_j}}{\text{tr}\left[e^{-\beta H_j}\right]}, \tag{3.29}$$

with $\beta = \frac{1}{k_B T}$ the inverse temperature. Using the transformations Eq. (3.7), Eq. (3.9) and Eq. (3.18), $\langle H_{\text{eff}} \rangle$ can be fully diagonalised. The internal energy $U = \langle H_{\text{eff}} \rangle$ for any separable state is bounded from below by zero point fluctuations, i.e.

$$\langle H_{\text{eff}} \rangle_{sep} \geq \frac{N\hbar}{2}\left(\Omega_x + \Omega_y + \Omega_{xy}\right), \tag{3.30}$$

and any state having a smaller energy must be entangled between the individual sites.

I now want to see how the ground state situation is modified at non-zero temperature. As the energy of the thermal state, i.e. the mean excitation of phonons, increases with temperature there exists a critical temperature, T_c, for each value of the trapping potential at which the thermal state matches the energy bound. The negativity between the y degrees of freedom of two nearest neighbours for NN Hamiltonian is evaluated numerically and plotted in Fig. 3.5 where the critical temperature for full separability is also indicated as a red-line. When the trapping potential is lowered, the

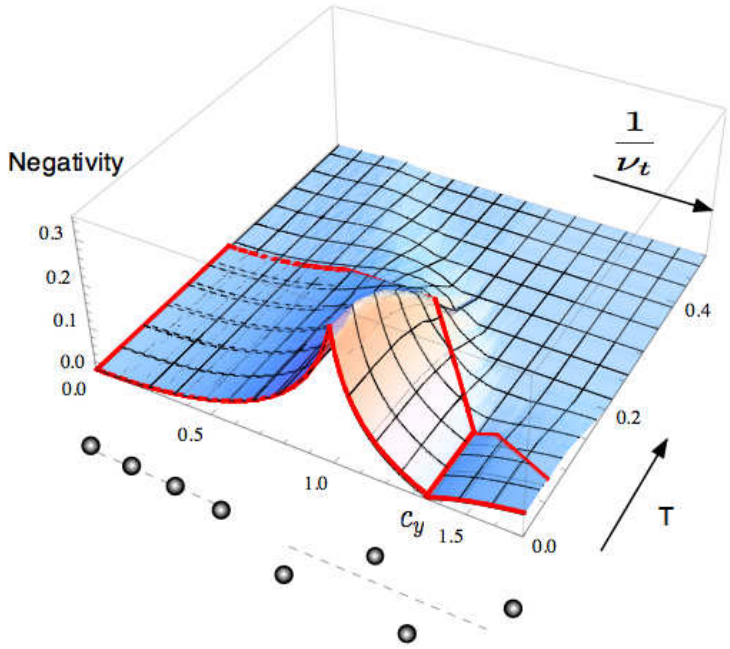

Figure 3.5: This graphic shows the negativity in y direction of two neighbouring ions for decreasing trapping potential and increasing temperature (in units of $[\nu_t] = \sqrt{\frac{Q^2}{ma^3}}$ and $[T] = [\nu_t]\frac{\hbar}{2k_B}$, $N = 20, Q = a = 1, m = 2$). The red line indicates the critical temperature, obtained with the energy witness argument, below which entanglement of some form must be present in the chain.

negativity increases until reaching its maximal value at the critical $\nu_{t,crit}$. Further lowering leads to a decrease of the negativity until it vanishes at point c_y. However, when further decreasing ν_t the negativity grows again, yet the two entanglement criteria $S_{1,2}$ are now switched. As expected, increasing the temperature leads to smaller values of negativity and smoothens the entanglement measures to make it differentiable at the critical point. For large ν_t the negativity is small, but remains finite until relatively high temperature. The sharp peak at the QPT remains almost constant for finite T and decreases fast. Thermal states within the red outlined area have a smaller energy than any separable state and their entanglement is therefore detected by the energy witness. Remarkably, states at c_y are entangled for temperatures up to $T_c[1/\nu_t = c_y] = 0.12\frac{[\nu_t]\hbar}{2k_B}$, even though there is no nearest neighbour entanglement in y direction. This is because there is still nearest neighbour entanglement in x direction and possibly also multipar-

tite entanglement the chain.

3.6 Conclusions

I revised the classical phase transition in a long range harmonic chain (53) using a fully quantised model. Two measures of entanglement display critical behaviour: The von Neumann entropy of a single site and blocks of two and three sites diverge at the critical point while the negativity is not differentiable. Thus also in this continuous variable system entanglement indicates a QPT, as previously shown for discrete systems (35). The negativity depends only on single site and nearest neighbour correlations; the single site von Neumann entropy even only depends on single site measurements. My calculation shows that even this local, single site function is able to detect a global change in configuration. This implies that instead of examining two point correlations functions one can alternatively consider the entanglement measures stated. This will be advantageous in experimental situations when the number of different measurement procedures is best kept as low as possible. I am aware that for the moment ion traps cannot yet perform the required measurements of e.g. single site variance of space and momentum operator, but this is a technical, not a fundamental problem. Furthermore, the results confirm that this phase transition is of second order as indicated in (53). At finite temperature, the negativity still displays critical behaviour, as seen in Fig. 3.5, however the non-differentiable cusp fades out quickly with increasing thermal noise. Tuning across a QPT provides a means of changing the amount and structure of continuous variable. Experiments with ion-traps are ideally suited to study QPTs with great precision.

4

Quantum information in DNA

Can quantum effects influence information processing in DNA? In order to answer I will develop a simple model describing the quantum degrees of freedom along the chain of DNA. I will show that, according to this model, the electronic degree of freedom is even at room temperature de-localised, i.e. maintains coherence. In chapter 5 I will mention possible effects on information flow.

I model the electron clouds of nucleic acids in DNA as a chain of coupled quantum harmonic oscillators with dipole-dipole interaction between nearest neighbours resulting in a van der Waals type bonding. Crucial parameters in my model are the distances between the acids and the coupling between them, which I estimate from numerical simulations (64). I show that for realistic parameters nearest neighbour entanglement is present even at room temperature. I quantify the amount of entanglement in terms of negativity and single base von Neumann entropy. I find that the strength of the single base von Neumann entropy depends on the neighbouring sites, thus questioning the notion of treating single bases as logically independent units. I derive an analytical expression for the binding energy of the coupled chain in terms of entanglement and show the connection between entanglement and correlation energy, a quantity commonly used in quantum chemistry.

4.1 Introduction

The precise value of energy levels is of crucial importance for any kind of interaction in physics. This is also true for processes in biological systems. It has recently been shown

for the photosynthesis complex FMO (8, 65, 66, 67) that maximum transport efficiency can only be achieved when the environment broadens the systems energy levels. Also for the olfactory sense the energy spectra of key molecules seem to have a more significant contribution than their shape (15). In (68) the possibility of intramolecular refrigeration is discussed. A common theme of these works is the system's ability to use non-trivial quantum effects to optimise its energy levels. This leads to the question whether a molecule's energy levels are only determined by its own structure, or if the environment *shapes* the molecule's energy level? Entanglement between system and environment is a necessary condition to alter the system's state. Here I study the influence of weak chemical bonds, such as intramolecular van der Waals interactions, on the energy level structure of DNA and discuss its connection to entanglement. To describe the van der Waals forces between the nucleic acids in a single strand of DNA, I consider a chain of coupled quantum harmonic oscillators. Much work has been done investigating classical harmonic oscillators. However, this cannot explain quantum features of non-local interactions. Also, classical systems can absorb energy quanta at any frequency, whereas quantum systems are restricted to absorb energy quanta matching their own energy levels. This is of importance for site specific DNA-Protein interaction, as the probability of a protein to bind to a specific sequence of sites in DNA is governed by the relative binding energy (69).

My work was motivated by a numerical study on the importance of dispersion energies in DNA (64). Dispersion energies describe attractive van der Waals forces between non-permanent dipoles. Recently their importance to stabilise macromolecules was realised (70, 71). Modelling macromolecules, such as DNA, is a tedious and complex task. It is currently nearly impossible to fully quantum mechanically simulate the DNA. Quantum chemistry has developed several techniques that allow the simulation of DNA with simplified dynamics. In (64) the authors first quantum mechanically optimise a small fragment of DNA in the water environment. Then, the potential energy of the system (see eq 1) is described by molecular dynamics (MD) and is divided into the electrostatic and Lennard-Jones terms. The former term is modelled by the Coulomb interaction of atomic point-charges, whereas the latter describes repulsion and dispersion energies,

$$V(r) = \frac{q_i q_j}{4\pi\epsilon_0 r_{ij}} + 4\epsilon \left[\left(\frac{\sigma}{r_{ij}} \right)^{12} - \left(\frac{\sigma}{r_{ij}} \right)^{6} \right] , \tag{4.1}$$

where the strength of the dispersion energy is scaled with the parameter ϵ. For $\epsilon = 1$ the dynamics of the DNA strand is normal. For a weaker dispersion, $\epsilon = 0.01$, there is in increase of 27% in energy in the DNA. This increase of energy induces the unravelling of the double helix to a flat, ladder-like DNA. Many factors contribute to the spatial geometry of DNA, e.g. water interaction, the phosphate backbone, etc. However, one of the strongest contributions is the energy of the electronic degree of freedom inside a DNA strand, which is well shielded from interactions with water. Stronger interaction ($\epsilon = 1$) allows the electrons clouds to achieve spatial configurations that require less structural energy. This allows a denser packing of the electron charges inside the double helix.

Here I investigate with a simple model of DNA whether continuous variable entanglement can be present at room temperature, and how this entanglement is connected to the energy of the molecule. There are many technically advanced quantum chemically calculations for van der Waals type interaction, i.e. (72). The aim of this work is not to provide an accurate model, but to understand underlying quantum mechanical features and their role in this biological system. Also, there are many parallel developments between quantum information and quantum chemistry. This work bridges the concepts of entanglement and dispersion energies between the two fields. Finally, the advantages of quantifying chemical bonds in terms of entanglement were already mentioned in (73). Here I give the first example of a system whose chemical bonds are described by entanglement.

4.2 Dispersion energies between nucleic acids

The nucleic bases adenine, guanine, cytosine and thymine are planar molecules surrounded by π electron clouds. I model each base as an immobile positively charged centre while the electron cloud is free to move around its equilibrium position, see Fig. 4.1. There is no permanent dipole moment, while any displacement of the electron cloud creates a non-permanent dipole moment. Denoting the displacement of two centres by (x, y, z), I assume the deviation out of equilibrium $|(x, y, z)|$ to be small compared to the distance r between neighboring bases in chain. The displacement of each electron cloud is approximated to second order and described by a harmonic oscillator

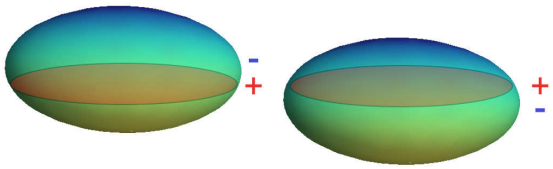

Figure 4.1: This graphic shows a sketch of a DNA nucleic acid. The mostly planar molecules are divided into the positively charged molecule core (red) and the negatively charged outer π electron cloud (blue-yellow). In equilibrium the centre of both parts coincide, thus there is no permanent dipole. If the electron cloud oscillates around the core, a non permanent dipole is created (74). The deviation out of equilibrium is denoted by (x, y, z). The corresponding dipole is $\vec{\mu} = Q(x, y, z)$. This oscillation might be caused by an external field, or induced by quantum fluctuations, as it is given in a DNA strand.

with trapping potential Ω that quantifies the Coulomb attraction of the cloud to the positively charged centre. A single DNA strand resembles a chain of harmonic oscillators, see Fig. 4.2, where each two neighboring bases with distance r have dipole-dipole interaction.

The Hamiltonian for the DNA strand of N bases if given by

$$H = \sum_{j,d=x,y,z}^{N} \left(\frac{p_{j,d}^2}{2m} + \frac{m\Omega_d^2}{2} d_j^2 + V_{j,dip-dip} \right) \tag{4.2}$$

where d denotes the dimensional degree of freedom, and the dipole potential

$$V_{j,dip-dip} = \sqrt{\epsilon} \frac{1}{4\pi\epsilon_0 r^3} \left(3(\vec{\mu}_j \cdot \vec{r}_N)(\vec{\mu}_{j+1} \cdot \vec{r}_N) - \vec{\mu}_j \cdot \vec{\mu}_{j+1}\right) \tag{4.3}$$

with $\vec{\mu}_j = Q(x_j, y_j, z_j)$ dipole vector of site j and $\vec{r}_N$ normalised distance vector between site j and $j+1$. Due to symmetry $\vec{r}_N$ is independent of j. I choose periodic boundary conditions, i.e. $\vec{\mu}_{N+j} = \vec{\mu}_j$. The dimensionless scaling factor ϵ is varied to study the effects on entanglement and energy identical as in (64). In order to compare this model with (64), I consider 'normal' interaction, where the dipole-dipole interaction has full strength modelled by $\epsilon = 1$ and 'scaled' interaction, where the dipole-dipole interaction is reduced to a hundredth of the original strength modelled by $\epsilon = 0.01$. The distance between neighbouring bases in DNA is approximately $r_0 = 4.5\mathring{A}$. For generality I will not fix the distance.

In general the single strand of DNA will not be perfectly linear and thus the dipole

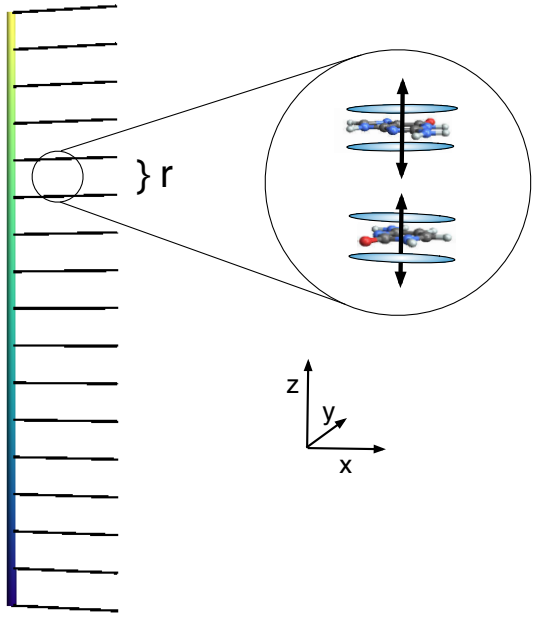

Figure 4.2: This graphic shows a sketch of a single DNA strand. The chain is along z direction. Each bar in the single strand DNA represents one nucleic acid: adenine, thymine, guanine or cytosine. Around the core of atoms is the blue outer electron cloud. The oscillation of these electron clouds is modelled here as non-permanent harmonic dipoles, depicted by the arrows, with trapping potential Ω_d in dimension $d = x, y, z$.

potential has coupling terms of the form xz etc. Detailed analysis following (75) shows that the energy contribution from the cross coupling terms is small, and they will be ignored here. This leads to the interaction term

$$V_{j,dip-dip} = \frac{Q^2}{4\pi\epsilon_0 r^3}\left(+x_j x_{j+1} + y_j y_{j+1} - 2z_j z_{j+1}\right) \ . \tag{4.4}$$

The different signs for x, y and z reflect the orientation of the chain along z direction.

A discrete Fourier transformation of the form

$$\begin{aligned} d_j &= \frac{1}{\sqrt{N}}\sum_{l=1}^{N} e^{i\frac{2\pi}{N}jl}\tilde{d}_l \\ p_{j,d} &= \frac{1}{\sqrt{N}}\sum_{l=1}^{N} e^{-i\frac{2\pi}{N}jl}\tilde{p}_{l,d} \end{aligned} \tag{4.5}$$

decouples the system into independent phonon modes. These modes can be diagonalized by introducing creation $a_{d,l} = \sqrt{\frac{m\Omega_d}{2\hbar}}\left(\tilde{d} + \frac{i}{m\Omega_d}\tilde{p}_{l,d}\right)$ and annihilation operator $a^\dagger_{d,l}$.

This results in the dispersion relations

$$\begin{aligned}
\omega_{xl}^2 &= \Omega_x^2 + 2\left(2\cos^2\left(\frac{\pi l}{N}\right) - 1\right)\frac{Q^2}{4\pi\epsilon_0 r^3 m} \\
\omega_{yl}^2 &= \Omega_y^2 + 2\left(2\cos^2\left(\frac{\pi l}{N}\right) - 1\right)\frac{Q^2}{4\pi\epsilon_0 r^3 m} \\
\omega_{zl}^2 &= \Omega_z^2 + 4\left(2\sin^2\left(\frac{\pi l}{N}\right) - 1\right)\frac{Q^2}{4\pi\epsilon_0 r^3 m}
\end{aligned} \tag{4.6}$$

and the Hamiltonian in diagonal form

$$H = \sum_{l=1,d=x,y,z}^{N} \hbar\omega_{dl}\left(n_{d,l} + \frac{1}{2}\right) \ , \tag{4.7}$$

where $n_{d,l} = a_{d,l}^\dagger a_{d,l}$ is the number operator of mode l in direction d.

The trapping potentials Ω_d can be linked to experimental data (see table 4.2) through the relation $\Omega_d = \sqrt{\frac{Q^2}{m_e \alpha_d}}$, where α_d is the polarizability of the nucleid base. So far I did not discuss the number of electrons in the cloud. Both the trapping potential Ω_d^2 as well as the interaction term $\frac{Q^2}{m}$ depend linearly on the number of electrons, and thus the dispersion frequencies $\omega_{d,l}^2$ have the same dependence. The quantities of interest in this chapter are entanglement and energy ratios, which are both given by ratios of different dispersion frequencies and are thus invariant of the number of electrons involved. In Table 4.2 I assumed the number of interacting electrons to be one, but the final results are independent of this special choice.

Table 4.1: Numerical values for polarizability of different nucleid acid bases (76) in units of $1au = 0.164 \cdot 10^{-40} Fm^2$. The trapping frequencies are calculated using the formula $\Omega = \sqrt{\frac{Q^2}{m_e \alpha}}$ and are given in units of $10^{15} Hz$.

nucleic acid	α_x	α_y	α_z	Ω_x	Ω_y	Ω_z
adenine	102.5	114.0	49.6	4.1	3.9	6.0
cytosine	78.8	107.1	44.2	4.7	4.1	6.3
guanine	108.7	124.8	51.2	4.0	3.8	5.9
thymine	80.7	101.7	45.9	4.7	4.2	6.2

Although the values for the four bases differ, all show similar $\Omega_x \approx \Omega_y$ (transverse), while there is an increase of 50% in the longitudinal direction, $\Omega_z \approx \frac{3}{2}\Omega_{x,y}$. In the

following I will approximate the chain to have the same value of trapping potential at each base. In x, y direction I will use $\Omega_{x,y} = 4 \cdot 10^{15} Hz$, and in z direction $\Omega_z = 6 \cdot 10^{15} Hz$.

4.3 Entanglement and Energy

I now investigate the influence of entanglement on energy. I will also derive an analytic expression for the change in binding energy depending on entanglement witnesses.

The chain of coupled harmonic oscillators is entangled at zero temperature, but is it possible to have entanglement at room temperature? There is a convenient way to calculate a criterion for nearest neighbour entanglement for harmonic chains (36), which compares the temperature T with the coupling strength ω between neighbouring sites. In general, for $\frac{2k_BT}{\hbar\omega} < 1$ one can expect entanglement to exist. Here the coupling between neighbouring clouds is given by $\omega = \sqrt{\sqrt{\epsilon}\frac{Q^2}{4\pi\epsilon_0 m r^3}} \approx \epsilon^{1/4} 1.6 \cdot 10^{15} Hz$ for $r = 4.5\mathring{A}$, which leads to $\frac{2k_B 300K}{\hbar\omega} = 0.05$ for $\epsilon = 1$ and 0.16 for $\epsilon = 0.01$. This means that the coupling between electron clouds is dominant compared to the temperature, and thus implies the existence of entanglement even at biological temperatures. An exact method to quantify the amount of entanglement in harmonic states is the violation of one of the two inequalities, related to the covariance matrix the state (63).

$$0 \leq S_1 = \frac{1}{\hbar^2} \left\langle (d_j + d_{j+1})^2 \right\rangle \left\langle (p_{d,j} - p_{d,j+1})^2 \right\rangle - 1 \tag{4.8}$$

$$0 \leq S_2 = \frac{1}{\hbar^2} \left\langle (d_j - d_{j+1})^2 \right\rangle \left\langle (p_{d,j} + p_{d,j+1})^2 \right\rangle - 1 \tag{4.9}$$

with d_j the position operator of site j in direction d and $p_{d,j}$ the corresponding momentum operator. If one of the inequalities is violated, the sites j and $j+1$ are entangled. The negativity, a widely used measure for entanglement, is calculated using the formula $Neg = \sum_{k=1}^{2} \max\left[0, -\ln\sqrt{S_k + 1}\right]$. The negativity measures the amount of entanglement between two subsystems. It can be directly calculated from space and momentum operator expectation values, namely the above defined $S_{1,2}$ criteria. The amount of negativity between neighbouring bases for room temperature is shown in Fig. 4.3. For the normal coupling there is substantially more entanglement present than for the scaled interaction. This correlates with the amount of binding energy found in (64), where

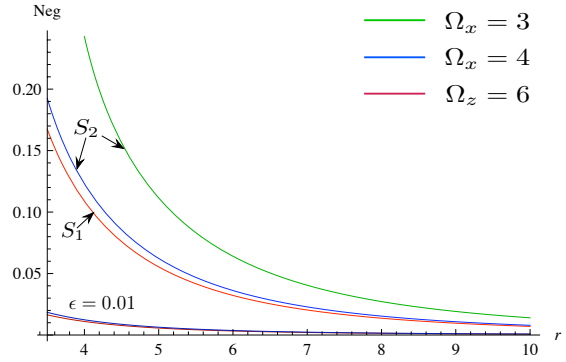

Figure 4.3: This graphic shows the nearest neighbour negativity as a function of distance between sites in $\mathring{A}$ at $T = 300K$. The three upper curves are for scaling factor $\epsilon = 1$, the lower two curves are for scaling factor $\epsilon = 0.01$. The red curve is for z direction and $\Omega_z = 6 \cdot 10^{15} Hz$. The blue and green curve are for x direction and $\Omega_x = 4 \cdot 10^{15} Hz$ and $\Omega_x = 3 \cdot 10^{15} Hz$. The negativity for $\epsilon = 0.01$ is much smaller than in the unscaled case. The amount of negativity strongly depends on the distance r between sites and the value of trapping potential Ω. The lower the potential, the higher the negativity. A typical distance between neighbouring base pairs in DNA is approximately $r = 4.5\mathring{A}$. Along the chain (z-direction) the S_1 criterion is violated, whereas transversal to the chain S_2 (x-direction) is violated. This reflects the geometry of the chain. Along the main axes of the chain energy is reduced by correlated movement. Transversal to the chain it is energetically better to be anti-correlated.

the DNA with normal coupling has a lower energy than the DNA with scaled coupling.

The above result motivates the question whether the binding energy can be expressed in terms of entanglement measures. In the limit of long distances, an analytical expression connects the amount of binding energy in the chain of oscillators with the values of $S_{1,2}$. Due to the strong coupling the chain of oscillators is effectively in its ground state, which I will assume in the following analysis.

The dispersion relations of the electron cloud oscillations can be expanded for large distances, i.e. $r^3 \to \infty$

$$\omega_{zl} \approx \Omega_z - 4\frac{Q^2}{4\pi\epsilon_0 m}\frac{1}{2\Omega_z}\cos\left(\frac{2\pi l}{N}\right)\frac{1}{r^3} + O\left[\frac{1}{r^6}\right] \tag{4.10}$$

and similarly $1/\omega_{zl}$

$$\frac{1}{\omega_{zl}} \approx \frac{1}{\Omega_z} + 4\frac{Q^2}{4\pi\epsilon_0 m}\frac{1}{2\Omega_z^3}\cos\left(\frac{2\pi l}{N}\right)\frac{1}{r^3} + O\left[\frac{1}{r^6}\right] \tag{4.11}$$

Inserting this expansion into the entanglement criterion S_2 gives:

$$S_{z,2} \approx -\frac{Q^2}{\pi\epsilon_0 m}\frac{1}{2\Omega_z^2}\frac{1}{r^3} \ , \tag{4.12}$$

while the corresponding expression for $S_{z,1}$ has a positive value. A similar expansion of the dispersion relation in the x direction leads to:

$$S_{x,1} \approx -\frac{Q^2}{2\pi\epsilon_0 m}\frac{1}{2\Omega_x^2}\frac{1}{r^3} \ . \tag{4.13}$$

This implies that nearest neighbor (n.n.) electronic clouds are entangled even at large distances. However the amount of entanglement decays very fast. I will now compare this result with the binding energy in the ground state. The binding energy is defined as the difference of energy of the entangled ground state and any hypothetical separable configuration

$$E_{z,bind} = \langle \hat{H}_z \rangle - \sum_{I=1}^{N} \langle \hat{H}_{zI} \rangle = \hbar/2 \left(\sum_{l=1}^{N} \omega_{zl} - N\Omega_z \right) \ . \tag{4.14}$$

This definition is analogous to the definition of correlation energy in chemistry (77). The first approximation to the full Schrödinger equation is the Hartree-Fock equation and assumes that each electron moves independent of the others. Each of the electrons feels the presence of an average field made up by the other electrons. Then the electron orbitals are antisymmetrised. This mean field approach gives rise to a separable state, as antisymmetrisation does not create entanglement. The Hartree-Fock energy is larger than the energy of the exact solution of the Schrödinger equation. The difference between the exact energy and the Hartree-Fock energy is called the correlation energy

$$E_{corr} = E_{exact} - E_{HF} \ . \tag{4.15}$$

This definition of binding energy is a special case of the correlation energy, but the analysis here is restricted to phonons (bosons) instead of electrons. This model describes the motional degree of freedom of electrons, namely the displacement of electron clouds out of equilibrium. I show for this special case that the amount of correlation energy is identical to entanglement measures.

Expanding the binding energy for $r^3 \to \infty$, the leading term is of order $\frac{1}{r^6}$

$$E_{z,bind} \approx \hbar/2 \left(-\left(\frac{Q^2}{\pi\epsilon_0 m} \right)^2 \frac{N}{16\Omega_z^3}\frac{1}{r^6} \right) = -\frac{N\hbar\Omega_z}{8} S_2^2 \ , \tag{4.16}$$

since the first order vanishes due to symmetry and similarly for x direction:

$$E_{x,bind} \approx -\frac{N\hbar\Omega_x}{8} S_1^2 \ . \tag{4.17}$$

Eqs. 4.16, 4.17 show a simple relation between the entanglement witnesses $S_{1,2}$ and the binding energy of the chain of coupled harmonic oscillators. The stronger the entanglement, the more binding energy the molecule has. Interestingly, along the chain the S_1 criterion is violated, whereas transversal to the chain S_2 is violated. This reflects the geometry of the chain. Along the main axes of the chain energy is reduced by correlated movement. Transversal to the chain it is energetically better to be anti-correlated. This means that the entanglement witnesses $S_{1,2}$ not only measure the amount of binding energy, but also the nature of correlation which gives rise to the energy reduction. This relation motivates the search for entanglement measures describing the binding energies of complex molecules. While the binding energy just measures energy differences the corresponding entanglement measures reflect more information. Without correlations between subsystems there would not be a chemical bond. It is precisely the purpose of entanglement measures not only to quantify, but also to characterise these correlations.

4.4 Aperiodic potentials and information processing in DNA

In the above calculations I assumed a periodic potential, which allowed me to derive analytical solutions. Here I investigate the influence of aperiodic potentials and discuss the robustness of the previous conclusions.

Firstly I note that the potentials for different nucleic acids do not differ significantly, see table 4.1. Hence one would intuitively assume that a sequence of different local potentials changes the amount of entanglement but does not destroy it. To check this intuition more thoroughly, one can use the phonon frequencies of the aperiodic chain of oscillators. For a finite one-dimensional chain of 50 bases without periodic boundary conditions and with the sequence of nucleic acids randomly chosen, I solve the resulting coupling matrix numerically. The smallest dispersion frequency determines the thermal robustness; the smaller the frequencies ω_l the larger the probability that the thermal heat bath can excite the system. Sampling over 1000 randomly chosen sequences yielded $\min(\omega_l) = 3.2 \cdot 10^{15} Hz$ as the smallest dispersion frequency. Comparing this with the

thermal energy gives $\frac{2k_B 300K}{\hbar\omega_l} \approx 0.03$, which is still very small.
Thus the thermal energy is more than 20 times smaller than the smallest phonon frequency, which allows to continue working with the ground state of the system.
Different sequences will cause fluctuations in the amount of entanglement in the chain of bases. I determine for each string the average of single site von Neumann entropy and compare it with the classical amount of information measured by the Shannon entropy of each string. The von Neumann entropy of a single site j is obtained following (63) with the formula

$$S_V(r_j) = \frac{r_j+1}{2}\ln\left(\frac{r_j+1}{2}\right) - \frac{r_j-1}{2}\ln\left(\frac{r_j-1}{2}\right) \tag{4.18}$$

where $r_j = \frac{1}{\hbar}\sqrt{\langle x_j^2\rangle\langle p_{x_j}^2\rangle}$, is the symplectic eigenvalue of the covariance matnrix of the reduced state.
To check whether the relative frequency of A,C,G and T influences the amount of entanglement within the coupled chain of oscillators, I also calculate the classical Shannon entropy of each string. Fig. 4.4 shows the average amount of single site quantum entropy vs. classical entropy. There is, within this model, no direct correlation between classical and quantum entropy. For the same amount of Shannon entropy, i.e. same relative frequencies of A,C,G and T, the value of quantum correlations varies strongly between around $vNE = 0.007$ and $vNE = 0.025$. One notes that for achieving a comparable amount of local disorder by thermal mixing a temperature of more than $2000K$ is needed. This is a quantum effect without classical counterpart. Each base without coupling to neighbours would be in its ground state, as thermal energy is small compared to the energy spacing of the oscillators. As the coupling increases, the chain of bases evolves from a separable ground state to an entangled ground state. As a consequence of the global entanglement, each base becomes locally mixed. This feature cannot be reproduced by a classical description of vibrations. When a classical system is globally in the ground state, also each individual unit is in its ground state. Although it is already well known that globally entangled states are locally mixed, little is known about possible consequences for biological systems. In the following paragraph I discuss one such quantum effect on the information flow in DNA.

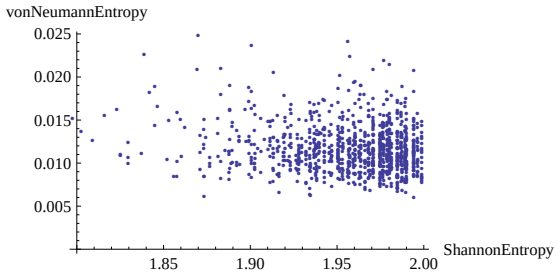

Figure 4.4: This graphic shows the average single site von Neumann entropy of a chain of nucleic acids dependant on the classical Shannon entropy of the string. Each string contains 50 bases with a random sequence of A,C,G, or T. The distribution of nucleic acids determines the classical Shannon entropy. For each nucleic acid the value of polarizability of Table 4.1 in x direction is used. The distance between sites is $r = 4.5 \cdot 10^{-10} m$. The plot has a sample size of 1000 strings. There is no direct correlation between quantum and classical information. The average amount of von Neumann entropy varies strongly for different sequences.

How much information about the neighbouring sites is contained in the quantum degree of freedom of a single base? Is it accurate to describe the electronic degree of freedom of a single nucleic acid as an individual unit or do the quantum correlations between bases require a combined approach of sequences of nucleic acids?

This will be of importance in the following chapter dealing with information flow in biological systems. There I will consider a model describing mutations in DNA. A crucial component for that model is energy quanta taken from the electronic degree of freedom of nucleic acids. If the amount of available energy is sequence dependent, i.e. changes with changing neighbours, then there could be non-random mutations. In the previous sections I showed that there is a correspondence between the amount of entanglement present and the binding energy of nucleic acids. Therefore, instead of checking the available energy levels, I will look at the von Neumann entropy. I will restrict myself to proof-of-principle, i.e. showing that the quantum state of an aperiodic chain of coupled harmonic oscillators in principle encodes information about its neighbours and is hence sequence dependent.

The single site von Neumann entropy measures how strongly a single site is entangled with the rest of the chain and is therefore a good measure to answer how strongly the quantum state of a single site depends on its neighbours. In the following I consider

a string with 17 sites of a single strand DNA. Site 9 as well as sites 1-7 and 11-17 are taken to be Adenine. The identity of nucleic acids at sites 8 and 10 varies. Table 4.2 shows the resulting von Neumann entropy of site 9 dependent on its neighbours. The value of a single site depends on the direct neighbourhood. There is, for example, a distinct difference if an Adenine is surrounded by Cytosine and Thymine ($vNE = 0.078$) or by Cytosine and Guanine ($vNE = 0.084$). On the other hand, in this model there is little difference between Adenine and Guanine in site 8 and Guanine in site 10. Of course this model has not enough precision to realistically quantify how much a single site knows about its surroundings. Nevertheless it indicates that the quantum state of a single base should not be treated as an individual unit. When quantifying the information content and error channels of genetic information, the analysis is usually restricted to classical information transmitted through classical channels. While I agree that the genetic information is *stored* using classical information, e.g. represented by the set of molecules (A,C,G,T), I consider it more accurate to describe the *processing* of genetic information by quantum channels, as the interactions between molecules are determined by laws of quantum mechanics.

Table 4.2: Numerical values for the von Neumann entropy of site 9 (Adenine) in a chain with open boundary condition containing 17 bases. The bases 1-7 and 11-17 are taken to be Adenine. The column gives the nucleic acid of site 8, the rows of site 10. The von Neumann entropy of site 9 varies with its neighbours.

	Adenine	Cytosine	Guanine	Thymine
Adenine	0.077	0.082	0.078	0.081
Cytosine	0.082	0.079	0.084	0.078
Guanine	0.078	0.084	0.079	0.083
Thymine	0.081	0.078	0.083	0.078

4.5 Conclusions and discussion

In this chapter I modelled the electron clouds of nucleic acids in a single strand of DNA as a chain of coupled quantum harmonic oscillators with dipole-dipole interaction between nearest neighbours. The main result is that the entanglement contained

in the chain coincides with the binding energy of the molecule. I derived in the limit of long distances and periodic potentials analytic expressions linking the entanglement witnesses to the energy reduction due to the quantum entanglement in the electron clouds. Motivated by this result I propose to use entanglement measures to quantify correlation energy, a quantity commonly used in quantum chemistry. As the interaction energy given by $\hbar\omega$ is roughly 20 times larger than the thermal energy $k_B 300K$ the motional electronic degree of freedom is effectively in the ground state. Thus the entanglement persists even at room temperature. Additionally, I investigated the entanglement properties of aperiodic potentials. For randomly chosen sequences of A,C,G, or T I calculated the average von Neumann entropy. There exists no direct correlation between the classical information of the sequence and its average quantum information. The average amount of von Neumann entropy varies strongly, even among sequences having the same Shannon entropy. Finally I showed that the quantum state of a single base contains information about its neighbour, questioning the notion of treating individual DNA bases as independent bits of information.

5

Information flow in biological systems

Mankind has entered the era of information processing. Leaving the century of thermodynamics, it is now a fashion to explain everything in terms of information. This includes biological systems. But what exactly is bio-logical information? And how is it processed? Biological information processing takes place at the challenging regime where quantum meets classical physics. Quantum effects will not play a large scale role in biology. Not only is it difficult to maintain coherence at body temperature in a noisy system, but living systems themselves have little use of phase information (except for transport problems, see introduction), a crucial component of quantum computers. The functionality of cells or bacteria depends on a delicate balance of concentrations of different molecules. Therefore the majority of information in a cell is classical information which has the advantage of being reliable and easy to store. The quantum aspects enter when information is processed. Any interaction in a cell relies on chemical reactions, which are dominated by quantum aspects of electron shells, i.e. quantum mechanics controls the flow of information. This insight is far from being new. The division of molecules into a classical part and a quantum part is a key aspect of the Born-Oppenheimer approximation (78), which is used successfully for many problems in computational chemistry since 1927. In a nutshell, as the nuclei of molecules are roughly a 1000 times heavier than the electrons, they can be approximated as classical particles. For a given set of nuclei coordinates (classical information), the Schrödinger equation is solved for the electrons, giving the solution of the quantum part. The

idea of the Born-Oppenheimer approximation will be re-examined in this chapter under the aspect of information processing in living systems, see fig. 5.1. I will discuss

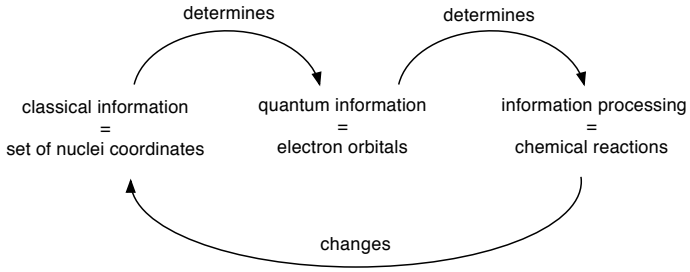

Figure 5.1: The Born-Oppenheimer approximation starts with separating complex molecules into the set of coordinates of the heavy nuclei, which are treated as classical particles, and the light electrons, which are treated fully quantum mechanically. The set of nuclei determines via the Schrödinger equation the electronic state of the molecule. Any interaction in a cell uses chemical reactions, which are determined by the electronic states of the molecules. A chemical reaction can turn a given molecule into a different one, thus changing the classical information.

in detail the interplay between classical information-storage and quantum controlled information-processing in living systems. First I give a small review on the meaning of information and entropy. One problem of quantifying information in biological systems is that usually neither the coding part nor decoding part of a molecule is known. The formalism of channel capacities is able to circumvent this problem, and will be introduced in the first part of this chapter. Then I will give examples of biological information processing and introduce the concepts of classical-quantum (cq) states in biology. This formalism is able to keep track of the combined classical-quantum aspects of information processing. In more detail I will study information processing in DNA. Copying genetic information is modelled as a two-step mechanism. The first step measures the quantum part, which determines the actual copying process in the second step, see fig. 5.1 and section 5.2.5. This simple model of copying genetic information allows to study general properties of quantum and classical capacities of genetic channels. The model uses three parameters, whose biological meaning will be explained in table 5.1. A copying mistake is also referred to as a mutation. In section 5.3 I will review experimental results on apparently non-random mutations in bacteria. So far no model can explain the existence of non-random mutations, which would require us to

re-think our understanding of genetics. Section 5.5 shows for which parameter values the experiments could be explained by the simple classical-quantum two-step mutational mechanism. Section 5.4 discusses possible quantum mechanisms for achieving these parameters values.

Last but not least, the consequences of sequence dependent mutations will be discussed.

5.1 Information theory

'Information means in-formation'.

- What is information?
  The mathematical definition of information was first given by Shannon (79). The information content of a message is given by the decrease of uncertainty after receiving the message. The information content can be quantified in two steps: first one has to choose an alphabet Σ, which is suitable to describe the message. An alphabet is a finite set of symbols, $\Sigma = \{x_i, i \in \{1...N\}\}$, where each symbol x_i occurs in the message with probability $p_i \geq 0$, s.t. $\sum_{i=1}^{N} p_i = 1$. This leads to a probability distribution $P = \{p_i, i \in \{1, ..., N\}\}$. Then the well known formula
  $$H(P) = -\sum p_i \log p_i \ , \tag{5.1}$$
  where $H(P)$ denotes the Shannon entropy of the probability distribution P, quantifies the entropy of a message. This formalism is exact in the limit of infinite messages. For messages of finite size errors occur, which can be quantified by smooth entropies (80).

- Information is physical
  Although information itself is an abstract concept, its realisation always needs a physical system (81). Understanding the physics of a system is crucial for understanding its information processing capacity. Every logical bit encoded in a physical degree of freedom has a non-zero probability to be corrupted by the environment. When a system has two different physical states, representing for example logical 0 and 1, interactions with the environment can alter the system's state and thus lead to logical errors. This idea will be discussed throughout the whole chapter.

5.1.1 Channels - sending and storing

Channels provide the most general formalism on how information can be sent from one party to another, see (82) for a general introduction. One advantage of using the channel picture of information is that it makes no assumption about the way a physical system encodes information. For a given physical system, the channel capacities determine how much information can be sent *in principle*. When dealing with biological systems, little is known for certain due to the complexity of the system. For a suitable approximation of the system, channel capacities allow to estimate the physically-possible information processing capacity, which is an upper bound on the actual information processing taking place. In the following I will explain some basics of channels. This knowledge will be used later to discuss possible quantum influences on the copying of genetic information in section 5.2.5.

In order to store or send information, its physical realisation needs to be stored or sent. A classical message is encoded in code words ρ_x , $x \in \{1...n\}$, which are sent through a channel denoted by G. A channel can be used once or several times, see fig. 5.2. Sometimes the message and the code word coincide. Each single letter of the Latin alphabet encodes its own message. However, the message of a single word is encoded in sequences of letters. Unless one writes Chinese, the message of a single word and its encoding is not the same. This will be important when dealing with the question how exactly information is encoded in biological systems, i.e. in which physical degree of freedom. Inevitably, sending the code words through a noisy channel will induce errors in the message. An elegant formalism to keep track of the information sent and to describe the main effects causing errors is given by the channel picture in computer science. In general a message is encoded into a physical system, which can constitute of one or more particles. This encoding, symbols, is sent through a usually noisy channel, after which a measurement determines the symbols and following decoding gives the retrieved message, see fig. 5.2. The channel G itself is usually defined in terms of Kraus operators. If the underlying physics of the channel is classical (quantum) it is referred to as a classical (quantum) channel.

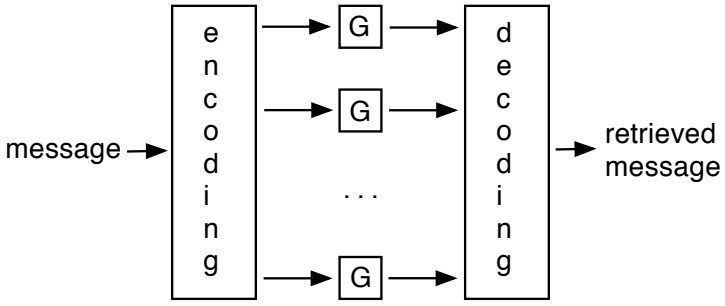

Figure 5.2: This graphic shows the most general description of a channel. A message is encoded into an alphabet of code symbols, which are sent through a possibly noisy channel G. After measurement of the symbols decoding gives the retrieved message. The channel can be used one time or several times.

In mathematical terms this is described as

$$\rho_{out} = G(\rho_{in}) = \sum_{i=1}^{M} E_i \rho_{in} E_i^\dagger \ , \tag{5.2}$$

where E_i are the Kraus operators fulfilling $\sum_{i=1}^{M} E_i^\dagger E_i = \mathbb{1}$, ρ_{in} is the input state, ρ_{out} the corresponding output state of the channel.
Suppose the alphabet consists of the letters $\{\rho_i, i \in \{1,2\}\}$ and there exists decodings that can perfectly distinguish the two states. The initial state is, for example, $\rho_{in} = \rho_1$. After passing through the noisy channel, the output state is $\rho_{out} = (1-p)\rho_1 + p\rho_2$, i.e. with probability $1-p$ the state is sent correctly as ρ_1 and with prob. p a different state, here ρ_2, exits the channel. An important question is how many bits k of information can be sent reliably through the channel G with n uses of the channel. In other words, what is the maximal rate $R \cdot n = k$ of sending reliably information? The maximal rate is also known as the channel capacity. In the following paragraph I will calculate the channel capacity for the simplest channel, the identity channel.

5.1.2 Identity Channel

Here I will consider the ideal scenario, namely the channel transmits the message correctly, without changing anything, i.e. $G(\rho) = \rho \ , \forall \rho \in \mathcal{H}$. The aim is to transmit k bits of information without error. It is possible to use the channel G n times, which

leads to a rate of transmission of $R = k/n$. A state ρ_x is chosen to encode the message x, $x \in \{0,1\}^{\otimes nR}$. After passing through the channel the output state is given by $\rho_{out} = G^{\otimes nR}(\rho_x)$. For the decoding a measurement POVM D_x is applied on the state ρ_{out} such that $Tr(D_x(\rho_x)) = 1$ while $Tr(D_x(\rho_{y\neq x}) = 0$.

The probability of decoding the state correctly is given by

$$P_{succ}(Rn = k) = \max_{\{D_x\}_x, \{\rho_x\}_x} \frac{1}{2^{nR}} \sum_{x\in\{0,1\}^{\otimes nR}} Tr\left(D_x(G^{\otimes nR}(\rho_x))\right) \ . \tag{5.3}$$

Note that for any channel G the maximisation is performed over all possible encodings (states ρ_x) and decodings (measurements D_x). For the identity channel the maximal rate, i.e. the channel capacity, can be determined analytically. Eq. 5.3 simplifies to

$$\begin{aligned} P_{succ}(Rn = k) &= \max_{\{D_x\}_x, \{\rho_x\}_x} \frac{1}{2^{nR}} \sum_{x\in\{0,1\}^{\otimes nR}} Tr\left(D_x(\rho_x)\right) \\ &\leq \max_{\{D_x\}_x} \frac{1}{2^{nR}} \sum_{x\in\{0,1\}^{\otimes nR}} Tr\left(D_x\right) \\ &\leq 2^{-nR} Tr(\mathbb{1}) \\ &= 2^{n(1-R)} \ , \end{aligned} \tag{5.4}$$

where in the second line the Cauchy-Schwarz inequality was used, and the dimension of the measurement POVM is $d = 2^n$. If the rate is chosen to be larger than one, i.e. $k > n$, the probability of decoding the message correctly drops exponentially. The best achievable rate is $R = 1$.

5.1.3 More channel capacities

The above scenario is valid both for classical and quantum channels. How is it possible to calculate channel capacities for more interesting cases than the identity channel? There is a useful theorem by Holevo-Schumacher-Westmoreland (82) which quantifies how much classical information can be sent through a noisy quantum channel with one use of the channel.

Theorem: Classical one shot capacity for noisy channels
Let G be a trace-preserving quantum operation. The one-shot classical capacity can

be calculated as

$$C^1(G) = \max_{\{p_j,\rho_j\}} \left[S\left(G\left(\sum_j p_j \rho_j \right) \right) - \sum_j p_j S(G(\rho_j)) \right] \quad , \tag{5.5}$$

where S denotes the von Neumann entropy. It can be shown that the maximisation of 5.5 may be achieved using an ensemble of at most d^2 pure states, where d is the dimension to the input channel.

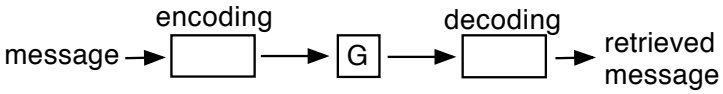

Figure 5.3: The one shot classical capacity quantifies how much information can be sent reliably if the channel G can be used only once.

It is straightforward to generalise the classical channel of 1 use, see fig. 5.3, of a quantum channel to n uses:

$$C^n(G) = \max_{\{p_j,\rho_j \in \mathcal{H}^{\otimes n}\}} \left[S\left(G^{\otimes n}\left(\sum_j p_j \rho_j \right) \right) - \sum_j p_j S(G^{\otimes n}(\rho_j)) \right] \quad . \tag{5.6}$$

If in addition sender and receiver also share an infinite amount of entanglement, they can use this entanglement to improve transmission of classical information (83, 84, 85), see fig. 5.4. The maximal transmission rate is now termed 'entanglement assisted classical capacity' and can be calculated in the following way :

$$C_E = \max_{\rho \in H} \left(S(\rho) + S(G(\rho)) - S((G \otimes \mathbb{1}_{anc})(\Phi)) \right) \quad , \tag{5.7}$$

where S is the von Neumann entropy, G the genetic channel and Φ the purification of ρ on the larger Hilbertspace.

Similar channel capacities exist for sending quantum information. The channel capacities (83, 85, 86, 87) are calculated as

$$Q_1 = \max_{\rho \in H} \left(S(G(\rho)) - S((G \otimes \mathbb{1}_{anc})(\Phi)) \right) \tag{5.8}$$

$$Q_E = C_E/2 \quad , \tag{5.9}$$

where Q_1 is the one-shot quantum capacity and Q_E denotes the entanglement assisted quantum capacity.

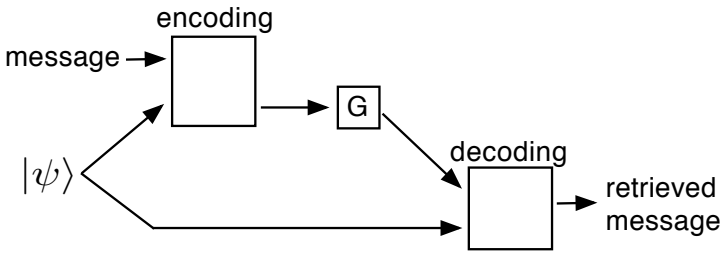

Figure 5.4: If the sender of the message and the receiver share initial entanglement denoted by $|\psi\rangle$, they can enhance both classical and quantum channel capacity, by applying teleportation protocols.

5.1.4 Examples of information processing in biology

When reading the words 'information processing' one thinks with a high likelihood of a computer, which is a well understood deterministic system. The basic unit of a computer is a transistor. Electrical currents control the flow of each single bit of information. On the contrary, biological systems are messy. Even a single cell consists of a plethora of different molecules. Everything moves and wiggles around. Instead of deterministic calculations, everything is based on statistical interaction. Two molecules only interact if they meet by chance. Yet, even in this chaos, there is an intricate information processing taking place. One type of molecule usually interacts non-trivially only with one or two other types of molecules.

This conditional interaction constitutes a powerful feedback system, keeping the cell in a functional non-equilibrium state. In the following I will mention some examples of molecules processing or storing information (88).

- DNA - information storage

  Deoxyribonucleic acid, or DNA, is a nucleic acid that contains the genetic instructions used in the development and functioning of all known living organisms. The main role of DNA molecules is the long-term storage of information. DNA is often compared to a set of blueprints, like a recipe or a code, since it contains the instructions needed to construct other components of cells, such as proteins and RNA molecules. The DNA segments that carry this genetic information are called genes, but other DNA sequences have structural purposes, or are involved in regulating the use of this genetic information. Along with RNA and proteins,

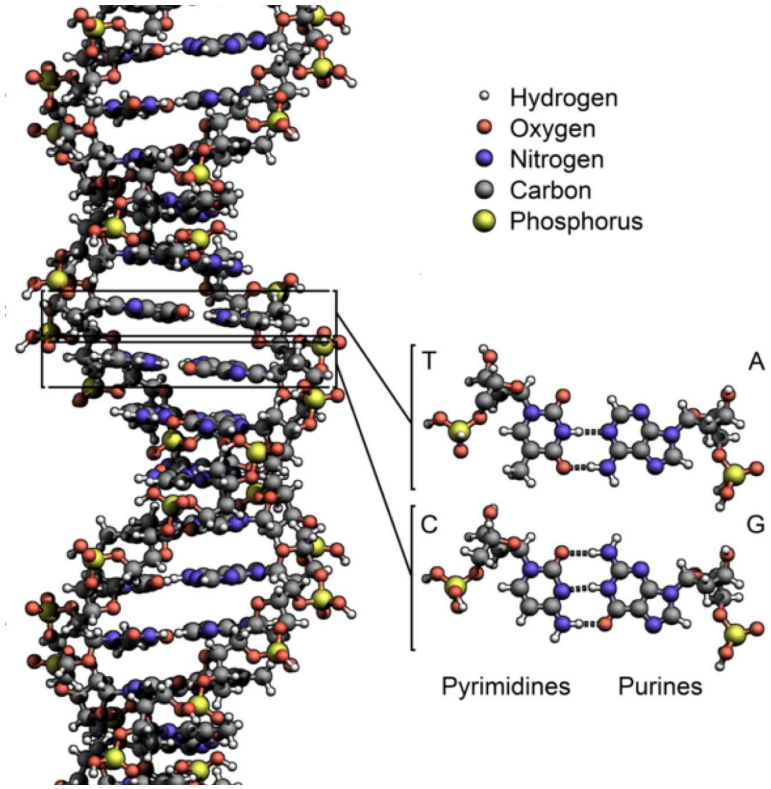

Figure 5.5: The B-DNA helix (89) consists of thymine-adenine and cytosine-guanine base pairs, held together by phosphor bonds at the backbone. T and C are larger nucleic bases, and constitute the pyrimidines, whereas the smaller nucleic acids A and G are purines. Two factors contribute to the base pairing: the position of protons and the size of base pairs.

DNA is one of the three major macromolecules that are essential for all known forms of life.

DNA consists of two long polymers of simple units called nucleotides, with backbones made of sugars and phosphate groups joined by ester bonds. These two strands run in opposite directions to each other and are therefore anti-parallel. Attached to each sugar is one of four types of molecules called nucleobases (informally, bases). It is the sequence of these four nucleobases along the backbone that encodes information. This information is read using the genetic code, which specifies the sequence of the amino acids within proteins. The code is read by copying stretches of DNA into the related nucleic acid RNA, in a process called

transcription.

- DNA polymerase- information read out and copying
  A DNA polymerase is an enzyme that helps catalyze in the polymerization of deoxyribonucleotides into a DNA strand. DNA polymerases are best-known for their feedback role in DNA replication, in which the polymerase "reads" an intact DNA strand as a template and uses it to synthesize the new strand. This process copies a piece of DNA. The newly-polymerized molecule is complementary to the template strand and identical to the template's original partner strand.

- Transcription- from DNA to RNA
  Transcription is the process of creating a complementary RNA copy of a sequence of DNA. Both RNA and DNA are nucleic acids, which use base pairs of nucleotides as a complementary language that can be converted back and forth from DNA to RNA by the action of the correct enzymes. During transcription, a DNA sequence is read by RNA polymerase, which produces a complementary, antiparallel RNA strand. As opposed to DNA replication, transcription results in an RNA complement that includes uracil (U) in all instances where thymine (T) would have occurred in a DNA complement.

- Kinase
  In chemistry and biochemistry, a kinase, alternatively known as a phosphotransferase, is a type of enzyme that transfers phosphate groups from high-energy donor molecules, such as ATP, to specific substrates. The process is referred to as phosphorylation, One of the largest groups of kinases are protein kinases, which act on and modify the activity of **specific** proteins. Kinases are used extensively to transmit signals and control complex processes in cells. Up to 518 different kinases have been identified in humans. The enormous diversity, as well as their role in signalling, makes them an object of study.

5.1.5 Biology's measurement problem

One of the key questions in biology is how certain molecules are recognised (= 'decoding' in channel capacity language). A good example for the complexity of this problem is the olfactory sense. Our nose enables us to acquire information about our surroundings by

identifying fragrant molecules in the air. If it smells of smoke, we know we are in danger of fire. The question is how a human perceives the smell of a certain molecule, and which molecules smell similar and which smell different. One of the scientific approaches to identifying a molecule is to specify which atoms bond to each other. This leads to the well known graphical representations filling chemical textbooks. It might have been this static, visual representation that lead scientists to believe that the sense of smell has something to do with the shape of a molecule. Recent experimental evidence on fruit flies (90) implies the contrary, namely that not the shape, but the vibrations of a molecule characterise its smell. This leads to the question how biological systems perform measurements? Which degrees of freedom, e.g. shape or vibration, participate in the measurement? Physicists spend a great deal of time discussing the question of what exactly constitutes a measurement. While there is no final agreement on the philosophical aspects, at least there is a useful mathematical formalism describing how a system and its measurement device interact, such that the measurement device is able to read out information about the system. I model the measurement problem in biology, i.e. how one molecules recognises the identity of another molecule, in the following way. One molecule acts as a measurement device on the target molecule. In the olfactory sense, the receptors in our nose constitute the measurement device, and the fragrant molecules the target. The target's degrees of freedom that do not participate in the measurement process are denoted by $|x\rangle$. The target's quantum degrees participating are denoted by $|\psi_x\rangle$ in the pure case, and ρ_{Qx} in the generalised mixed case. The measurement apparatus starts in a pure state $|\Phi_0\rangle$. The interaction between the system - molecule and measurement apparatus is given by the unitary time evolution $\hat{U}(t) = e^{i\hat{H}_{int}t/\hbar}$,

$$|x\rangle \otimes \hat{U}(t)\left(|\psi_x\rangle \otimes |\Phi_0\rangle\right) = |x\rangle \otimes \sum_i c_i(t)|\xi_i\rangle|\Phi_i\rangle \ . \tag{5.10}$$

In general the measurement will change the target's quantum state $|\psi_x\rangle$, such that the resulting target's quantum states after the measurement are $|\xi_i\rangle$. Note that neither the accessible set of states $\{|\psi_x\rangle\}$ before the measurement nor the accessible set of states $\{|\xi_i\rangle\}$ after the measurement need to be mutually orthogonal. In a physics experiment the measurement device's states are usually chosen such that different measurement outcomes j, k are perfectly distinguishable, i.e. $\langle\Phi_k||\Phi_j\rangle = \delta_{kj}$. While this is the best choice for minimising measurement mistakes, there might be other chemical constraints

leading to not perfectly distinguishable measurement states. Ideally, the interaction $\hat{U}(t)$ is such that $|c_x(t)|^2 = 1$, i.e. the measurement outcome is always correctly x. While it is in general too difficult to give a closed form of the time evolution, it can be written in terms like

$$\hat{U}(t)|kl\rangle \approx e^{i(\omega_k - \omega_l)t}|kl\rangle \ , \tag{5.11}$$

where $|kl\rangle$ represents the diagonal basis of the system-measurement interaction with corresponding eigenvalues ω_l, ω_k. That means in general the time evolution of two interacting states $|kl\rangle$ will depend on the relative value of their eigenvalues. If the eigenvalues are nearly the same, the states will evolve very slowly, in the extreme case of $\omega_k = \omega_l$ the states will not evolve at all. If the eigenvalues are of different orders of magnitude, the states $|kl\rangle$ will evolve rapidly.

Here, at the moment when the measurement takes place, is a possibility to externally alter the measurement outcome. If in addition to the measurement interaction an external field is applied, in general the eigenvalues are going to change. Consider the scenario that $0 < \omega_k - \omega_l << 1$, i.e. the eigenvalue ω_k is just a little larger than ω_l. If an external field makes ω_k a little smaller, then suddenly $0 > \omega_k - \omega_l$, i.e. the exponent of the time evolution has a different sign! This will give rise to a possibly completely different time evolution of the state. The possibility that weak fields change the measurement outcome of such a biological measurement, thus leading to errors in the cell's information processing, will be discussed in section 5.1.8.

5.1.6 Does QM play a non-trivial role in genetic information processing?

DNA stores the blueprints for sequences of amino acids, which fold into functional proteins. These sequences consist of classical information, there is little need to invoke quantum information processing. But the processing of genetic information relies on chemical reaction. As seen in chapter 2, even small amounts of energy can change the outcome of chemical reactions. Is there a way the laws of QM contribute non-trivially to the processing of genetic information? In previous literature (91) this was denied, arguing with the impossibility to copy quantum information perfectly, the so called 'no-cloning theorem' (82). Although it is evidently impossible to design a quantum information replicator, this says nothing about the possibility of employing quantum

assisted copying of classical information. The following sections will deal with the question to which extent quantum degrees of freedom can influence information processing in biological systems.

5.1.7 Classical quantum states in genetic information

It is in general not an easy problem to decide what exactly constitutes a quantum effect. The scientific community itself still discusses which parts of quantum computing are *really* quantum. In the following, I will introduce a pragmatic definition of what can be considered quantum and classical in a biological system. The idea underlying the Born-Oppenheimer approximation, i.e. separating molecules into a classical and quantum part, is as follows: A key difference between classical and quantum physics is that quantum particles can exist in a superposition of two or more states. Consequently, the classical part of a molecule is defined as everything that is, for all practical purposes, impossible to superimpose, because, for example, it is too heavy. Straightforwardly, everything about a molecule that can exist in superpositions, is considered to be the quantum part of a molecule. Usually both the electrons and single protons can exist in superposition of different states. Only in very controlled experimental situations can whole molecules show interference properties (92).

I propose to use cq states for describing information processing in living systems. The chemical identity of a molecule, given mainly by the nuclei, constitutes without doubt classical information. However, the processing of this classical information is governed by chemical reactions. Therefore, quantum degrees of freedom presumably influence the flow of biological information by governing the outcome of chemical reactions.

The mathematical definition of a cq state is

$$\rho_{cq} = \sum_{x \in \Sigma} p_x |x\rangle\langle x| \otimes \rho_{Q,x} \ , \tag{5.12}$$

where the first classical part $|x\rangle\langle x|, x \in \Sigma$, Σ being the corresponding alphabet of the biological problem, describes the classical information (=message) of, for example, the identity of a molecule, say adenine or cytosine. The second part $\rho_{Q,x}$ represents the corresponding quantum part of the molecule, which is determined by the classical information x. This quantum part plays a crucial role for the outcome of chemical

reactions and will constitute in the following paragraphs the code words in the channel formalism. The term $p_x \geq 0$ with $\sum_{x\in\Sigma} p_x = 1$ describes the probability that molecule x enters the chemical reaction. As it is impossible to superimpose different classical information in the same space volume there are no off diagonal elements in the first part. The second part describes its corresponding quantum state, i.e. the electronic degrees of freedom and possibly also the single protons constituting the H-bonds in DNA base pairs.

For example, consider the protons of the nucleic acid cytosine, see fig. 5.6.

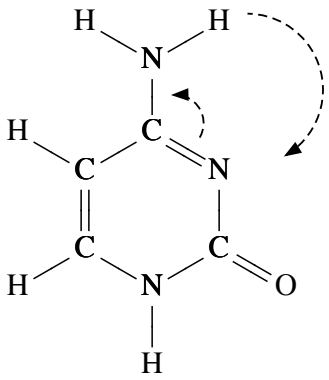

Figure 5.6: This figure shows the normal form of the nucleic acid cytosine. If sufficient energy is applied, the upper right proton can tunnel to the middle nitrogen atom, see dotted arrow, leading to the tautomeric form. At the same time the electronic double bond switches accordingly.

The proton position at the upper nitrogen atom is the ground state of the molecule. However, it is also possible that the proton binds to the middle nitrogen, see dotted arrow in fig. 5.6, which requires a higher energy. It is conjectured (93) that the proton distribution of nucleic acids determines the copying process of genetic information. This idea will be discussed in detail in section 5.2. In order to focus on the key aspects of this copying process, a simplified version of nucleic acids will be developed.

Instead of having four different genetic letters, only two, denoted by logical '0' and '1', will be considered. Let me consider the example of two molecules encoding logical '0' and '1'. Because they are different molecules the single protons 'see' different potentials for their position. Fig. 5.7 shows an example of proton position coding.

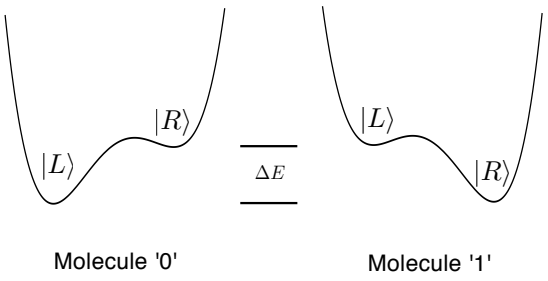

Figure 5.7: I consider the scenario that information is encoded in the position of a single proton (left or right). This figure shows the potential for a single proton for two different molecules. If the energy gap ΔE between ground state and first excited state is sufficiently big, the ground state can be used reliably to encode classical information, here logical '0' is encoded in $|L\rangle$ and logical '1' in $|R\rangle$. For finite temperature the tunnel probability to the excited state gives rise to errors in this encoding.

Assuming that information is encoded in the ground states, the cq states of this coding scheme are

$$\rho_0 = |0\rangle\langle 0| \otimes |L\rangle\langle L| \tag{5.13}$$

$$\rho_1 = |1\rangle\langle 1| \otimes |R\rangle\langle R| \ . \tag{5.14}$$

The two different molecules represent different classical information, i.e. different nuclei coordinates. This leads in the Born-Oppenheimer approximation to different potentials for the quantum part of the molecules.

In general, each molecule has its own unique quantum part. In this example, the ground state $|L\rangle$ encodes the classical information 0. However, the excited state of molecule '1' is also given by $|L\rangle$. That means if molecule '1' is in its excited state, it could be mistaken to be molecule '0'. This idea will be explained in more detail in the following paragraphs of the chapter.

The key ideas of using cq states to describe information flow in biological systems are the following:

(1) The classical information of the identity of molecules is encoded in the quantum states of each molecule.

(2) Chemical reactions only interact with the quantum part $\rho_{Q,x}$ of molecule x.

(3) If environmental influences change the quantum part of a molecule, logical errors

for the classical information can occur, for example because the altered quantum part leads to different chemical reactions.

If we continue to model chemical reactions in the channel picture, then each molecule has its own set of Kraus operators describing the possible ways to act on the cq state of the molecule. In general it is very difficult to correctly describe all environmental influences that could change the quantum part of a molecule. One cause of error is body temperature, leading to a thermal state of the quantum part, see sec. 5.2.4. But also weak oscillating fields could corrupt the signal, see chapter 2 and the following paragraph. Finally, in sec. 5.4 of this chapter I will discuss the possibility that neighbouring nucleic acids within a strand of DNA influence the probability of changing the quantum state of a certain nucleic acid.

Because of the interplay between the classical and the quantum part of molecules it is important to treat both parts together in the same formalism provided by the cq states.

5.1.8 Weak external fields

Ever since mankind started changing its environment, people have discussed the possible consequences for ourselves. With the intensive use of radio signals the potentially harmful influence of so called 'electro-smog' is investigated. It is an ongoing discussion whether electro-smog, here modelled as weak external fields, can influence living systems despite its weak amplitude. Mean field models, neglecting quantum details, usually cannot find a possible influence (2). However, in this paragraph I show how arbitrarily weak fields, if on resonance, can alter information processing in living systems.

Suppose there is one type of molecule, denoted by logical '0', whose quantum degree of freedom can be approximated as a pure state $|\psi_0\rangle$. The corresponding cq-state takes the form $\rho_0 = |0\rangle\langle 0| \otimes |\psi_0\rangle\langle\psi_0|$. Similarly, there exists another type of molecule, denoted by logical '1', whose quantum degree of freedom can be approximated as pure state $|\psi_1\rangle$, leading to the cq-state $\rho_1 = |1\rangle\langle 1| \otimes |\psi_1\rangle\langle\psi_1|$. In addition I assume that $\langle\psi_0|\psi_1\rangle = 0$, i.e. under normal situations the two molecules can in principle be perfectly distinguished. Let me furthermore suppose that there exists an excited quantum state $|\Psi_0\rangle$ of molecule '0' which resembles the quantum state of molecule '1', s.t. $\langle\Psi_0|\psi_1\rangle \approx 1$.

That means the excited state of one type of molecules resembles the ground state of another type. Normally this does not cause problems, because I defined $|\psi_0\rangle$ as the quantum state that molecule '0' typically exists in. However, a weak field on resonance with the energy gap between the states $|\psi_0\rangle$ and $|\Psi_0\rangle$ can change the quantum part of molecule '0', such that

$$\hat{E}_{ext}\rho_0\hat{E}_{ext}^{\dagger} = |0\rangle\langle 0| \otimes (p_0|\psi_0\rangle\langle\psi_0| + p_1|\Psi_0\rangle\langle\Psi_0|) \quad , \tag{5.15}$$

where I assumed that the cell environment destroys any coherence between the states $|\psi_0\rangle$ and $|\Psi_0\rangle$, and $p_{0,1}$ are the corresponding probabilities to be in the state $|\psi_0\rangle, |\Psi_0\rangle$. Now, with probability p_1, the target molecule is mis-decoded as logical '1'. The key question is which values p_1 can have, i.e. how strongly an external field can corrupt a quantum state.

In the following part of this section I will review results from (94) on quantum resonance to answer this question.

Molecule '0' has two states of importance, $|\psi_0\rangle$ and $|\Psi_0\rangle$. A two level system is described by the Hamiltonian

$$H = \frac{\hbar}{2}\Delta\sigma_z \quad , \tag{5.16}$$

where σ_z denotes the pauli z matrix, and $\hbar\Delta$ is the energy gap between ground and excited state. In general $\hbar\Delta >> k_BT$, otherwise the signal would be too easily corrupted by thermal noise. Even small external fields, if on resonance, can have a large impact on a quantum system. If the system is under influence of a weak external field oscillating in the $x-y$ plane, it is described by

$$H = \frac{\hbar}{2}\Delta\sigma_z + \frac{\hbar}{2}A\cos(\omega t)\sigma_x + \frac{\hbar}{2}A\sin(\omega t)\sigma_y \quad , \tag{5.17}$$

with $\sigma_{x,y}$ being the Pauli x, y matrix, A the amplitude of the external field, and ω the frequency of its oscillation. A suitable rotation brings this system into the form

$$H_{eff} = -\frac{1}{2}\hbar\alpha\sigma_a \quad , \tag{5.18}$$

with

$$\begin{aligned} \sigma_a &= \frac{(\Delta+\omega)\sigma_z + A\sigma_x}{\alpha} \\ \alpha &= \sqrt{(\Delta+\omega)^2 + A^2} \quad , \end{aligned} \tag{5.19}$$

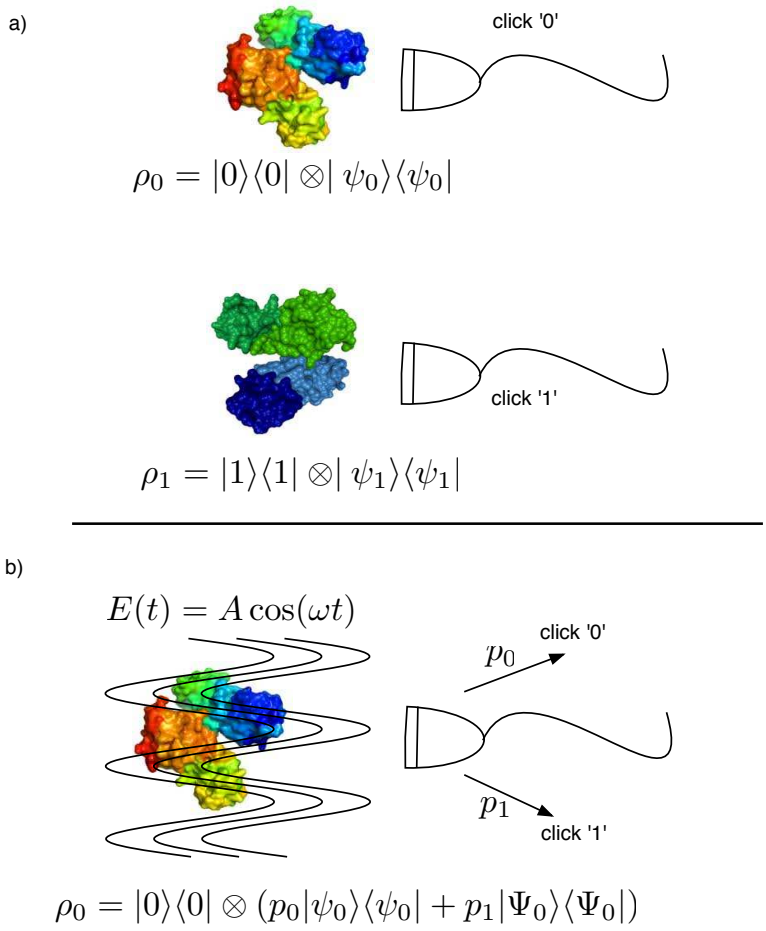

Figure 5.8: This graphic sketches the recognition of molecules by using their quantum degree of freedom. In *a* the normal situation is shown, where two different kinds of molecules have two different quantum states, and are thus reliably distinguishable. In *b*, a noise field is applied on the molecule encoding logical '0'. The effect of the noise field, see main text for detailed explanation, is to change the quantum state, such that it is mis-decoded with probability p_1.

Is it possible that this weak field can corrupt the signal by bringing the system into the excited state? The probability to find the system in the excited state at time T is given by

$$P_{exc} = \left| \frac{A}{\alpha} \sin\left(\frac{1}{2}\alpha T\right) \right|^2 \quad , \tag{5.20}$$

This formula has a time dependant oscillating part, and an amplitude part. The am-

plitude is

$$\frac{A^2}{\alpha^2} = \frac{A^2}{(\Delta+\omega)^2 + A^2} \leq 1 \ , \tag{5.21}$$

The maximum is taken at resonance $\Delta+\omega = 0$, which is given when the oscillating field rotates in clockwise direction. No matter how small the amplitude A of the external field, if the frequency ω is sufficiently close to resonance, the probability for the system to be in the excited state reaches 1 and will then oscillate. That means that even very weak external fields can have a non-trivial influence on living systems, *if they resonate with coding quantum states*. This is exactly what is happening in the avian compass, see chapter 2. A very weak oscillating field is able to corrupt the bird's sense of magnetoreception, because it is on-resonant with the two important quantum states needed for navigation.

5.2 Copying genetic information

In the previous section I discussed abstract properties of channels and measurements. In this section I will apply these concepts to the problem of copying genetic information.

DNA stores the genetic blueprint for assembling functional proteins. The genetic alphabet consists of four nucleic acids, adenine, cytosine, guanine and thymine. All nucleic acids are mostly planar, and can thus be easily put into sequence. In addition, H-bonds allow the nucleic acids to form pairs of two, adenine-thymine and cytosine-guanine, see fig. 5.9. Sequences of these two base pairs form the double helix.

Both when DNA is replicated and genes are read-out (transciption), the information stored in DNA needs to be accessed. The double strand is separated into two single strands, each serving as a template for copying.

The molecule DNA polymerase reads out the genetic information stored in the single strand, namely the sequence of four different nucleic acids, and assembles a complementary DNA strand. Following the line of argument of the previous section, it is now time to discuss which physical degrees of freedom participate in the measurement.

The bonding properties of nucleic acids are determined by two parameters. Firstly, the proton positions have to be anticorrelated, to allow hydrogen bonding, see fig. 5.9. Secondly, the nucleic acids have different sizes. Adenine and guanine are purines, i.e. big (b) molecules. On the other hand, cytosine and thymine are pyrimidines, i.e. small (s) molecules. The width of DNA, including the base pair and its phosphate backbone,

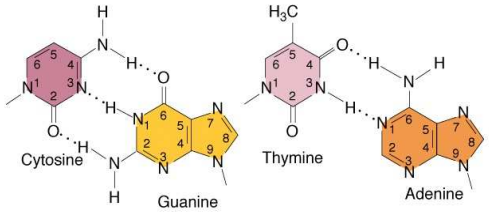

Figure 5.9: In the normal form, the ground state of the molecules, there are two possible nucleic acid combinations, adenine-thymine and cytosine-guanine, so called base pairs. Two parameters determine the base pairing. The proton position of the two nucleic acids have to be anti-correlated, to allow H-bonding. In addition, purines, i.e. the bigger molecules, are matched with pyrimidines, i.e. the smaller molecules, such that the total width of the two different base pairs is the same.

is limited to about $2nm$, that means the small and big molecules are matched. If two small (big) nucleic acids bind, the resulting position in the DNA is strand is to narrow (thicken), and this error is corrected. This is summarised in fig. 5.9 and eq. 5.22.

The following equations summarise in informal notation the two parameters determining how nucleic acids bind. This notation will never be used in any formula and just serves to emphasise certain aspects of nucleic acids. The first ket denotes the proton position distribution, where 0 represents no proton, and 1 represents proton present at that position in the nucleic acid, compare with Fig. 5.9. The second ket describes the size of the nucleic acids, i.e. either purines (b) or pyrimidines (s).

$$\begin{aligned} \text{Adenine} &= |001\rangle|b\rangle \\ \text{Cytosine} &= |001\rangle|s\rangle \\ \text{Guanine} &= |110\rangle|b\rangle \\ \text{Thymine} &= |010\rangle|s\rangle \quad . \end{aligned} \tag{5.22}$$

When reading out the information stored in DNA, both degrees of freedom are accessed. This is necessary, because the proton distribution itself does not allow to distinguish Adenine and Cytosine.

5.2.1 Mutations and its causes

Although DNA replication is in general quite precise, it is not perfect. Copying errors are usually referred to as mutations. Some mutations are due to classical physics, for example breakage of DNA strands. Other errors like point mutation (substituting one genetic letter with a different one) and $\pm x$ frameshift mutations, i.e. inserting or deleting x nucleic acids in a single DNA strand, are more difficult to explain. While the approximate mutation rate (copy errors per genome per generation) for most organisms is known, little is understood about the mechanism how and why these mutations actually occur. Using the concepts of computer science, the problem is phrased as follows: It is known that the storage of genetic information constitutes a noisy channel. Similarly, copying genetic information is also subject to noise. It is unknown how to best describe the channels, i.e. which physical processes exactly are the cause for a mutation. Löwdin argued (93) that tautomeric forms of nucleic acids, i.e. excited nucleic acids having a different proton distribution, may be the cause of point and frameshift mutations. For an overview on mutation see (95).

5.2.2 Tautomeric base pairing

While the size of a nucleic acid cannot be changed or superimposed, the proton position of a nucleic acid can be altered. It was proposed by Löwdin (93) that such a shift in proton position can be the cause of point mutations, see also fig. 5.11. Following the concepts of the previous section, the size of a nucleic acid is part of the classical degrees of freedom, whereas the proton positions are treated as quantum degrees of freedom.

Shifting protons changes the energy of the nucleic acid. The amount of energy required to do that exceeds kT by roughly an order of magnitude, see later discussion, so this is a rare event. If one of the nucleic acids is in its tautomeric form, the binding to other nucleic acids changes, as summarised in fig. 5.10.

Using the same informal notation as above, the shifted proton position are sum-

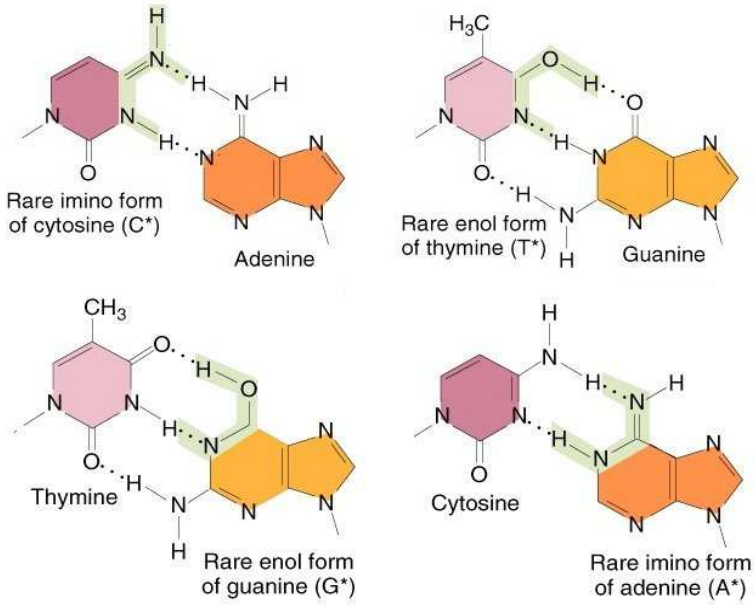

Figure 5.10: When one of the nucleic acids is in an excited tautomeric form, the proton position is changed. Adenine*, for example, cannot bind any longer with thymine, because the protons would repel each other. Instead, it is now possible to bind with cytosine.

marised as follows:

$$\begin{aligned} \text{Adenine}^* &= |010\rangle|b\rangle \\ \text{Cytosine}^* &= |010\rangle|s\rangle \\ \text{Guanine}^* &= |101\rangle|b\rangle \\ \text{Thymine}^* &= |001\rangle|s\rangle \quad . \end{aligned} \tag{5.23}$$

Fig. 5.10 shows how the altered proton position leads to different base pairing. As the tautomers constitute an excited state, they will automatically return to the ground state after a while. Only if the genetic information is copied during the lifetime of the tautomer, it causes a mutation.

5.2.3 Non-coding tautomeric base pairing

In the previous section I discussed the nucleic acid's base pairing properties for the case that a single nucleic acid is in a tautomeric form, which is mis-interpreted as a different

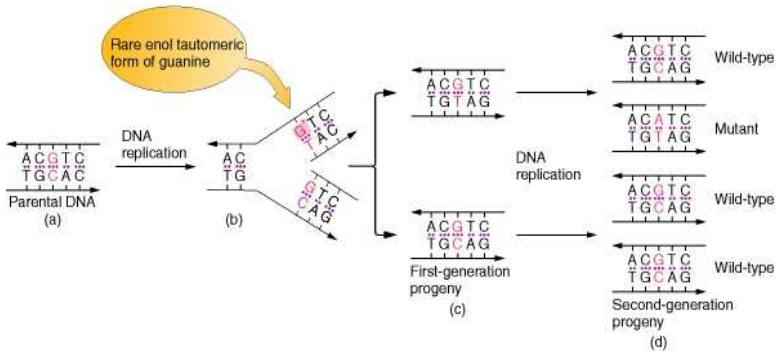

Figure 5.11: This picture shows how a tautomeric form (unstable) can be transformed into a permanent mutation in the copying processes. In *a* the parental DNA is in its normal form. After the double helix was opened to access the nucleic acids in the single strand, the guanine molecule became excited into its tautomeric form. G^* is now matched with thymine instead of adenine, *b*. While one of the two resulting first generation daughter strands is a perfect copy, the other has an abnormal $G^* - T$ base pair, *c*. In the next copying process, *d*, the abnormal base pair is copied into two normal base pairs, one having a permanent point mutation, replacing the inital guanine-cytosine pair with a adenine-thymine pair.

genetic letter, leading to different base pairing. This is important for dividing cells. But also stationary, i.e. non-dividing, cells are subject to mutations. One explanation is given by single and double proton tunneling within a base pair.

5.2.3.1 Double proton tunnelling

Base pairs are held together by the H-bonds between the nucleic acids, two proton bonds for an $A - T$ pair and three for a $C - G$ pair. In an H-bond, the proton is in a covalent bond with its original bonding atom, and interacts non-covalently with the closed electron orbitals of the oxygen or nitrogen atom of the other molecule. It is possible that protons tunnel from their original molecule to the other molecule. When two protons tunnel within a base pair, the excited base pair resembles the other one concerning proton position, i.e. $A^* - T^* \approx G - C$ and $C^* - G^* \approx T - A$. When a DNA polymerase reads out the genetic information, it separates the two strands. The altered proton position is measured and gives rise to a genetic error. This is widely believed to be a cause for point mutations.

5.2.3.2 Single proton tunneling

In the previous examples about tautomeric base pairing, one genetic letter was misinterpreted to be a different genetic letter, which can lead to a mutation. However, there are also excited states, caused by single proton tunneling, which do not resemble any genetic letter, for example:

$$\begin{aligned} \text{Adenine}^\dagger &= |011\rangle|b\rangle \\ \text{Cytosine}^\dagger &= |011\rangle|s\rangle \\ \text{Guanine}^\dagger &= |100\rangle|b\rangle \\ \text{Thymine}^\dagger &= |000\rangle|s\rangle \ . \end{aligned} \tag{5.24}$$

This proton position coding scheme is not recognised as a valid genetic letter. It is believed that such a single proton tunneling event is the cause for -1 frameshift deletions. When DNA polymerase finds this excited base pair, it is taken out of the DNA strand because it does not resemble a valid DNA base pair.

5.2.4 The thermal error channel

Whenever information is encoded in a specific quantum state of a molecule at finite temperature, there is an error probability that the molecule is brought into a different state by interactions with the environment. Section 5.1.8 discussed the possibility that a weak, resonant external field might corrupt the quantum signal. A more common source of errors is temperature. I will show the effects of temperature on the example introduced in section 5.1.7. The system consists of two different classical letters, '0' and '1', where the ground state of the molecules encoding '0' is left $|L\rangle$ and '1' is right $|R\rangle$. There is an energy barrier ΔE to the first excited state. If, due to thermal energy, the molecule encoding logical '0' is in its first excited state $|R\rangle$, by measuring its quantum part, it will be mis-decoded. At zero temperature, the excited state of a molecule has a finite probability to decay into the ground state, while the ground state cannot become excited, as there are no energy quanta available. At finite temperature, the situation changes. Both ground and excited state have a non-zero probability to become corrupted. This is a well known physical problem. Which quantum operation describes the effect of dissipation to an environment at finite temperature? This process,

generalised amplitude damping (GAD), is defined for single qubits by the operation elements (82)

$$E_1 = \sqrt{p}\begin{pmatrix} 1 & 0 \\ 0 & \sqrt{1-\gamma} \end{pmatrix} \tag{5.25}$$

$$E_2 = \sqrt{p}\begin{pmatrix} 0 & \sqrt{\gamma} \\ 0 & 0 \end{pmatrix} \tag{5.26}$$

$$E_3 = \sqrt{1-p}\begin{pmatrix} \sqrt{1-\gamma} & 0 \\ 0 & 1 \end{pmatrix} \tag{5.27}$$

$$E_4 = \sqrt{1-p}\begin{pmatrix} 0 & 0 \\ \sqrt{\gamma} & 0 \end{pmatrix} \ , \tag{5.28}$$

with $\gamma = 1 - e^{-t}$, t time and $p \in [0,1]$. For $p = 0$ or $p = 1$ the channel reduces to an amplitude damping channel. The input state

$$\rho_{in} = \begin{pmatrix} p_L & c_{LR} \\ c_{LR}^* & 1-p_L \end{pmatrix} \ , \tag{5.29}$$

where p_L is the probability that the particle is in the left well, and c_{LR} describes the coherences of the particle being in the between left or right potential well, exits the GAD channel as $\rho_{out} = \sum_{i=1}^{4} E_i \rho_{in} E_i^\dagger$ with

$$\rho_{out} = \begin{pmatrix} p_L(1-\gamma)+p\gamma & c_{LR}\sqrt{1-\gamma} \\ c_{LR}^*\sqrt{1-\gamma} & 1-p_L(1-\gamma)-p\gamma \end{pmatrix} \ . \tag{5.30}$$

The steady state is achieved for $t \to \infty$ or $\gamma \to 1$ and is given by

$$\rho_\infty = \begin{pmatrix} p & 0 \\ 0 & 1-p \end{pmatrix} \ . \tag{5.31}$$

This final state is equivalent to a thermal state for $p = \frac{e^x}{e^x+e^{-x}}$ with $x = \frac{\hbar\Delta_0}{2k_BT}$, where $\hbar\Delta_0$ is the energy gap to the first excited state of molecule '0'. The thermal state is

$$\rho_{Therm} = \frac{e^{-\beta H}}{Z} = p_L|L\rangle\langle L| + p_R|R\rangle\langle R| \ , \tag{5.32}$$

where $\beta = \frac{1}{k_BT}$ the inverse temperature and $Z = Tr(e^{-\beta H})$ is the partition function. The probabilities are given as

$$p_L = \frac{e^x}{e^x + e^{-x}} \qquad p_R = \frac{e^{-x}}{e^x + e^{-x}} \ . \tag{5.33}$$

The larger the temperature, the more likely to find the molecule in its excited state. Now, at finite temperature, the cq state takes the form

$$\rho_{cq} = |0\rangle\langle 0| \otimes (p_L|L\rangle\langle L| + p_R|R\rangle\langle R|) \ . \tag{5.34}$$

Fig. 5.12 and 5.13 show the probabilities to be in the excited state. The larger the temperature T compared to the energy gap $\hbar\Delta$, the larger the probability for the molecule to be in the excited state, i.e. only for low temperatures do ground states provide a good coding scheme.

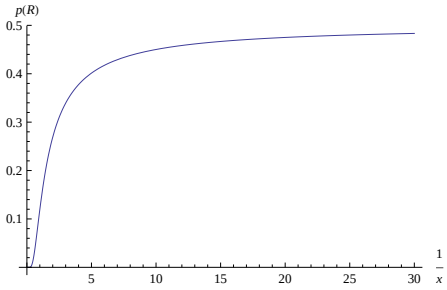

Figure 5.12: This graphic shows the probability to be in the excited state p_R dependent on $\frac{1}{x} = \frac{2k_BT}{\hbar\Delta}$. For large temperatures, the error probability approaches asymptotically 1/2.

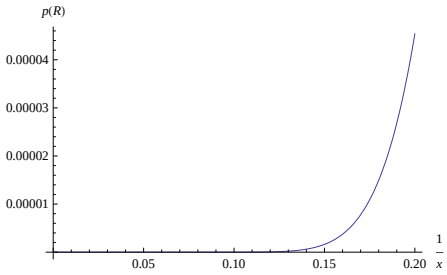

Figure 5.13: This graphic shows the probability to be in the excited state p_R dependent on $\frac{1}{x} = \frac{2k_BT}{\hbar\Delta}$ for small temperatures.

5.2.5 Channel picture of genetic information

A quantum system can have many degrees of freedom. Modelling many degrees of freedom exactly is practically impossible. Therefore, the analysis is usually restricted to small systems, which are well approximated by a small number of dimensions. Examples include glass fibre cables, electro-magnetic waves and single spins in quantum dots. Here, in contrast, I want to quantify the amount of information transmitted in

DNA. DNA stores reliably classical information. There are earlier attempts to quantify the amount of information processed in genetic channels, see (96). However, this work focuses entirely on classical channels. In the following I will show that even in the absence of quantum coherences, the mere existence of a quantum channel can in principle influence non-trivially the flow of genetic information.
There is good reason to believe that the quantum part of nucleic acids contributes to the information processing, which a purely classical description cannot capture. In order to study the influence of quantum information on genetic channels, I will investigate different channel capacities for a simplified genetic system. Instead of four nucleic acids I will only model two genetic (classical) symbols, denoted by '0' and '1'. The principle of proton position coding for genetic symbols is kept but simplified. Only one proton can be in either (or both) wells of a skewed double well potential, see fig. 5.7.

For genetic / logical 0 the ground state consists of proton left $|L\rangle$, and the first excited state of proton right $|R\rangle$, and vice versa for genetic 1. The quantum part interacts with an environment at finite temperature. Each molecule is excited with rate γ_{exc}, and decays with rate γ_{dec}. If a molecule, while copying, is detected in the excited state, it is switched with rate σ to the complementary genetic symbol. Fig. 5.14 summarises the combined classical and quantum aspect of genetic information for a simple model.

In section 5.1.7 I already discussed the scenario of a molecule identifying other molecules by measuring their quantum degree of freedom. If the target molecule occupies a 'wrong' quantum state, its information is misinterpreted and lead to a different signalling pathway, but the target molecule itself would not change. However, when DNA is copied, a 'wrong' quantum state leads to a logical error on the classical part, and the new daughter DNA strand keeps the change. The model for copying genetic information can be decomposed into two single channels: One channel acts only on the quantum part ($|L\rangle, |R\rangle$), and models how the environment acts on the quantum register, while the other channel changes the classical, logical, bit ($|0\rangle\langle 0|, |1\rangle\langle 1|$) dependent on the quantum state of the system, and models the actual copying process. This interplay of classical and quantum information is best described by cq states introduced in section 5.1.7.

I will use the following Hilbert space structure: the first Hilbert space describes the classical part, tensored by the quantum part, leading to pure state basis

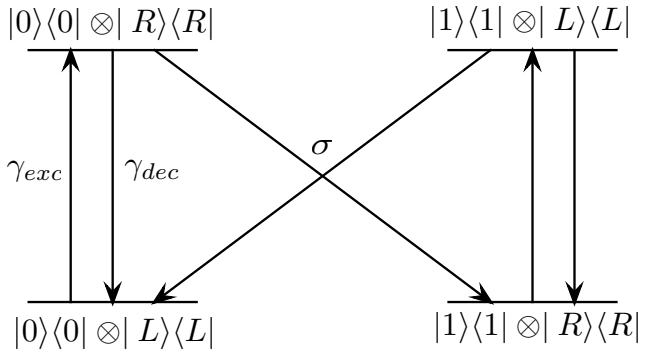

Figure 5.14: This graphic shows a toy model of genetic information flow. Each molecule has a classical part, encoding '0' or '1', and and a quantum part, with a ground and excited state. The ground state of one molecule corresponds to the first excited state of the other. The quantum part interacts with an environment at finite temperature, which is described with the parameters γ_{exc} (excitation rate) and γ_{dec} (decay rate). The interaction of quantum part with the environment constitutes a generalized amplitude damping channel. In addition, a second channel acts on the classical part. Conditional on the quantum register, it can switch the classical symbol with rate σ. See main text for detailed description.

$(|0,L\rangle, |0,R\rangle, |1,L\rangle, |1,R\rangle)$. The first and the fourth entry represent ground states, whereas the second and third entry are excited states. As the classical part cannot be in superposition, this restricts the possible input states to the following form

$$\begin{aligned}\rho_{in} &= p_0|0\rangle\langle 0| \otimes \rho_0 + p_1|1\rangle\langle 1| \otimes \rho_1 \\ &= p_0 \begin{pmatrix} p_{0L} & c_{0LR} & 0 & 0 \\ c^*_{0LR} & p_{0R} & 0 & 0 \\ 0 & 0 & 0 & 0 \\ 0 & 0 & 0 & 0 \end{pmatrix} + p_1 \begin{pmatrix} 0 & 0 & 0 & 0 \\ 0 & 0 & 0 & 0 \\ 0 & 0 & p_{1L} & c_{1LR} \\ 0 & 0 & c^*_{1LR} & p_{1R} \end{pmatrix} , \end{aligned} \tag{5.35}$$

where p_i is the probability that the molecule encoding logical i , $i \in \{0,1\}$ is present with $p_0 + p_1 = 1$, p_{iL}, p_{iR} describes the probability for molecule i to be in the quantum state $|L\rangle, |R\rangle$, and c_{iLR} quantifies the coherence between between the states $|L\rangle, |R\rangle$. Although the matrix representation uses four dimensions, the above considered cq state has only two dimensions. The dimension of the tensor product is the product of dimensions of the original spaces. The classical part consists only of two probabilities, which are positive and real valued. The first space therefore has one dimension. The second space describes a qubit, and has two dimensions, $\rho_i \in \mathbb{C}^{\otimes 2}$.

The system is embedded into an environment at finite temperature, which is described with the following master equation

$$\begin{aligned}\dot{\rho} = -\frac{i}{\hbar}[\rho, \hat{H}] &+ \gamma_{exc}\left(2\sigma_-\rho\sigma_+ - \sigma_+\sigma_-\rho - \rho\sigma_+\sigma_-\right) \\ &+ \gamma_{dec}\left(2\sigma_+\rho\sigma_- - \sigma_-\sigma_+\rho - \rho\sigma_-\sigma_+\right) \quad , \end{aligned} \tag{5.36}$$

where γ_{exc} describes the excitation of a molecule from the ground to the excited state, and γ_{dec} the opposite, and $\sigma_\pm = \sigma_x \pm i\sigma_y$ is the raising and lowering Pauli operator. The excitation and decay of each molecule constitutes a generalised amplitude damping (GAD) channel. Its Kraus operators on the molecules encoding '0' take the form

$$E_{0,1} = |0\rangle\langle 0| \otimes \sqrt{p}\begin{pmatrix} 1 & 0 \\ 0 & \sqrt{1-\gamma} \end{pmatrix} \tag{5.37}$$

$$E_{0,2} = |0\rangle\langle 0| \otimes \sqrt{p}\begin{pmatrix} 0 & \sqrt{\gamma} \\ 0 & 0 \end{pmatrix} \tag{5.38}$$

$$E_{0,3} = |0\rangle\langle 0| \otimes \sqrt{1-p}\begin{pmatrix} \sqrt{1-\gamma} & 0 \\ 0 & 1 \end{pmatrix} \tag{5.39}$$

$$E_{0,4} = |0\rangle\langle 0| \otimes \sqrt{1-p}\begin{pmatrix} 0 & 0 \\ \sqrt{\gamma} & 0 \end{pmatrix} \quad , \tag{5.40}$$

with $p = \frac{\gamma_{dec}}{\gamma_{exc}+\gamma_{dec}}$ and $\gamma = 1 - \exp(-t/(\gamma_{exc} + \gamma_{dec}))$. The parameter γ_{exc} describes the temperature of the environment and the likelihood that a molecules absorbs an energy quantum. The parameter γ_{dec} describes the rate of emitting a quantum to the environment. This depends both on the temperature and the lifetime of the excited state. The larger γ, i.e. the more time t the particle spends in the generalised amplitude damping channel, the closer the output state to the thermal state, which is independent of its initial configuration. For a biological scenario large values of γ seem reasonable, as most of the time the DNA is just stored, with the environment acting on the quantum part. The parameter p will have a value close to 1. In general de-excitation will be much more likely than excitation of a nucleic acid. Similar Kraus operators $E_{1,i}, i \in \{1, 2, 3, 4\}$ describe the channel for the molecules encoding '1'.

The switching channel measures the quantum part, and then acts on the classical part. If the measurement outcome of the quantum register is for example $|L\rangle\langle L|$, then there are two possible events. The quantum register belongs to a molecule encoding logical '0'. In this case nothing happens, the measurement outcome will be correctly

decoded as '0'. However, if molecule '1' was measured, during the copying process it will be decoded as logical '0' and the next strand of daughter DNA will have a different bit value at this position. This constitutes an amplitude damping (AD) channel. Its Kraus operators are

$$F_{L,1} = \begin{pmatrix} 1 & 0 \\ 0 & \sqrt{1-\sigma} \end{pmatrix} \otimes |L\rangle\langle L| \tag{5.41}$$

$$F_{L,2} = \begin{pmatrix} 0 & \sqrt{\sigma} \\ 0 & 0 \end{pmatrix} \otimes |L\rangle\langle L| \tag{5.42}$$

$$F_{R,1} = \begin{pmatrix} \sqrt{1-\sigma} & 0 \\ 0 & 1 \end{pmatrix} \otimes |R\rangle\langle R| \tag{5.43}$$

$$F_{R,2} = \begin{pmatrix} 0 & 0 \\ \sqrt{\sigma} & 0 \end{pmatrix} \otimes |R\rangle\langle R| \ , \tag{5.44}$$

with σ describing the average rate at which the information is copied. There are many interactions in a living cell that can lead to a measurement of the quantum register of the kind $|R\rangle\langle R|, |L\rangle\langle L|$, leading to a projection of the quantum state to the $|R\rangle, |L\rangle$ basis. But not every measurement is connected to actually copying the genetic information. The higher (lower) the value of σ the more (less) likely it is that a projection of the quantum register is due to a copying process. For a realistic biological scenario σ is very small. Table 5.1 provides a summary of the parameters and their meaning in a cell or bacteria.

The overall channel is given by the concatenation of the two channels,

$$G(\rho_{in}) = \sum_{q=R,L,i=1,2} \sum_{m=0,1,j=1-4} F_{q,i} E_{m,j} \rho_{in} E_{m,j}^{\dagger} F_{q,i}^{\dagger} \ . \tag{5.45}$$

It is worth discussing whether this channel description of copying genetic information is the most accurate one. The quantum degrees themselves are not used for storing genetic information; they just act as the code words of the channel encoding. Once the copying process is finished, it can be argued that the quantum degree if forgotten by the system, and should be traced out in the channel description. This would imply that once a copying mistake happened, it cannot be corrected, as the channels forgets everything about its history. However, life is more complicated. There are post-copying DNA error-correcting mechanisms. One of them uses methyl groups (95). Suppose a copying mistake happens, and guanine is matched with thymine instead of cytosine. An enzyme is able to determine that a copying mistake occurred, as $G-T$ is not a normal

parameters in genetic model	biological meaning
$p = \frac{\gamma_{dec}}{\gamma_{exc}+\gamma_{dec}}$	-usually $\gamma_{exc} << \gamma_{dec}$ s.t. $p \approx 1$ - can differ over orders of magnitude for different base pairs - two ways to change value of p: - increased probability to excite base pair (possible mechanism discussed in this thesis) - increased life time of excited state
$\gamma = 1 - e^{-t/(\gamma_{exc}+\gamma_{dec})}$	measures time it takes to equilibriate to effective temperature
σ	read-out probability influenced by stress, i.e. starving, and how often DNA polymerase in vicinity of excited base pair, $\rightarrow$ double stranded breaks also influence value of σ

Table 5.1: Each of the parameters in the genetic channel model corresponds to parameters in living systems. Section 5.3 explains the biological terms used here.

base pair. Given only the $G-T$ pair itself it would be impossible to decide which is the true original and which the faulty copying mistake. However, another effects helps to decide which strand is the original. The nucleic acid adenine becomes methylated, i.e. a methyl group attaches itself to adenine in a DNA sequence. This takes some minutes after copying. This means the old template strand has all adenine molecules methylated, whereas the new strand has not. If an enzyme detects the faulty $G-T$ base pair before the surrounding adenine molecules become methylated, the copying mistake can be corrected. That means that a genetic channel stores more information than just the classical symbols of the genetic alphabet. Here I consider the more general scenario of keeping track of the quantum register. As tracing out only looses information, the channel rates here can be taken as upper bounds on the channels which do forget the quantum part.

The channel measures first the classical part, and acts conditionally on the quantum part. The measurement on the classical register is an important part of the system, as it determines the corresponding Kraus operators for the quantum part. The system considered here is symmetric with respect to the classical information '0','1'. Both

quantum parts have equal probability to be corrupted by interactions with the environment. However, one of the molecules might have a different energy gap between ground and first excited state, leading to different parameters values in the Kraus operators for the channel. Then, the channel measures the quantum part, and replaces the classical symbol with its corresponding quantum measurement outcome. Because of the second measurement, the state looses all coherence, and exits the channel in diagonal form. The output state is

$$\begin{aligned}\rho_{out} = G(\rho_{in}) = diag\{&p_0(p_{0L}(1-\gamma)+p\gamma) - p_1(p_{1L}(\gamma-1)+(p-1)\gamma)\sigma, \\ &p_0(1+p_{0L}(\gamma-1)-p\gamma)(1-\sigma), \\ &p_1(p_{1L}(1-\gamma)+(1-p)\gamma)(1-\sigma), \\ &p_1(1+p_{1L}(\gamma-1)+(p-1)\gamma)+p_0(1+p_{0L}(\gamma-1)-p\gamma)\sigma\} \ .\end{aligned} \tag{5.46}$$

For $t >> \gamma_{exc} + \gamma_{dec}$ the output state ρ_{out} will thermalise to the new effective temperature p. In the limit of $t \to \infty$ or equivalently $\gamma \to 1$ the output state takes the form

$$\begin{aligned}\rho_{out} = G(\rho_{in}) = diag\{&p_0 p - p_1(p-1)\sigma, \\ &p_0(1-p)(1-\sigma), \\ &p_1(1-p)(1-\sigma), \\ &p_1 p + p_0(1-p)\sigma\} \ .\end{aligned} \tag{5.47}$$

The initial terms $p_{0,L}$ etc. all vanish and the thermal state is independent of the initial state.

The channel is chosen to be symmetric with regard to logical '0' and '1'. Therefore the most efficient coding requires as many molecules encoding logical '0' as logical '1', which means $p_0 = p_1 = 1/2$. Comparison with section 5.2.4 shows that the effective temperature T_{eff}, i.e. the population of the excited state compared to the ground state, is given by

$$\frac{e^x}{e^x + e^{-x}} = p - \sigma p + \sigma \ , \tag{5.48}$$

with $x = \frac{\hbar\Delta}{2k_B T_{eff}}$. Inverting eq. 5.48 gives the dependence of the inverse temperature on the channel parameters p, σ

$$\frac{\hbar\Delta}{2k_B T_{eff}} = \frac{1}{2}\log\left(\frac{y}{1-y}\right) \tag{5.49}$$

with $y = p - \sigma p + \sigma$.

This example shows that the concept of temperature, in the sense of occupation of

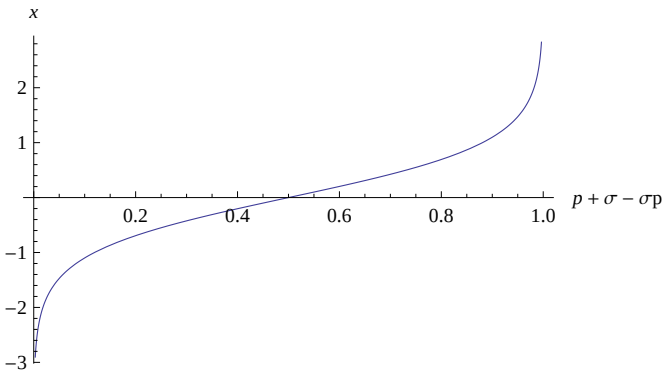

Figure 5.15: This graphic shows the parameter $x = \frac{\hbar\Delta}{2k_B T_{eff}}$ over the channel parameters $y = p - \sigma p + \sigma$. The effective temperature is zero for $y = 1$. For $y = 1/2$ T_{eff} is infinite. As y further decreases, the effective temperature becomes negative, as the population of the excited states becomes more likely than the population of the ground states.

excited states, in biological is complicated. Not only external parameters like γ_{exc} contribute, but also internal parameters like γ_{dec} and σ determine the effective temperature of the system.

5.2.5.1 Results for quantum capacity

The measurement on the quantum register has consequences for the quantum capacity Q_1 of the channel, namely it vanishes for all values of channel parameters p, γ, σ. This can be explained when looking again at the formula for the quantum capacity:

$$Q_1 = \max_{\rho \in H} \left(S(G(\rho)) - S((G \otimes \mathbb{1}_{anc})(\Phi)) \right) \quad , \tag{5.50}$$

Whereas the first terms quantifies the entropy of the output state ρ_{out}, the second term gives the entropy of the purification of the output state on a larger Hilbert space. In general, if the channel G were, for example, the identity channel $G(\rho) = \rho$, then the pure state of the purification $Tr_2|\psi\rangle\langle\psi| = \rho$ could be chosen to be a maximally entangled state, such that $\rho = \mathbb{1}/4$. In this case, the entropy of the output state is $S(G(\rho)) = S(\rho) = \log 2 = 1$, as $d = 2$, but the entropy of the purification is zero, because it is a pure state. Thus the positive value of the quantum capacity is due to the

channels ability to sustain entanglement between the particle sent through the channel and the remaining particle. Here, the genetic channel G performs a measurement on the quantum part. This measurement destroys any potential entanglement between the state ρ and its environment. In addition, as the resulting switch operation is restricted to the classical degree of freedom $|0\rangle\langle 0|, |1\rangle\langle 1|$, there is no possibility that the measurement $|L\rangle\langle L|, |R\rangle\langle R|$ leads to entanglement between the quantum state of ρ and the measurement device. That means the genetic channel fully breaks entanglement, such that $(G \otimes \mathbb{1}_{anc})(\Phi) = \sum_{i=1}^{d} \rho_{out,i} \otimes \rho_{anc,i}$, where the $\rho_{anc,i}$ are the final states of the ancilla. This separable mixture of states has at least as much entropy as the output state ρ_{out} itself. Therefore the quantum capacity Q_1 is zero.

5.2.5.2 Results for one-shot classical capacity

How much classical information can be sent through the noisy channel? The one-shot classical capacity can be calculated using the following equation

$$C_1(G) = \max_{\{p_j,\rho_j\}} \left[S\left(G\left(\sum_j p_j \rho_j \right) \right) - \sum_j p_j S(G(\rho_j)) \right] \quad , \tag{5.51}$$

where it suffices to optimise over d^2 pure states. Here $d = 2$, and thus four pure states are required for the maximal classical one-shot capacity.

The pure states here take the form

$$\begin{aligned} |\psi_1\rangle &= |0\rangle|L\rangle \\ |\psi_2\rangle &= |0\rangle|R\rangle \\ |\psi_3\rangle &= |1\rangle|L\rangle \\ |\psi_4\rangle &= |1\rangle|R\rangle \,. \end{aligned} \tag{5.52}$$

Numerical optimisation of eq. 5.51 leads to the following results. For any value of p, the classical one-shot capacity is maximal $C_1 = 2$ for $\gamma = \sigma = 0$. With growing value of σ and γ the one-shot classical capacity drops, until it reaches zero for $\gamma = \sigma = 1$ and $p = 0.5$, see fig. 5.16. In a biological setup a large value of γ seems reasonable. DNA read-out requires the movement of macro molecules, which is slow compared to the time it takes for a quantum system to equilibrate. In the rest of the chapter I will work with the assumption that each nucleic acid is thermalised with its environment,

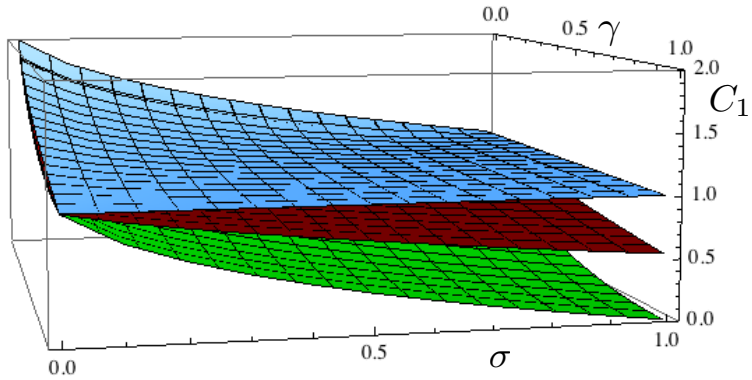

Figure 5.16: This graphic shows the one-shot classical capacity for $p = 1$ (light blue), $p = 0.9$ (red), and $p = 0.5$ (green). The classical capacity decreases as the parameters γ and σ increase.

i.e. $\gamma = 1$. As a consequence, maximal one bit of information can be sent through the genetic channel, compare with fig. 5.16.

The two-step mechanism for mutations will be of importance later in this chapter. The parameter σ depends on classically observable processes in the cell, i.e. which DNA polymerase reads out the information, how often a certain gene is accessed, etc. On the contrary, the parameter p is more difficult to observe and depends on the precise quantum properties of the system. While a lot is known about the classical properties influencing the value of σ, little is known of p.

5.2.5.3 Results for entanglement assisted classical capacity C_E

The numerical results for the entanglement assisted classical capacity C_E are shown in Fig. 5.17. For $\gamma = \sigma = 0$ the entanglement assisted classical capacity takes its maximum of $C_E = 2 \log d = 2$ as $d = 2$. For larger value of γ and σ the classical capacity drops quickly and vanishes completely for $p = 0.5$ and $\sigma = \gamma = 1$. For biological systems a large value of γ is plausible. Hence the entanglement assisted classical capacity yields here little advantage over the one-shot classical advantage.

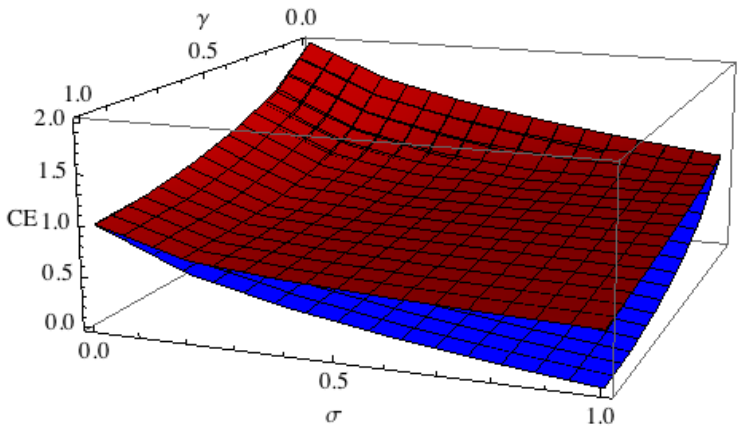

Figure 5.17: This graphic shows the entanglement assisted classical capacity (numerical results) for $p = 0.1$ (red curve) and $p = 0.5$ (blue curve).

5.3 Sequence dependent mutations

In the previous paragraphs I discussed the mechanism of random mutations. But is that all to mutations? Is it possible to have non-random mutations? Note that there are two possible distinctions between non-random mutations. The one that is often discussed in existing literature is Lamarckian mutations, where an organism changes its genome to a certain environment to achieve better performance. The causal line of argument is that mutations leading to an advantage for the organism are preferentially induced. Up to now there exists no detailed explanation how this should be possible. Selection, up to current understanding, only acts on the phenotype, and not on the genotype. It seems very difficult to imagine how a living systems figures out itself which mutations are beneficial and induce these preferentially. These kind of models will not be discussed here. On the contrary, non-random mutations can also mean sequence dependant mutations (SDM), i.e. the probability of a base pair to mutate depends on the neighbouring nucleic acids, simply because the relevant physical effects allow for it. This would mean that the neighbouring DNA sequence and maybe also other cell parameters influence non-trivially the mutation probability of a single site, independent of the consequences for the phenotype. Nevertheless, living systems which randomly evolve to exploit these SDM for their own good would have evolutionary

advantages. In appropriate circumstances, where a SDM leads to an advantage for the organism, it would appear to be a Lamarckian mutation, although the underlying mechanism would be very different. This will be discussed again in section 5.5.

However, if such a mutational mechanism exists, it would, in a given set of DNA sequences, eliminate itself. Any base pair having a neighbourhood that increases its mutation rate will eventually mutate. After long time the DNA strands will equilibrate to special sequences where each base pair has the same mutation probability, such that the sequence dependant mutation channel is indistinguishable from thermal random mutations. Such a mechanism would drastically change our understanding of information storage in DNA. It would mean that firstly not all possible sequences of DNA are equally likely and secondly mutations leading to deviation from equilibrium sequences should lead to further mutations. In this section I first review the experimental evidence supporting such a theory, the codon bias and adaptive mutations. Then I will introduce a physical mechanism that could give rise to sequence dependent mutations and discuss its plausibility.

5.3.1 Codon bias

If a SDM mechanism exists, its actions should be clearly visible in the statistics of DNA. While a bias in DNA does not prove directly the existence of SDMs, the absence of such a bias would instantly disprove the idea. Generally, there is a competition between mutational forces, changing an organism's genotype, and selection forces, acting on the phenotype. If a mutation turns out to be lethal for the organism, it will not be passed on to future generations. But not all mutations compete with selection forces. Firstly, there are non-coding regions of the genome, so called intergenic regions, which are not translated into proteins, and therefore do not directly influence the phenotype. Secondly, some mutations are 'silent', because they do not change the resulting protein. As these two kinds of mutations do not directly compete with evolution, they should contain a fingerprint of SDM. In (97) the authors count the occurrence of codons, i.e. three consecutive nucleic acids, in the genome of a 100 different species. The codon code maps triplets of nucleic acids into amino acids, see table 5.2. There are 64 possible codons, but only 20 used amino acids. That means the mapping has some redundancy. Some amino acids are only encoded by two codons ($'AAA', 'AAG' \rightarrow 'Lysine'$) , while others are represented by 6 different codons

($'CGA', 'CGC', 'CGG', 'CGT', 'AGA', 'AGG \rightarrow Arginine$). The resulting functionality of a protein is invariant under different coding for its amino acids. Therefore, one would expect the occurrence of codons to be randomly distributed. When a codon starts with 'CG', the third position should not matter, as all nucleic acids maps to the same amino acid 'Arginine'. Therefore, random mutations should fully randomise the third position of a CG codon.

Amino acid	Codons	Amino acid	Codons
Alanine	GCT, GCC, GCA, GCG	Cysteine	TGT, TGC
Aspartic acid	GAT, GAC	Glutamic acid	GAA, GAG
Phenylalanine	TTT, TTC	Glycine	GGA, GGC, GGG, GGT
Histidine	CAT, CAC	Isoleucine	ATT, ATC, ATA
Lysine	AAA, AAG	Leucine	CTA, CTC, CTG, CTT TTA, TTG
Methionine	ATG	Asparagine	AAT, AAC
Proline	CCA, CCC, CCG, CCT	Glutamine	CAA, CAG
Arginine	CGA, CGC, CGG, CGT AGA, AGG	Serine	TCT, TCC, TCA, TCG AGT, AGC
Threonine	ACT, ACC, ACA, ACG	Valine	GTT, GTC, GTA, GTG
Tryptophan	TGG	Tyrosine	TAT, TAC
Start	ATG	Stop	TAA, TGA, TAG

Table 5.2: Each of the amino acids as well as the start and stop codon are encoded by a sequence of three nucleic acids, A,C,G, and T. As there are 20 different amino acids, and 64 possible triplets, the code has some redundancy. For example the amino acid Leucine is encoded by 6 different triplets. Note that if there are multiple codons for the same amino acid, usually the third position varies.

On the contrary, the distribution of codons is biased. For example, a hypothetical organism uses only $'CGA', 'CGC'$ in its genome, but not the other four possibilities. The authors of (97) furthermore show that the bias can be effectively described by two parameters. That means that the bias is not random, but has structure. The first parameter relates to the GC content of the genome. As the GC bond is stronger than the AT, AT is more likely to mutate. The second parameter correlates with the intergenic codon bias. DNA consists of regions that code for proteins (genes), and intergenic

regions whose function is not yet entirely understood. As the intergenic region is not translated into tRNA (which might provide an explanation for the gene codon bias [1]), this bias is difficult to explain with selection pressure. As discussed earlier in (82), the most efficient codes are completely random. Any correlations between sections of the DNA strand reduce the genetic code's efficiency. However, it was found out that (97) *'the nearest neighbour nucleotide biases found in the intergenic region are in all cases positively correlated with biases in the third codon position of genes from the same origin'*. Both the non-coding DNA regions as well as many third position of codons do not directly influence the phenotype of an organism. Changes at those position in the genome do not alter the resulting proteins, and are thus not affected by selective pressure. In the absence of other directional mutational forces, random mutations should fully randomise any non-coding part of DNA. Each bias, in the non-coding DNA and third codon position, could have its own independent explanation. However, the correlations between the biases indicate a common cause, namely a new mutational mechanism.

This is strong evidence that not all sequences are equally likely. How is it possible that the non-coding regions of DNA are correlated with codon biases in coding regions? The authors (97) conclude that the easiest explanation is a genome wide mutational event, although they do not specify the detailed mechanism. Even more surprisingly, the bias depends on the species (97, 98), i.e. different species have a different bias. This implies that the underlying mechanism not only depends on the DNA itself, but possibly also on other influences inside a cell.

5.3.2 Adaptive mutations

Another hint at the existence of sequence dependant mutations would be given by 'follow-up' mutations. An initial mutation in a gene might increase the probability of having further mutations. After a long time different sequences equilibrate such that the mutation probability for each base pair is roughly the same, and thus indistinguishable from thermal noise. A random mutation is likely to increase the probability of SDM

[1] For each different codon a cell needs to synthesize a matching tRNA molecule. It would be energetically favourable to produce only two different tRNA instead of six for mapping to the same amino acid.

occuring, especially at the position of the original random mutation, as the disturbance out of equilibrium is biggest there, see fig. 5.29.

A beautiful example of this is given by the experimental evidence of adaptive mutations, where an unknown mechanism reverts the original mutation. The phenomena of adaptive mutations present a riddle to the science community. Pioneering experiments on adaptive mutations were performed by Cairns et al in 1988 (99) and much work has been undertaken to confirm and refine these initial findings (100, 101, 102). A typical experiment is this. A colony of E-coli bacteria is prepared with a lac^- gene [1] which renders it unable to process lactose, due to a +1 frameshift mutation. The colony is subsequently incubated in an environment where lactose is the only energy source. Surprisingly, the lac^- gene mutates to lac^+, −1 frameshift, with a hundred-fold rate compared to the mutation rate in a non-lactose environment (103), thus enabling lactose processing. Other genes also show a small increase in their mutation rate (104, 105, 106) and a few genes have an increase in rate comparable to that of the lac gene (107, 108). This indicates that the lac mutations are induced preferentially to allow the bacteria to adapt to their environment at a rate faster than if the mutations were genuinely random. Indeed, the bacteria seem to "know" which mutations will be most beneficial for their survival and appear to "stimulate" these. While the lac mutation in E-coli is only one example of adaptive mutations, they have also been confirmed in other bacteria and yeast in the presence of lactose and in absence of important amino acids (100). As neatly put by Rosenberg (101) "The emerging mechanisms of adaptive genetic change cast evolution, development and heredity into a new perspective, indicating new models for the genetic changes that fuel these processes."

5.4 A quantum resonance model

The key question of this paragraph is the following: Is there a physical mechanism, that would 'selectively' excite, dependant on the environmental conditions, only one specific base pair into its tautomeric form, thus leading to a sequence dependant mutation?

Resonance model.– The experimental data on adaptive mutations indicates an extremely selective underlying mechanism. In physical experiments such behaviour is

[1] The $gene^-$ notation means that the protein expressed from a certain gene is not functional. Similarly, the $gene^+$ notation means that a protein expressed from that gene is functional.

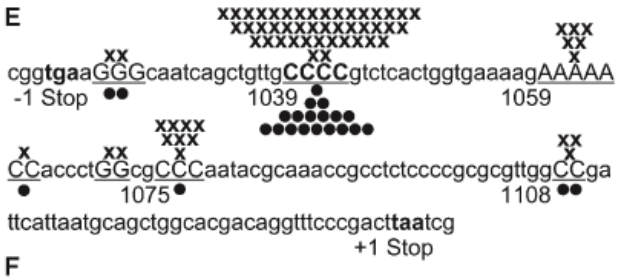

F

	WT	cis DSBs
- 1 at hotspot 1039	43	18
- 1 at other repeats	22	6
Other	1	0
Total	66	24

Figure 5.18: Experimental results taken from (109). In the lac reversion experiments, in initial +1 frameshift mutation at position 1039 is, under certain environmental circumstances, reverted by a -1 frameshift mutation, thus restoring the functionality of the resulting protein. The crosses and dots mark where such a -1 frameshift mutation occurred. Remarkably, most reverting mutations occur exactly at the same position where the genome was originally altered.

produced by resonance effects that can be incredibly sensitive to miniscule changes (110, 111). I propose that such a resonance effect underlies the phenomenon of adaptive mutations. This would explain how a specific base pair in a specific gene can be targeted, a common feature of adaptive mutations. Here, the bacteria are in stationary phase. They cannot divide, because not enough energy is available. As a consequence I will now look into the mutational mechanism during stationary phase, induced by errors of the DNA polymerase molecule. That means that a complete base pair, AT or CG, is corrupted, see section 5.2.3. In the experiments a -1 frameshift mutation restores the functionality of the gene's resulting protein, see fig. 5.18. This seems easiest explained by a single or double proton shift within a base pair. The new proton positions would not constitute a valid genetic letter, and thus the base pair would be discarded by DNA polymerase. In the following I will concentrate on single proton shifts within a base pair.

The key quantity from the physics perspective is the energy gap required to shift protons. I model each base pair as a two level system separated by the energy $\hbar\Delta$ [1],

[1] The energy levels need not be sharp, it suffices to assume that their broadening is significantly

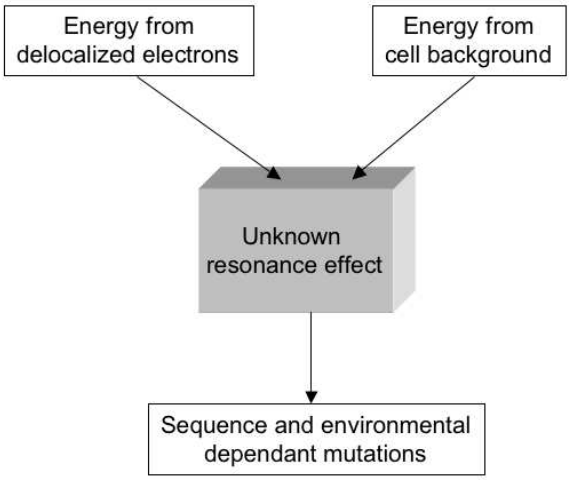

Figure 5.19: Section 5.3.1 discussed the experimental evidence on mutation events dependant on the species, and section 5.3.2 summarised the occurrence of adaptive mutations mutations. In this paragraph I will suggest a quantum resonance model that can explain both experimental findings.

where the excited state describes the shifted proton. The two different base pairs (AT and CG) have different energy gaps, simply due to their different chemical composition. These energy levels will change (albeit by a small amount compared with the gap itself) depending on the neighbouring base pairs, see fig. 5.20. This model discusses the source for bridging this energy gap. In Löwdin's analysis the proton transfer occurs via quantum tunnelling, which is a static process independent of the environment. The tunneling probability is roughly the same for all base pairs. In contrast, I propose a resonant energy transfer between the two proton states, which is a dynamic effect. Importantly, the excitation probability depends sensitively on a number of parameters, and thus could differ over orders of magnitudes for different base pairs, see fig. 5.27.

5.4.1 Directed generation or directed capture

The creation of a sequence dependent mutation requires three components: Firstly, the energy gap to a tautomeric form has to be bridged, i.e. some physical process needs to supply energy. Secondly, the lifetime of the excited state has to be sufficiently long.

smaller than the energy gap itself.

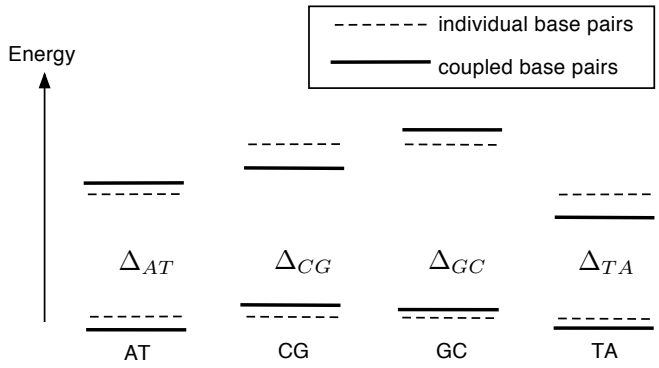

Figure 5.20: This graphic shows the energies of base pairs in their normal form (ground state) and tautomeric form (excited state). The dashed lines describe individual base pairs, while the solid lines sketches how the energy levels shift when the base pairs are embedded in a gene's sequence. Without coupling both AT and TA (CG and GC) have the same energy gap between normal and tautomeric form. However, this is not the case with coupling, where the precise value of the energy gap depends on the neighbourhood of the base pair. While it is difficult to determine the precise value of the energy gap, the order of magnitude ranges from $\hbar\Delta \in 0.5 - 0.8eV$

Thirdly, a DNA polymerase has to be in the vicinity, to transform the excited state into a permanent mutation. The first two points are not completely independent of each other. If the lifetime of the excited state is independent of the sequence of nucleic acids, then SDM requires a directed energy transfer into the target base pair. If, on the contrary, the lifetime of the excited state **is** sequence dependent, then simple thermal tunneling would be sufficient for creating SDM. While random base pairs become excited, only special base pairs have a long enough lifetime to lead to a permanent mutation. This second possibility, sequence dependant capturing, requires detailed calculations of DNA strands, which are currently out of reach of numerical simulations. In the following I will focus on the first possibility, sequence dependent generation of excited states.

The problem of proton movement is, contrary to electron movement, poorly understood. As protons have a 1836 times larger mass than electrons, they couple differently to light. For example, it would be unlikely for a proton to directly absorb a high energy photon (around the missing $0.6eV$) to get into the excited state. Because of its mass

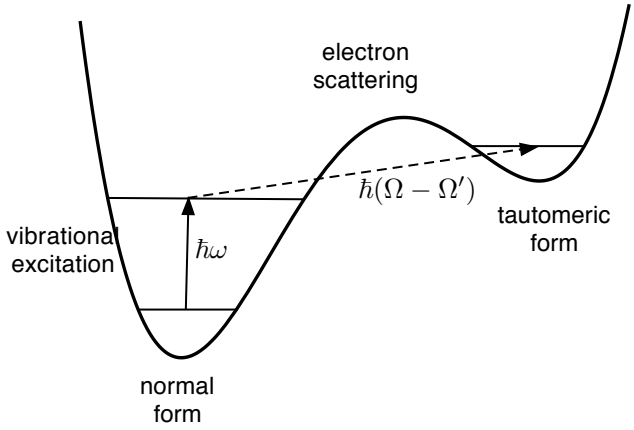

Figure 5.21: The proposed mechanism for selected excitation of base pairs has two steps. First, a base pair is excited into a vibrational mode of energy $\hbar\omega$, where one of the protons constituting the H-bonds within the base pairs oscillates strongly out of equilibrium. This first excitation can either be thermal or through photon absorption. In the second step, the moving proton scatters with the electrons, whereby the missing energy $\hbar(\Omega - \Omega')$ for reaching the tautomeric form is transferred from electrons to the proton.

the proton has high inertia. Before the proton starts moving the photon is already gone. One way to deal with the proton's inertia is to consider vibrations. The O-H and N-H bonds within a base pair can undergo vibrations. Numerical studies (112) show that there exist vibrations within A-T and C-G pairs, where a single proton oscillates out of equilibrium position. The basic idea is that the moving proton couples strongly to the delocalized electron cloud. Electrons and proton scatter, whereby the missing energy quantum is transferred from the electrons to the proton, causing it to shift its position in the base pair, leading to a tautomeric form, see fig. 5.21 for an overview. In the following, each step of the model will be explained in more detail.

5.4.2 Vibrational states of base pairs

In (112) single proton oscillations in base pairs are numerically investigated. The wavenumber of proton vibrations ranges from $500cm^{-1}$ to $3550cm^{-1}$. In addition, it was found that the energy of vibration depends on the neighbourhood. The peaks of the vibrational spectra shift up to $500cm^{-1}$ when adding a second base pair as a neighbourhood for the first. The results for double base pairs are shown in fig.'s 5.22

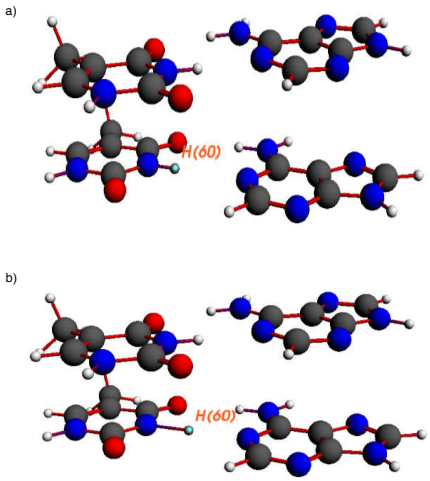

Figure 5.22: This graph shows a snapshot from the numerical simulations performed in (112). In (a), a two AT-AT base pairs are shown in their normal configuration, i.e. ground state. In figure (b) the same double base pair is shown where one base pair is in a vibrationally excited state. The proton H60 oscillates out of equilibrium and comes close to the neighbouring nitrogen atom. The energy of this vibration is around $3680cm^{-1}$, which corresponds to 0.46 eV.

and 5.23 for AT-AT as well as fig.'s 5.24 and 5.25 for CG-GC.

5.4.3 Electron scattering

The single proton vibrations discussed in the previous section can supply up to approximately $0.46eV$ of energy. The energy needed to create a tautomer is around $0.5 - 0.8eV$, which is more than the energy of proton vibrations. I propose that the electronic vibrational degree of freedom of the DNA's π-stacks provides the missing energy. It is experimentally known that electron scattering, induced by visible light in Raman spectroscopy, transfers energy to vibrational degrees of freedom in the range of $1200cm^{-1} - 900cm^{-1}$, equivalent to $\hbar\Omega = 0.15eV - 0.11eV$ (113). It is natural that the gene's electrons interact electrostatically with the base pair's protons. When protons move, these electrons invariably must undergo vibrations and vice versa. The tautomeric forms discussed in section 5.2.3, where a single proton completely tunnels to the opposite nucleic acid, need more energy than is provided by the single proton oscillation. This additional energy might come from electronic vibrations (114). These

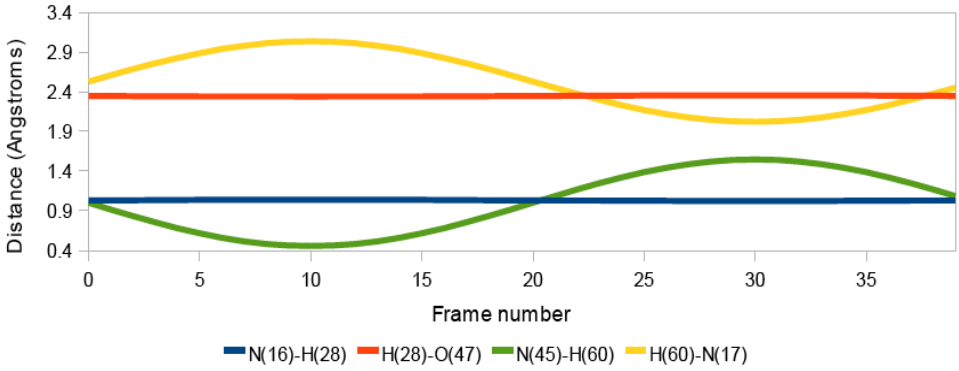

Figure 5.23: This graph shows the distance variation of the strong part of the H-bond H(60)-N(45) and the weak part H(60)-N(17) of the AT-AT double base pair. Due to the vibration the distance of the proton H60 to the nitrogen atom of the opposite nucleic acid shortens significantly from around 2.5$\mathring{A}$ to 1.9$\mathring{A}$, which is only 0.4$\mathring{A}$ more distance than the strong part of the H-bond.

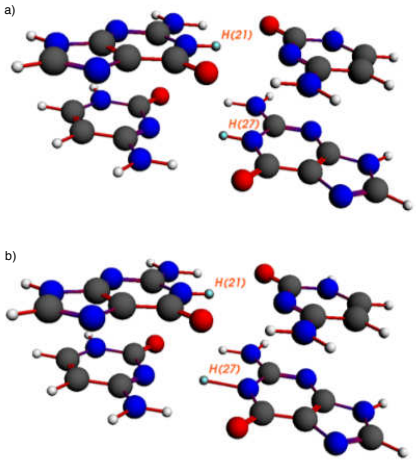

Figure 5.24: This graph shows a snapshot from the numerical simulations performed in (112). In (a), a two CG-GC base pairs are shown in their normal configuration, i.e. ground state. In figure (b) the same double base pair is shown where one base pair is in a vibrationally excited state. The proton with number H27 oscillates out of equilibrium and comes close to the neighbouring nitrogen atom. The energy of this vibration is around 3630cm^{-1}, which corresponds to 0.45 eV.

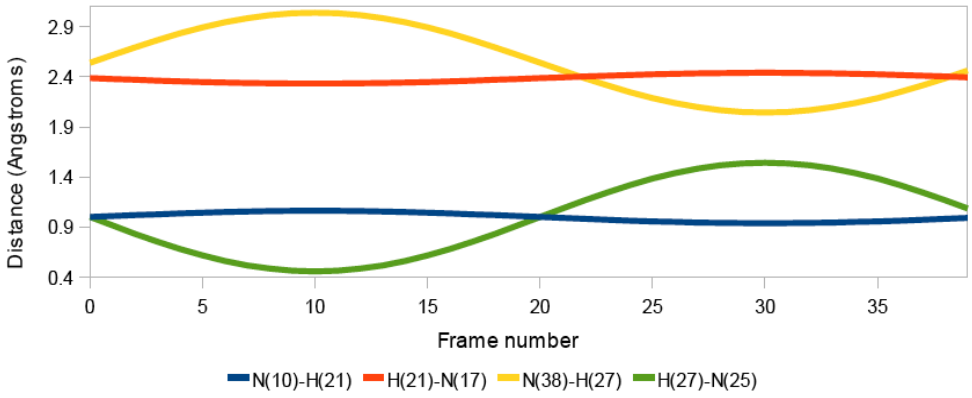

Figure 5.25: This graph shows the distance variation of the strong part of the H-bond H(27)-N(25) and the weak part H(27)-N(38) of the AT-AT double base pair. Due to the vibration the distance of the proton H27 to the nitrogen atom of the opposite nucleic acid shortens significantly from around 2.5$\mathring{A}$ to 1.9$\mathring{A}$, which is only 0.4$\mathring{A}$ more distance than the strong part of the H-bond.

depend strongly on the base pair sequence. This is because each base pair has a specific local potential for its π electron clouds. The coupling between the electronic degrees of freedom of different base pairs gives rise to unique vibrational energies in the sense that replacing one base pair with another will change these energies. This sequence dependence goes beyond the boundaries of a gene and extends to the neighbourhood. The same gene, surrounded by a different base pair sequence, will have different electronic vibrational energies. This is in agreement with experimental data. Firstly, the higher than normal mutation rate occurs only if the lac^- gene is located on the episome and not on the chromosome (115, 116). The neighbourhood of the lac^- gene is totally different for the two locations. This leads to different vibrational energies, turning the lac^- gene on the chromosome off-resonant with the lactose radiation field.

Secondly, in an experiment (108) a $Tn10$ gene was inserted at different distances to the lac^- gene on the episome. It was observed that the closer the $Tn10$ gene to the lac^- gene, the stronger the repression of the lac^+ mutation. Qualitatively this is exactly what this model would predict. The closer the insertion of the $Tn10$ gene, the stronger the perturbation of the electronic vibrations which again leads to off-resonance. To confirm that such an influence can exist at large distances of several 1000 base pairs, as reported in the experiment, will require extensive calculations.

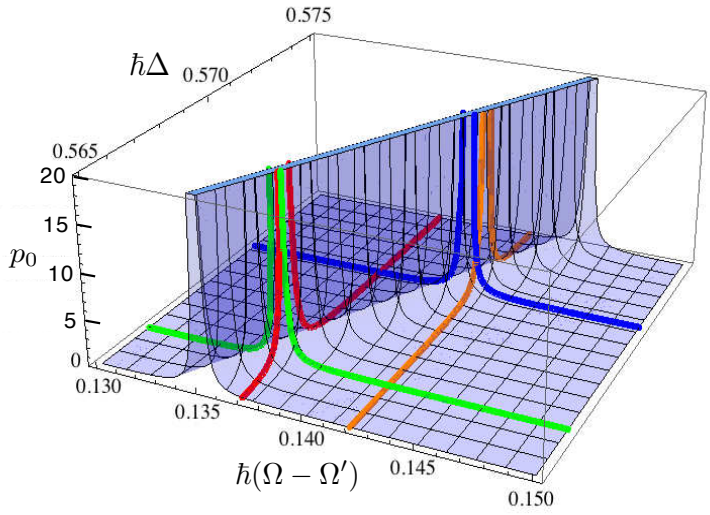

Figure 5.26: This graphic shows the time-independent part, p_0 in 10^{-6}, of the excitation probability (5.53) over the electronic vibrational energy $\hbar(\Omega-\Omega')$ and the base pair's energy gap $\hbar\Delta$. The ridge visualises the resonance condition. The energy of the proton vibration is $\hbar\omega = 0.43eV$ and the coupling proton vibration is chosen as $2\hbar\lambda = 10^{-6}eV$, motivated from standard physics experiments, see supplement. I have highlighted two different base pair energy gaps, blue curve ($\hbar\Delta = 0.572eV$) and green curve ($\hbar\Delta = 0.567eV$). Exciting these base pairs with two different electronic energies, red curve ($\hbar(\Omega - \Omega') = 0.137eV$) and orange curve ($\hbar(\Omega - \Omega') = 0.142eV$), gives very different probabilities. The excitation probability is high only when the combined energy of electronic vibration together with the proton vibration energy matches the base pair energy gap. This is the case for the combinations of green&red curves, $p_0 = 12\cdot10^{-6}$, and blue&orange curves, $p_0 = 2\cdot10^{-6}$. In contrast, the off-resonant combinations, such as green&orange have a much lower excitation probability, $p_0 = 1.8\cdot10^{-8}$. This quantitative analysis shows that with realistic parameters the resonance model predicts the increase in mutation rate by a factor of 100 for a specific gene - base pair combination, as found in experiment.

Base pair excitation probability.– The emphasis of the model is on two energetic contributions, one energy quantum from the delocalised gene's electronic vibrations and another thermal proton vibration, that resonates with the base pair.

As resonance is an ubiquitous phenomenon in physics there are a number of different physical couplings that would produce similar resonance observations. More experimental data are needed to pinpoint the precise coupling mechanism.

Typically electrons absorb energy quanta to transfer to excited orbitals. In contrast, the excited state considered here consists of *protons* that have transferred to different positions in the base pair with higher energy.

As a consequence, neighbouring base pairs, although embedded in nearly the same electronic vibrations, can have, due to small differences in base pair energy gap $\hbar\Delta$, very different probabilities to become excited. For a first approximation of the resonant energy transfer from electrons to protons, I take a standard model from quantum optics methods (117), which is also commonly used in quantum biology. For this coupling process the probability for a base pair to transfer to its tautomeric form is

$$p_{excite}(t) = \frac{4\lambda^2}{4\lambda^2 + (\Delta - (\Omega - \Omega') - \omega)^2} \sin^2\left(\frac{Rt}{2}\right), \tag{5.53}$$

where λ is the coupling constant between the base pair combined with the electronic vibration and the proton vibration. The energy matching condition is expressed by the term $\hbar(\Delta - \Omega + \Omega') - \hbar\omega$. The probability of excitation oscillates in time, t, with the so-called *Rabi frequency*, given as $R = \sqrt{(\Delta - \Omega + \Omega' - \omega)^2 + 4\lambda^2}$.

Formula (5.53) shows the two key features relevant for the discussion of adaptive mutations. One is that the probability is highly sensitive to the energy difference $\hbar(\Delta - \Omega + \Omega') - \hbar\omega$. For a given proton vibration, i.e. fixed ω, even a small change in the combined base pair and electron vibration energy, $\hbar(\Delta - \Omega + \Omega')$, can lead to a sharp drop in probability of excitation. The time-independent part of the excitation probability, $p_0 = \frac{4\lambda^2}{4\lambda^2 + (\Delta - \Omega + \Omega' - \omega)^2}$, is shown in fig. 5.26. The second feature is that the coupling to the proton vibration, 2λ, determines the width of the resonance peak. In the following I show how our model qualitatively explains known experimental data.

This mechanism is not limited to the lac gene; it can also induce non-selected mutations. A set of experiments (107, 108) show a higher than normal reversion rate of the mutant *Tn10* gene during lactose selection. The initial +1 frameshift mutation makes the bacteria sensitive to the antibiotic tetracycline (tet^s). Here the *tet* mutation

rate is comparable to the *lac* mutation rate. This is remarkable as the presence of lactose is not immediately causally connected to the resistance to antibiotics. This model can explain such a fact if the electronic gene vibration of the mutated gene, is in resonance with the energy needed for exciting a base pair in the tet gene. The degree of mis-tuning determines the rate of mutations: a gene-base pair combination with bigger mismatch to resonance will mutate at a much lower rate than one with strong resonance, see eq. (5.53) and fig. 5.26. The expected picture is that many genes mutate at a slightly increased rate. This is observed in several experiments (104, 105, 106, 107).

5.4.3.1 Excitation mechanism

There are two possible excitation mechanisms, the thermal tunnelling and the resonant energy transfer. In order to compare the two mechanisms, fig. 5.27 shows the excitation probability for thermal tunneling (red) and resonant excitation transfer (blue) given that an initial energy of $0.43eV$ is supplied. The thermal tunnelling and resonant excitation transfer have a distinct excitation profile for different energy gaps $\hbar\Delta$. However, so far the influence of thermal line broadening is not discussed here. While in principle such a resonant excitation transfer can lead to sequence dependent excitation of base pairs, a more detailed calculation is required to confirm the mechanism.

5.4.4 The importance of selective pressure

The simple model of copying genetic information sensitively depends on the switching parameter σ. It was mentioned a couple of times that this parameter can be actively changed by a cell or bacteria. Here I will mention two ways of doing so. All experiments on adaptive mutations put selective pressure on the bacteria. In the case of the lac mutation, lactose is the only available carbon source and this lactose environment selects bacteria which develop mutations in the lac^- gene. Firstly, the lack of usable nutrition puts the bacteria into stress, which alters their metabolism (109), which changes the switching parameter σ introduced. A more error prone DNA polymerase will lead to a higher value of σ. Secondly, although the lactose cannot be utilised, its presence leads to a higher read-out rate of the lac gene (see lactose regulatory network), and thus also increases the value of σ. This is of importance for the generation of mutations. So far I discussed mechanisms how to excite a special base pair. For turning the excitation into a permanent mutation a second step, the copying or error

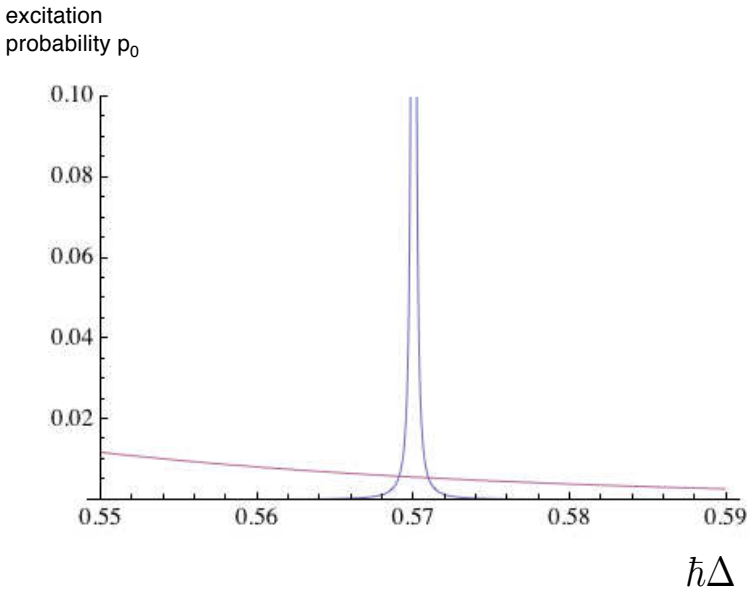

Figure 5.27: This graphic compares the thermal (red) excitation probability with the resonant mechanism (blue) given that energy of $\hbar\omega = 0.43eV$ is externally supplied. The thermal excitation probability is given by $p_0 = \exp(-\hbar\Delta + 0.43eV)/kT)$. Over the range of $\hbar\Delta$, i.e. the energy gap of a base pair, the thermal excitation probability is roughly constant. For the resonant excitation mechanism, given by eq. 5.53 with $2\lambda = 10^{-4}$, there is a sharp excitation peak.

correction of DNA polymerase, is required. The general interplay between excitation of base pairs and read-out rate of genes is discussed in the next section.

5.5 Change or die!

Mutations are important for life. Without genetic change, life would be stuck in its present form, and have little chance of further development. Viruses and bacteria seem to be masters of using mutations to develop new skills and fight, for example, antibiotics. But when a random mutation occurs, there are two possible effects. Firstly, the mutation does nothing harmful, i.e. all proteins and their expression mechanisms stay functional, or even improves the performance of the bacteria. Such mutations are good for the organism. Secondly, a mutation destroys an important functional protein. In severe cases this might, in the long run, lead to the death of the organism. Before

that, the bacteria will enter a state of stress, possibly because of starvation as in the lac experment, see section 5.3.2. Is there a way of selectively undoing harmful mutations? This would provide enormous evolutionary advantages. The problem is, after a mutation becomes permanent[1], there is no way for the bacteria to find out where exactly the mutation occurred. The DNA itself is the backup of genetic information, and if the backup is corrupted, it is impossible to tell where the error happened. However, if sequence dependant mutations are physically possible, there is a mechanism to achieve exactly this. In the previous section I discussed the possibility that a quantum resonance effect excites mainly only a specific base pair in a specific genetic neighbourhood into the excited tautomeric form. If the resonance condition is sufficiently sharp, effectively only a single base pair is excited. But can this quantum signal indeed be the cause of the observed mutation events? More precisely, it is in principle possible to undo a malevolent mutation without mutating other, correct, base pairs? Similarly, if the initial mutation causes no harm, is it possible not to increase the mutation rate? To answer these questions, I will look again at the one-shot classical capacity discussed in section 5.2.5.2. There are three parameters entering the formula of C_1: the parameter $\gamma = 1 - \exp(-t/(\gamma_{exc} + \gamma_{dec})$ describes how far a single base pair is in equilibrium with its environment. Here I set $\gamma = 1$. It takes a relatively long time for a DNA polymerase to reach the targeted base pair, hence it seems reasonable to assume that the base pair is fully thermalised. Secondly, the parameter $p = \frac{\gamma_{dec}}{\gamma_{exc}+\gamma_{dec}}$ is the probability that the system, once thermalized, is in the ground state. Usually, $p \approx 1$, i.e. with nearly certainty the base pair is in its ground state. The action of the quantum resonance effect is to decrease this probability for a specific base pair. Note that this a physical effect bound to the DNA sequence itself, not to a DNA polymerase molecule. If such a resonance effect is possible within DNA, it would be nearly impossible for a living cell to develop methods to avoid this signal corruption. Finally, the third parameter is the copying probability σ. This parameter describes the likelihood that a measurement is due to a DNA polymerase molecule, which would change the excited state into a permanent mutation. Contrary to the parameter p, a cell can influence the value of σ. It is, for example, known that in starvation bacteria change their DNA error correcting mechanism. Instead of the normal DNA polymerase, a more error prone polymerase is

[1] I.e. enough time after copying has past such that no post-copying error correction scheme can locate the error.

used. This increases the value of σ. Fig. 5.28 shows the one-shot capacity dependent on p and σ.

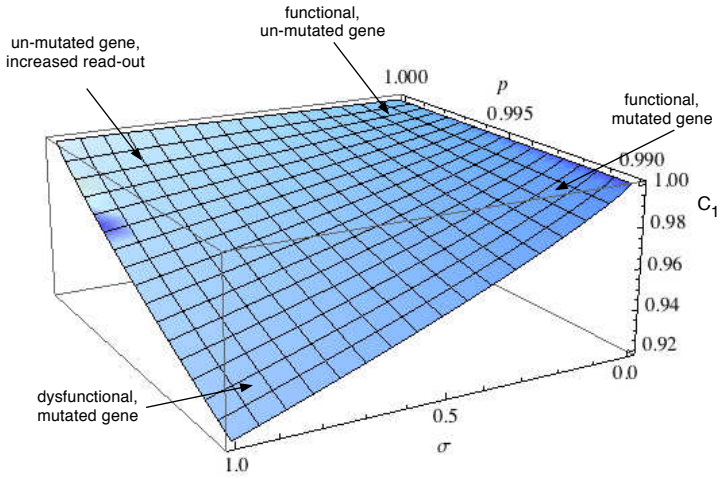

Figure 5.28: This graphic shows one-shot classical capacity C_1 dependant on p and σ for $\gamma = 1$, i.e. the quantum state is fully thermalized for the effective temperature given by p. In the normal case, un-mutated genome (p large) and cell not starving (σ small) the classical capacity is maximal. In the case a random mutation decreases p, but is otherwise harmless (σ small), the classical capacity is only little smaller. However, if an initial mutation (p small) does harm to the cell (σ large), the prob. for a mutation increases strongest. Other base pairs, with large p, have even in this changed DNA error mechanism (σ large) little increased error probability. Thus a cell would in principle be able to repair preferentially an initially mutated base pair.

Using a two step mechanism indeed allows to increase the mutation rate locally where a harmful mutation occurred. The first parameter, the effective temperature p, increases for initial mutations. If the mutation are harmless, σ remains unchanged. That means the mutation out of an equilibrium sequence would only slightly increase the mutation rate at this point. This effect might be so small that it remains unnoticed in the thermal noise of random mutations. The bias in the codon code might have developed this way. Mutations in the third position of a codon do not change the functionality of the resulting protein. If, however, a mutation is harmful, and puts stress on the bacteria, the bacteria will change its genetic read-out mechanism to a more error-prone polymerase, which is described by a higher value of σ. This will lead

to preferentially mutating sequences which already have mutations out of equilibrium. Once the gene is 'repaired', the bacteria changes again to the normal DNA read-out mechanism, to prevent further mutations.

Such a change of DNA repair mechanism of course also has consequences for other genes. If a gene has acquired neutral or beneficial mutations, under normal, un-stressed conditions the probability for mutations increases little, see blue dot in fig. 5.29a. However, if other genes activate a more error-prone DNA polymerase, excited base pairs are more likely to mutate, fig. 5.29b. Thus a mutation in one gene could lead to follow-up mutations in other genes. As this line of argument is only qualitative, it needs further calculations to check the quantitative aspects of this model.

5.6 Summary

In this chapter I discussed information processing in living systems with focus on copying genetic information. I applied the concept of cq states to chemical reactions, and showed how the occupancy of different quantum states influences the classical information processing. I showed that in principle, given a small number of realistic assumptions, bacteria can **on average** undo malevolent mutations. Indeed, the effects discussed in this chapter do not need any coherence. By setting the parameter $\gamma = 1$, all initial coherences of the involved cq states vanish, but still the existence of quantum states plays a non-trivial role. But without coherences, is it still adequate to talk about quantum effects? Violation of Bell's inequality, quantum computers, etc. heavily rely on the magic ingredient superposition aka coherence. Here, however, I mainly discussed energy levels and effective temperatures. By considering the modest, down-to-earth beginning of quantum mechanics, one realises these two concepts are at the very heart of quantum mechanics, and should not be dismissed as 'trivial quantum mechanics', as they have considerable impact on the macroscopic world. The first breakthrough to our modern understanding of the quantised world was in 1900, when Planck published his work 'on the theory of the distribution law of the normal spectrum'. He realised that the spectrum of a black body can only be explained by assuming that energy is only exchanged in discrete quanta. Five years later Einstein published that the existence of discrete energy levels underlies the photoelectric effect. It is precisely these physical effects that could enable living systems to exploit the possibility of sequence dependent

mutations.

I hope the reader does not mind me to summarise again the key assumptions which would enable sequence dependent mutations:

Existence of quantum state signalling point mutation

Some point mutations are induced by the occupancy of an excited state of nucleic base pairs. Without the existence of such an energy level there is little possibility to signal that this specific base pair should be mutated. In section 5.4 I estimated that such an energy level can at least in principle exist.

Effective temperature changes significantly over different base pairs

In section 5.2.5 I showed that the occupancy of different states resembles an effective temperature for the system. Three effects contribute to the effective temperature, namely the likelihood of excitation (γ_{exc}), the life time of the excited state (γ_{dec}) and the copying probability (σ). While the copying probability can be influenced actively by a bacterium, the excitation and de-excitation of a base pair are fundamental quantum parameters determined by the physics of DNA itself (and its surrounding solvent etc). If at least one of these two parameters is DNA sequence dependent, then a whole class of mutations is also sequence dependent. This would change our understanding of genetics drastically. One should note here that the computation of each parameter is currently for all practical purposes impossible. Moreover, as it simultaneously involves moving protons and electrons, most numerical approximations fail. Intensive research is needed to fully understand whether this mechanism actually takes place.

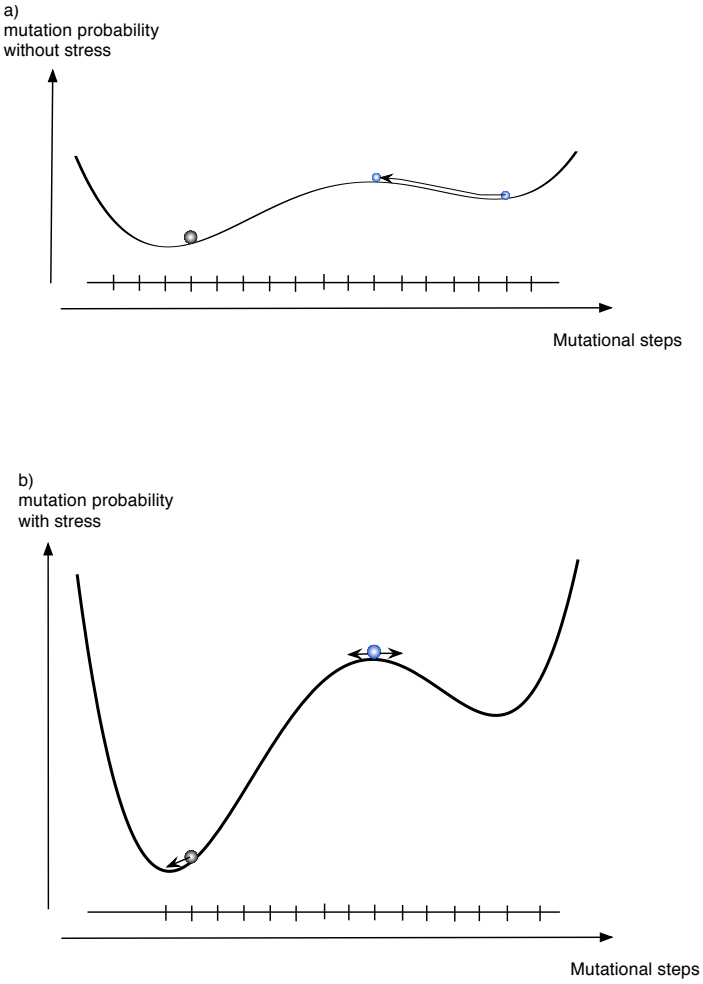

Figure 5.29: This graphic shows a sketch of the probability to mutate for a sequence of DNA. In reality the probability to mutate for each base pair within a sequence will depend on several parameters. Here, I consider only a one-dimensional mutation landscape. The bars at the x-axis represent the discrete mutational steps. In (a) the cell or bacteria is not subject to stress, i.e. has in general a smaller mutation probability, a relatively flat mutational landscape. Over time, the sequence dependent mutational mechanism will mutate genes along the landscape to the local minima, the equilibrium sequences. However, random mutations will shift these equilibrium sequences uphill the potential. For step local minimum random mutations can shift the equilibrium sequences only slightly uphill, i.e. few or single mutations, see black circle. In case of a relatively flat local potential minimum several mutations can occur without increasing the overall mutation probability significantly, see blue circles. In (b) the cell or bacteria is subject to stress. As a consequence, the mutation potential steepens. In case of single mutations there is a high probability that the stress leads to back-mutations, which undo the initial mutations, as in the case of adaptive mutations. In the case of several mutations, blue circles, the situation is different. In addition to the possibility of back-mutations (right arrow) there is also the possibility of on-going mutations (left arrow).

6

Conclusions and Outlook

Does quantum mechanics play a non-trivial role in life? If it is possible, and advantageous for the living system, the answer has to be yes! If there is a useful way of harnessing quantum correlations, Nature's 4 billion year research and development program is bound to have found it. Confirming that a living system employs quantum effects is hard, and needs to be proven individually for each system.

In the case of European Robin much progress has been achieved. The experimental evidence from weak oscillating fields together with the detailed analysis of chapter 2 of this thesis provides strong evidence about the long coherence time of electron spins in European Robins. However, it remains poorly understood **why** these this long coherence time is beneficial or **how** it is achieved.

The second biological system under consideration in this thesis is DNA. In chapter 4 the electronic degree of freedom of nucleic acids is investigated. A harmonic model for the coupling between electrons of neighbouring nucleic acids is developed. The polarizability, which is different for the four nucleic acids, constitutes a local trapping potential for the electrons. Van der Waals forces between neighbouring sites give a coupling mechanism between sites. For realistic parameters this model predicts that the electronic degree of freedom maintains coherence and entanglement even at body temperature. This also means that the electronic degree of freedom is delocalised. As a consequence, the precise value of the energy of the electronic eigenstates is also nucleic acid sequence dependent. The model so far does not include broadening of the energy levels due to coupling to vibrations. A more detailed analysis is needed to find out how far the electronic degree is sequence dependent.

While in chapter 4 the physical properties of DNA are investigated, in chapter 5 I discuss information flow in living systems from a general point of view. The concept of cq states, known from quantum cryptography, is applied to biological systems. The Born-Oppenheimer approximations motivates the separation of molecules into a classical part, that reliably encodes classical information, and a quantum part, that processes the classical information by determining the outcome of chemical reactions. If, due to environmental influences, a molecule is in an unusual quantum state, logical errors might occur. Sources for such errors are discussed.
In more detail the influence of quantum states on the copying fidelity of DNA is investigated. A simple model for copying genetic information is developed, which is strongly motivated by the current understanding of DNA. The model consists of two genetic letters encoding logical '0' and '1'. The classical information can only be accessed by measuring the quantum states of the two molecules, which are taken to be orthogonal. However, the excited state of one molecule resembles the ground state of another. This is taken to be the source of logical errors in copying genetic information. Mechanisms for bringing the molecules into excited states are discussed. One possible mechanism uses energy from the electronic degree of freedom. As the value of electronic eigen energies is possibly sequence dependent, a physical mechanism transferring this energy to the genetic letters might cause sequence dependent mutations. This is compared to the experimental evidence from biology on non-random mutations. The consequences of such a mechanism on bacteria are discussed. If possible, it would in-principle allow bacteria **on average** to undo malevolent mutations with a non-zero probability.

This thesis only shows that such non-random mutations events are in-principle possible, given that a number of physical parameters take certain values. More detailed analysis is needed to further investigate the possibility of non-random mutations.

In addition to the discussed ideas on how quantum mechanics can affect biological systems, here I will bring attention to two further concepts that might apply in biology.

6.1 Predictive power and QM

The title of this thesis is 'Quantum Coherence in biological systems'. So far everything I discussed could also have been 'Quantum Coherence in non-equilibrium physical systems'. Spin chemical effects are mainly studied outside living birds, and stacks of

nucleic acids are a priori not alive themselves. This reflects the problem of defining biological systems. Biology refers to the study of living systems, but this just shifts the problem to defining what life is. [1]

Let me compare the motion of a bird and a kite. Both are flying under suitable conditions in the sky, and yet there are distinct differences between the two systems. The kite just obeys laws of physics in the sense of the following: If the wind changes its direction, so will the kite, if the wind blows stronger or weaker, the kite will rise or fall. Birds are different. While birds and kites have to obey the same laws of physics, birds learned to **react**. Given a change in the wind, the bird will **decide** to change, for example, the position of its wings, to counteract the change in wind. Or it might just fly somewhere else, where the wind conditions are better for flying. The ability to react to its environment is a feature that all living systems share. If one were able to design a robot, that looks a bird, and makes the same decisions given a certain environmental input, like a bird, then most people would not be able to distinguish the robot from the living bird. How does a bird, or any other living system, achieve this? I will not attempt to answer the question how far a bird is conscious about itself flying. But there is clearly some sort of information-processing-and-predicting-the-future taking place in the bird. This requires a lot of computing inside the bird. In more detail, the bird needs to have a predictive model about itself and its environment. The bird needs to be able to predict, for example, 'If the wind slows down, I will lose height'. If losing height is not advantageous for the bird, it needs to decide what counter action to initiate. The more information one stores about its environment, the better one can react to it. If the future state about the environment is predicted correctly, one can either adapt to changes or exploit resources. Although little is known about how exactly the brain stores information, or how decisions are made, living organisms nevertheless have to obey fundamental laws of physics and computation. Even though it is difficult to determine how many bits of information an organism can store, it is easy to assert that the total memory is finite. The more information an organism wants to store and process, the more energy has to be spent on it. [2] One the other hand, just spending

[1] Well, life is what happens despite of what physicists consider possible.

[2] The required amount of energy can be substantial. Humans are better at abstract mathematics than monkeys because we optimised energy intake by cooking our food before eating, which allows us to sustain a bigger brain.

more energy on information processing does not necessarily improve predictions, as the computational models used might be wasteful. Is there a way to determine the minimal amount of resources that need to be spent for simulating one's environment, and classify the efficiency of the computational model? Computer science developed theoretical models to measure exactly this. It has been shown (118) that using QM allows to predict the future more efficiently, i.e. using less resources. The key idea is this: the state of the environment is partitioned into equivalence classes. If two states lead to the same future statistics, there is no need to distinguish between them, and they represent the same equivalence class. If two states lead to different futures, they are distinguished and stored as different states. Sometimes, however, the future statistics of two states are very similar, but not completely the same. If the information is stored classically, the two states leading to similar futures have to be stored fully distinguishable. Storing the same information quantum mechanically requires less resources.

Maximising the predictive power of a brain thus requires using quantum mechanical effects. While it is very difficult to determine whether living system actually use QM to maximise their predictive power with given resources, the physically-possible most efficient predictive black box does use quantum effects.

6.2 Life, levers and quantum biology

Levers are ubiquitous in everybody's life. Their technological advantage allowed humans to become ever more sophisticated. While there are many different kinds of levers, the simplest just needs a stone and a plank. Imagine a weight that is too heavy to be lifted. When putting the plank over the stone and under the heavy object in the correct way, it can be lifted with a relatively small amount of force. That means, with an appropriate construction, a small mass can affect the motion of a large mass. The principle of levers governs almost all processes of our daily life: any tool, from screw drivers to hammers, uses leverage. In our cars the turning of the key (which requires a tiny force) starts the engine (which sets free a big force). Computers are based on transistors, whose basic functional principle is that a small electrical current controls a bigger current. Levers are not bound to physical sytems. Even in the stock market there exist levers in the form of options. But how about life? Did humans invent the idea of levers, or did we just re-invent it?

In the following I will argue that this simple principle is one key feature of life: life is behaviour, life is physics beyond the postulate of equal a priori probability. Behaviour can be regarded as controlled reaction to an environmental stimulus, which can be decomposed into three key steps:
1) detecting a stimulus from the environment,
2) internal data processing leading to a decision about how to react (discussed in the previous paragraph) and finally
3) amplification of small-energy decision, e.g. firing of neurones in the brain, to large-scale reaction, for example moving one's hand.
The energy scale difference between (2) and (3) is needed for showing the phenomena of behaviour. Making a non-trivial decision usually requires to choose from many possible actions. If the decision is not made on a significantly smaller system than the organism itself, the whole organism would have to randomly stumble through the possible reactions, until reaching an advantageous one. This would hardly resemble the process of decision making. This is one of the reasons why biological phenomena so stubbornly refuse to fit into a nice physical formula: The work horses of physics, statistical physics and thermodynamics, are just not suitable to handle amplification processes. One might argue that the reason we understand quantum mechanics so well is that there is no lever effect possible. Each quantum is already the smallest possible energy, no other smaller energy can affect it.

Now that we established that levers are important for life, we have to identity which sort of levers actually occur in living systems. Shape is without doubt a lever, that controls the outcome of reactions. If the shape of two molecules do not fit, they do not react. Are there other possible levers? Presumably yes. Life is chemistry, and chemistry is quantum mechanics. The existence and occupation of discrete molecular eigenstates controls the outcome of chemical reactions. The spin chemical reactions underlying the avian compass recently received much attention, see chapter 2 of this thesis. The change of a single quantum number, the spin, may have macroscopic implication on the direction European Robins choose to fly to. The way quantum mechanics controls the outcome of chemical reactions constitutes a powerful lever. The physical possibility of using quantum mechanics as a lever for chemical reactions, and the potential powerful benefits for living systems, make it likely that Nature in its four billion year research and development program learned to exploit these kind of quantum effects.

The occurrence of adaptive mutations might be another example of a bio-quantum lever. In chapter 5 it was argued that quantum mechanics allows, in principle, to selectively excite a special base pair in a special gene into its tautomeric form. The tautomeric form resembles an option for a mutation. If DNA polymerase detects the tautomer quickly enough, it can lead to a permanent mutation. Other processes in the cell control how often a certain gene is read out, i.e. how likely the optional mutations are turned into actual mutations. A relatively small energy, around 20 times of thermal energy, is needed to create a tautomer. The energetic consequences of mutations on gene expression are huge, as they potentially decide between the life or death of an organism. Thus the optional mutations created by tautomers would constitute a powerful lever.

Das also war des Pudels Kern!

Quantum effects are ubiquitous in biological systems. Even though the **why** and **how** of existence of quantum effects is seldom understood, there is little doubt about the **that**. This thesis mentions many possibilities how harnessing quantum effects can be advantageous for biological systems. I hope this work will trigger further research into quantum biology.

References

[1] Albert Einstein. **Über einen die Erzeugung und Verwandlung des Lichtes betreffenden heuristischen Gesichtspunkt**. *Annalen der Physik*, **17**:132–148, 1905. 1

[2] K. R. Foster. **Mechanisms of interaction of extremely low frequency electric fields and biological systems**. *Radiation Protection Dosimetry*, **106**(4):301–310, 2003. 1, 70

[3] T. D. Ladd, F. Jelezko, R. Laflamme, Y. Nakamura, C. Monroe, and J. L. O/'Brien. **Quantum computers**. *Nature*, **464**(7285):45–53, 2010. 3

[4] Jianming Cai, Sandu Popescu, and Hans J. Briegel. **Dynamic entanglement in oscillating molecules and potential biological implications**. *Phys. Rev. E*, **82**(2):021921, Aug 2010. 3

[5] Christiane R. Timmel and Kevin B. Henbest. **A study of spin chemistry in weak magnetic fields**. *Philosophical Transactions of the Royal Society of London. Series A: Mathematical, Physical and Engineering Sciences*, **362**(1825):2573–2589, 2004. 3, 11

[6] Christopher T. Rodgers and P. J. Hore. **Chemical magnetoreception in birds: The radical pair mechanism**. *Proceedings of the National Academy of Sciences*, **106**(2):353–360, 2009. 3, 11, 13

[7] Alipasha Vaziri and Martin B Plenio. **Quantum coherence in ion channels: resonances, transport and verification**. *New Journal of Physics*, **12**(8):085001, 2010. 6, 7

[8] Gregory S. Engel, Tessa R. Calhoun, Elizabeth L. Read, Tae-Kyu Ahn, Tomás Mancal, Yuan-Chung Cheng, Robert E. Blankenship, and Graham R. Fleming. **Evidence for wavelike energy transfer through quantum coherence in photosynthetic systems**. *Nature*, **446**:782–786, 2007. 7, 42

[9] Akihito Ishizaki, Tessa R. Calhoun, Gabriela S. Schlau-Cohen, and Graham R. Fleming. **Quantum coherence and its interplay with protein environments in photosynthetic electronic energy transfer**. *Phys. Chem. Chem. Phys.*, **12**:7319–7337, 2010. 7

[10] W. Wiltschko and R. Wiltschko. **Magnetic compass of European robins**. *Science*, **176**(4030):62–64, 1972. 8, 12

[11] Wolfgang Wiltschko and Roswitha Wiltschko. **Magnetic compass orientation in birds and its physiological basis**. *Naturwissenschaften*, **89**:445–452, 2002. 8, 12

[12] T.Ritz, P. Thalau, J. B. Phillips, R. Wiltschko, and W. Wiltschko. **Resonance effects indicate a radical-pair mechanism for avian magnetic compass**. *Nature*, **429**:177–180, 2004. 8, 11, 12

[13] Ilia A. Solov'yov and Klaus Schulten. **Magnetoreception through Cryptochrome May Involve Superoxide**. *Biophysical journal*, **96**(12):4804–4813, 2009. 9, 14

[14] Jennifer C. Brookes, Filio Hartoutsiou, A. P. Horsfield, and A. M. Stoneham. **Could Humans Recognize Odor by Phonon Assisted Tunneling?** *Phys. Rev. Lett.*, **98**(3):038101, Jan 2007. 9

[15] Luca Turin. **A Spectroscopic Mechanism for Primary Olfactory Reception**. *Chemical Senses*, **21**(6):773–791, 1996. 9, 42

[16] Sonke Johnsen and Kenneth J. Lohmann. **Magnetoreception in animals**. *Physics Today*, **61**(3):29–35, 2008. 11

[17] Thorsten Ritz, Salih Adem, and Klaus Schulten. **A Model for Photoreceptor-Based Magnetoreception in Birds**. *Biophysical journal*, **78**(2):707–718, 02 2000. 11, 12, 14

[18] N. Keary et al. *Frontiers in Zoology*, **6**:25, 2009. 11

[19] Robert J. Gegear, Amy Casselman, Scott Waddell, and Steven M. Reppert. **Cryptochrome mediates light-dependent magnetosensitivity in Drosophila**. *Nature*, **454**(7207):1014–1018, 2008. 11

[20] T. Yoshii et al. *PLoS Biol.*, **7**:e1000086, 2009. 11

[21] Margaret Ahmad, Paul Galland, Thorsten Ritz, Roswitha Wiltschko, and Wolfgang Wiltschko. **Magnetic intensity affects cryptochrome-dependent responses in Arabidopsis thaliana**. *Planta*, **225**:615–624, 2007. 11

[22] Yan Liu, Ruth Edge, Kevin Henbest, Christiane R. Timmel, P. J. Hore, and Peter Gast. **Magnetic field effect on singlet oxygen production in a biochemical system**. *Chem. Commun.*, pages 174–176, 2005. 11

[23] T. Miura, K. Maeda, and T. Arai. *J. Phys. Chem. A*, **110**:4151, 2006. 11

[24] C.T. Rodgers. **Magnetic field effects in chemical systems**. *Pure and Applied Chem.*, **81**(1):19–43, 2009. 11

[25] Kiminori Maeda, Kevin B. Henbest, Filippo Cintolesi, Ilya Kuprov, Christopher T. Rodgers, Paul A. Liddell, Devens Gust, Christiane R. Timmel, and P. J. Hore. **Chemical compass model of avian magnetoreception**. *Nature*, **453**(7193):387–390, 05 2008. 11

[26] Jianming Cai, Gian Giacomo Guerreschi, and Hans J. Briegel. **Quantum Control and Entanglement in a Chemical Compass**. *Phys. Rev. Lett.*, **104**(22):220502, Jun 2010. 11, 13

REFERENCES

[27] Thorsten Ritz, Roswitha Wiltschko, P. J. Hore, Christopher T. Rodgers, Katrin Stapput, Peter Thalau, Christiane R. Timmel, and Wolfgang Wiltschko. **Magnetic Compass of Birds Is Based on a Molecule with Optimal Directional Sensitivity**. *Biophysical journal*, **96**(8):3451–3457, 04 2009. 12, 13, 14, 15

[28] Manuela Zapka, Dominik Heyers, Christine M. Hein, Svenja Engels, Nils-Lasse Schneider, Jorg Hans, Simon Weiler, David Dreyer, Dmitry Kishkinev, J. Martin Wild, and Henrik Mouritsen. **Visual but not trigeminal mediation of magnetic compass information in a migratory bird**. *Nature*, **461**(7268):1274–1277, 10 2009. 12

[29] Olga Efimova and Peter Hore. **Evaluation of nuclear quadrupole interactions as a source of magnetic anisotropy in the radical pair model of the avian magnetic compass**. *Molecular Physics*, **107**(07):665–671, 2009. 13

[30] C. T. Rodgers. *PhD thesis*. University of Oxford, 2007. 13

[31] E. Gauger, E. Rieper, J.J.L. Morton, S.C. Benjamin, and V. Vedral:. **Sustained quantum coherence and entanglement in the avian compass**. *Phys. Rev. Lett.*, **106**:040503, 2011. 14

[32] Miriam Liedvogel, Kiminori Maeda, Kevin Henbest, Erik Schleicher, Thomas Simon, Christiane R. Timmel, P. J. Hore, and Henrik Mouritsen. **Chemical Magnetoreception: Bird Cryptochrome 1a Is Excited by Blue Light and Forms Long-Lived Radical-Pairs**. *PLoS ONE*, **2**(10):e1106, 2007. 12, 17

[33] J. J. L. Morton et al. *J. Chem. Phys.*, **124**:014508, 2006. 18

[34] T. Ritz et al. **Magnetic Compass of Birds Is Based on a Molecule with Optimal Directional Sensitivity**. *Biophys. J.*, **96**:3451–3457, 2009. 20

[35] L.-A. Wu, M. S. Sarandy, and D. A. Lidar. **Quantum Phase Transitions and Bipartite Entanglement**. *Phys. Rev. Lett.*, **93**(25):250404, 2004. 25, 26, 34, 40

[36] Janet Anders. **Thermal state entanglement in harmonic lattices**. *Phys. Rev. A*, **77**(6):062102, 2008. 25, 26, 27, 31, 32, 38, 47

[37] Albert Einstein. **Die Plancksche Theorie der Strahlung und die Theorie der spezifischen Wärme.** *Annalen der Physik*, **22**:180–190, 1907. 25

[38] Vladimir Spirko, Jiri Sponer, and Pavel Hobza. **Anharmonic and harmonic intermolecular vibrational modes of the DNA base pairs**. *J. Chem. Phys.*, **106**:1472, 1997. 25, 27

[39] H. Fröhlich. **Long range coherence and the action of enzymes**. *Nature*, **228**:1093, 1970. 25

[40] K. Audenaert, J. Eisert, M. B. Plenio, and R. F. Werner. **Entanglement properties of the harmonic chain**. *Phys. Rev. A*, **66**(4):042327, 2002. 26, 36

[41] Juan Pablo Paz and Augusto J. Roncaglia. **Dynamics of the Entanglement between Two Oscillators in the Same Environment**. *Phys. Rev. Lett.*, **100**(22):220401, 2008. 26

[42] J. Eisert, M. B. Plenio, S. Bose, and J. Hartley. **Towards Quantum Entanglement in Nanoelectromechanical Devices**. *Phys. Rev. Lett.*, **93**(19):190402, 2004. 26

[43] Fernando Galve and Eric Lutz. **Energy cost and optimal entanglement production in harmonic chains**. *Phys. Rev. A*, **79**(3):032327, 2009. 26

[44] J. M. Yeomans. *Statistical Mechanics of Phase Transitions*. Clarendon Press, 1992. 26

[45] Sachdev. *Quantum Phase Transitions*. Cambridge University Press, 1999. 26

[46] A. Osterloh, L. Amico, G. Falci, and R. Fazio. **Scaling of entanglement close to a quantum phase transition**. *Nature*, **416**:608, 2002. 26

[47] J. Eisert and M.B. Plenio. **Introduction to the basics of entanglement theory in continuous-variable systems**. *Int. J. Quant. Inf.*, **1**:479, 2003. 26, 31

[48] S. Ghosh, T. F. Rosenbaum, G. Aeppli, and S. N. Coppersmith. **Entangled quantum state of magnetic dipoles**. *Nature*, **425**:48, 2003. 26

[49] Rainer Blatt and David Wineland. **Entangled states of trapped atomic ions**. *Nature*, **453**(7198):1008–1015, 2008. 26

[50] G Kirchmair, J Benhelm, F Zähringer, R Gerritsma, C F Roos, and R Blatt. **Deterministic entanglement of ions in thermal states of motion**. *New Journal of Physics*, **11**(2):023002, 2009. 26

[51] G. Birkl, S. Kassner, and H. Walther:. **Multiple-shell structures of laser-cooled 24Mg+ ions in a quadrupole storage ring**. *Nature*, **357**:310, 1992. 26, 27

[52] D. G. Enzer, M. M. Schauer, J. J. Gomez, M. S. Gulley, M. H. Holzscheiter, P. G. Kwiat, S. K. Lamoreaux, C. G. Peterson, V. D. Sandberg, D. Tupa, A. G. White, R. J. Hughes, and D. F. V. James. **Observation of Power-Law Scaling for Phase Transitions in Linear Trapped Ion Crystals**. *Phys. Rev. Lett.*, **85**(12):2466–2469, 2000. 26

[53] Shmuel Fishman, Gabriele De Chiara, Tommaso Calarco, and Giovanna Morigi. **Structural phase transitions in low-dimensional ion crystals**. *Phys. Rev. B*, **77**(6):064111, 2008. 26, 27, 40

[54] A. Retzker, R. C. Thompson, D. M. Segal, and M. B. Plenio. **Double Well Potentials and Quantum Phase Transitions in Ion Traps**. *Phys. Rev. Lett.*, **101**(26):260504, 2008. 26, 36

[55] J. Eisert, M. Cramer, and M. B. Plenio. **Colloquium: Area laws for the entanglement entropy**. *Rev. Mod. Phys.*, **82**(1):277–306, 2010. 27, 36

[56] Angela Kopp and Sudip Chakravarty. **Criticality in correlated quantum matter**. *Nature Physics*, **1**(53), 2005. 27

[57] I. Bloch. **Quantum coherence and entanglement with ultracold atoms in optical lattices**. *Nature*, **453**(1016), 2008. 27

[58] M. G. Raizen, J. M. Gilligan, J. C. Bergquist, W. M. Itano, and D. J. Wineland. **Ionic crystals in a linear Paul trap**. *Phys. Rev. A*, **45**(9):6493–6501, 1992. 27

[59] I. Waki, S. Kassner, G. Birkl, and H. Walther. **Observation of ordered structures of laser-cooled ions in a quadrupole storage ring**. *Phys. Rev. Lett.*, **68**(13):2007–2010, 1992. 27

[60] Charles H. Bennett, David P. DiVincenzo, John A. Smolin, and William K. Wootters. **Mixed-state entanglement and quantum error correction**. *Phys. Rev. A*, **54**(5):3824–3851, 1996. 29

[61] J. Williamson. *American Journal of Mathematics*, **58**:3658, 1936. 31

[62] A. Einstein, B. Podolsky, and N. Rosen. **Can quantum-mechanical description of physical reality be considered complete?** *Phys. Rev.*, **47**(777), 1935. 32

[63] Gerardo Adesso, Alessio Serafini, and Fabrizio Illuminati. **Extremal entanglement and mixedness in continuous variable systems**. *Phys. Rev. A*, **70**(2):022318, Aug 2004. 32, 47, 51

[64] Jirri Cerny, Matrin Kabelac, and Pavel Hobza. **Double-Helical -Ladder Structural Transition in the B-DNA is Induced by a Loss of Dispersion Energy**. *Journal of the American Chemical Society*, **130**(47):16055–16059, 2008. 41, 42, 44, 47

[65] Masoud Mohseni, Patrick Rebentrost, Seth Lloyd, and Alan Aspuru-Guzik. **Environment-assisted quantum walks in photosynthetic energy transfer**. *The Journal of Chemical Physics*, **129**(17):174106, 2008. 42

[66] F. Caruso, A. W. Chin, A. Datta, S. F. Huelga, and M. B. Plenio. **Highly efficient energy excitation transfer in light-harvesting complexes: The fundamental role of noise-assisted transport**. *The Journal of Chemical Physics*, **131**(10):105106, 2009. 42

[67] Francesca Fassioli, Alexandra Olaya-Castro, Simon Scheuring, James N. Sturgis, and Neil F. Johnson. **Energy Transfer in Light-Adapted Photosynthetic Membranes: From Active to Saturated Photosynthesis**. *Biophysical journal*, **97**(9):2464–2473, 11 2009. 42

[68] Hans J. Briegel and Sandu Popescu. **Intra-molecular refrigeration in enzymes**. *arXiv:0912.2365*, 2009. 42

[69] Gary D. Stormo and Yue Zhao. **Determining the specificity of protein–DNA interactions**. *Nat Rev Genet*, **11**(11):751–760, 11 2010. 42

[70] Jiří Černý, Jiří Vondrášek, and Pavel Hobza. **Loss of Dispersion Energy Changes the Stability and Folding/Unfolding Equilibrium of the Trp-Cage Protein**. *The Journal of Physical Chemistry B*, **113**(16):5657–5660, 2009. 42

[71] R. Luo, H. S. R. Gilson, M. J. Potter, and M. K. Gilson. **The Physical Basis of Nucleic Acid Base Stacking in Water**. *Biophys. J.*, **80**:140–148, 2001. 42

[72] Adam E. Cohen and Shaul Mukamel. **Resonant Enhancement and Dissipation in Nonequilibrium van der Waals Forces**. *Phys. Rev. Lett.*, **91**(23):233202, Dec 2003. 43

[73] Hefeng Wang and Sabre Kais. **Quantum Entanglement and Electron Correlation in Molecular Systems**. *Israel Journal of Chemistry*, **47**(1):59–65, 2007. 43

[74] G.C. Maitland, M. Rigby, E. Brian Smith, and W.A. Wakeham. *Intermolecular forces*. Clarendon Press, Oxford, 1981. 44

[75] Elisabeth Rieper, Janet Anders, and Vlatko Vedral. **Entanglement at the quantum phase transition in a harmonic lattice**. *New Journal of Physics*, **12**(2):025017, 2010. 45

[76] H. Barsch, D.R. Garmer, P.G. Jasien, M. Krauss, and W.J. Stevens. **Electrical properties fo nucleic acid bases**. *Chem. Phys. Lett.*, **163**(6):514–522, 1989. 46

[77] T. Engel and P. Reid. *Physical Chemistry*. Pearson, 2010. 49

[78] M. Born and R. Oppenheimer. **Zur Quantentheorie der Molekülen**. *Annalen der Physik*, **389**(20):457–484, 1927. 55

[79] C.E. Shannon. **A Mathematical Theory of Communication**. *Bell System Technical Journal*, **27**:379–423, 1948. 57

[80] O. Dahlsten, R. Renner, E. Rieper, and V. Vedral. **Inadequacy of von Neumann entropy for characterizing extractable work**. *New Journal of Physics*, **13**:053015, 2011. 57

[81] Rolf Landauer. **The physical nature of information**. *Physics Letters A*, **217**:188–193, 1996. 57

[82] M. A. Nielson and I. L. Chuang. *Quantum Computation and Quantum Information*. Cambridge University Press, 2000. 58, 60, 66, 79, 93

[83] Charles H. Bennett, Peter W. Shor, John A. Smolin, and Ashish V. Thapliyal. **Entanglement-Assisted Classical Capacity of Noisy Quantum Channels**. *Phys. Rev. Lett.*, **83**(15):3081–3084, 1999. 61

[84] C. Adami and N. J. Cerf. **von Neumann capacity of noisy quantum channels**. *Phys. Rev. A*, **56**(5):3470–3483, 1997. 61

[85] C.H. Bennett, P.W. Shor, J.A. Smolin, and A.V. Thapliyal. **Entanglement-assisted capacity of a quantum channel and the reverse Shannon theorem**. *IEEE*, **48**:2637, 2002. 61

[86] Seth Lloyd. **Capacity of the noisy quantum channel**. *Phys. Rev. A*, **55**(3):1613–1622, 1997. 61

[87] Howard Barnum, M. A. Nielsen, and Benjamin Schumacher. **Information transmission through a noisy quantum channel**. *Phys. Rev. A*, **57**:4153–4175, 1998. 61

[88] [online][link]. 62

[89] [online, cited 7.11.2011][link]. 63

REFERENCES

[90] Maria Isabel Franco, Luca Turin, Andreas Mershin, and Efthimios M. C. Skoulakis. **Molecular vibration-sensing component in Drosophila melanogaster olfaction**. *Proceedings of the National Academy of Sciences*, **108**(9):3797–3802, 2011. 65

[91] *Quantum Aspects of life*. Imperial College Press, 2008. 66

[92] Lucia Hackermüller, Stefan Uttenthaler, Klaus Hornberger, Elisabeth Reiger, Björn Brezger, Anton Zeilinger, and Markus Arndt. **Wave Nature of Biomolecules and Fluorofullerenes**. *Phys. Rev. Lett.*, **91**(9):090408, 2003. 67

[93] P.O. Löwdin. *Quantum Genetics and the Aperiodic Solid: Some Aspects on the Biological Problems of Heredity, Mutations, Aging, and Tumors in View of the Quantum Theory of the DNA Molecule*. Academic Press, 1966. 68, 75

[94] Leslie E. Ballentine. *Quantum Mechanics: A Modern Development*. Word Scientific, 1998. 71

[95] A.J.F. Griffiths, W. M. Gelbart, J.H. Miller, and R.C. Lewontin. *Modern Genetic Analysis*. W. H. Freeman and Company, 1999. 75, 84

[96] H. P. Yockey. *Information theory and molecular biology*. Cambridge University Press, 1992. 81

[97] Swaine L. Chen, William Lee, Alison K. Hottes, Lucy Shapiro, and Harley H. McAdams. **Codon usage between genomes is constrained by genome-wide mutational processes**. *Proceedings of the National Academy of Sciences of the United States of America*, **101**(10):3480–3485, 2004. 91, 92, 93

[98] Joshua B. Plotkin and Grzegorz Kudla. **Synonymous but not the same: the causes and consequences of codon bias**. *Nat Rev Genet*, 2010. 93

[99] John Cairns, Julie Overbaugh, and Stephan Miller. **The origin of mutants**. *Nature*, **355**:142–145, 1988. 94

[100] Patricia L. Foster. **Adaptive Mutation: The Uses of Adversity**. *Annual Reviews Microbiology*, **47**:467–504, 1993. 94

[101] Susan M. Rosenberg. **Evolving Responsively: Adaptive Mutation**. *Nature Reviews Genetics*, **2**(504-515), 2001. 94

[102] John R. Roth, Elisabeth Kugelberg, Andrew B. Reams, Eric Kofoid, and Dan I. Andersson. **Origin of Mutations Under Selection: The Adaptive Mutation Controversy**. *Annual Reviews Microbiology*, **60**:477–501, 2006. 94

[103] Patricia L. Foster. **Stress-Induced Mutagenesis in Bacteria**. *Critical Reviews in Biochemistry and Molecular Biology*, **42**:373–397, 2007. 94

[104] V. G. Godoy, F. S. Gizatullin, and Maurice S. Fox. **Some Features of the Mutability of Bacteria During Nonlethal Selection**. *Genetics*, **154**(1):49–59, 2000. 94, 104

[105] William A. Rosche and Patricia L. Foster. **The role of transient hypermutators in adaptive mutation in Escherichia coli**. *Proceedings of the National Academy of Sciences of the United States of America*, **96**(12):6862–6867, 1999. 94, 104

[106] Joel Torkelson, Reuben S. Harris, Mary-Jane Lombardo, Jayan Nagendran, Carl Thulin, and Susan M. Rosenberg. **Genome-wide hypermutation in a subpopulation of stationary-phase cells underlies recombination-dependent adaptive mutation**. *EMBO J*, **16**(11):3303–3311, 1997. 94, 104

[107] PL Foster. **Nonadaptive mutations occur on the F' episome during adaptive mutation conditions in Escherichia coli**. *J. Bacteriol.*, **179**(5):1550–1554, 1997. 94, 103, 104

[108] Jeffrey D. Stumpf, Anthony R. Poteete, and Patricia L. Foster. **Amplification of lac Cannot Account for Adaptive Mutation to Lac+ in Escherichia coli**. *J. Bacteriol.*, **189**(6):2291–2299, 2007. 94, 101, 103

[109] Rebecca G. Ponder, Natalie C. Fonville, and Susan M. Rosenberg. **A Switch from High-Fidelity to Error-Prone DNA Double-Strand Break Repair Underlies Stress-Induced Mutation**. *Molecular cell*, **19**:791–804, 2005. 95, 104

[110] J. D. Teufel, Dale Li, M. S. Allman, K. Cicak, A. J. Sirois, J. D. Whittaker, and R. W. Simmonds. **Circuit cavity electromechanics in the strong-coupling regime**. *Nature*, **471**(7337):204–208, 2011. 95

[111] K. R. Brown, C. Ospelkaus, Y. Colombe, A. C. Wilson, D. Leibfried, and D. J. Wineland. **Coupled quantized mechanical oscillators**. *Nature*, **471**(7337):196–199, 2011. 95

[112] Elisabeth Rieper Anna Muszkiewicz. **Atomic vibrations in DNA and their dependence on the sequence of the DNA base pairs – a theoretical study**. *private conservation*, 2011. 98, 99, 100

[113] M. Harz, P. Rösch, and J. Popp. **Vibrational spectroscopy—A powerful tool for the rapid identification of microbial cells at the single-cell level**. *Cytometry Part A*, **75A**(2):104–113, 2009. 99

[114] E. Rieper, J. Anders, and V. Vedral. **Quantum entanglement between the electron clouds Quantum entanglement between the electron clouds of nucleic acids in DNA**. *in preparation*, 2010. 99

[115] JP Radicella, PU Park, and MS Fox. **Adaptive mutation in Escherichia coli: a role for conjugation**. *Science*, **268**(5209):418–420, 1995. 101

[116] P L Foster and J M Trimarchi. **Adaptive reversion of an episomal frameshift mutation in Escherichia coli requires conjugal functions but not actual conjugation**. *Proceedings of the National Academy of Sciences of the United States of America*, **92**(12):5487–5490, 1995. 101

[117] C. Gerry and P. Knight. *Introductory Quantum Optics*. Cambridge University Press, 2004. 103

[118] M. Gu, K. Wiesner, Elisabeth Rieper, and V. Vedral. **Sharpening Occams Razor with Quantum Mechanics**. *submitted*, **arxiv 1102.1994**, 2011. 114